ORNL/TM-13660

ornl

OAK RIDGE NATIONAL LABORATORY

LOCKHEED MARTIN

Status Report on Solid Control in Leachates

E. C. Beahm
C. F. Weber
D. D. Lee
T. A. Dillow
R. D. Hunt
C. M. Keswa
K. Osseo-Asare
K. E. Spear

MASTER

Tanks
Focus
Area

DISCLAIMER

Portions of this document may be illegible in electronic image products. Images are produced from the best available original document.

Chemical Technology Division

Status Report on Solid Control in Leachates

E. C. Beahm   R. D. Hunt
C. F. Weber[*]   C. M. Keswa[†]
D. D. Lee   K. Osseo-Asare[†]
T. A. Dillow   K. E. Spear[†]

---

[*]Computational Physics and Engineering Division.
[†]Pennsylvania State University, University Park.

Date Published: July 1998
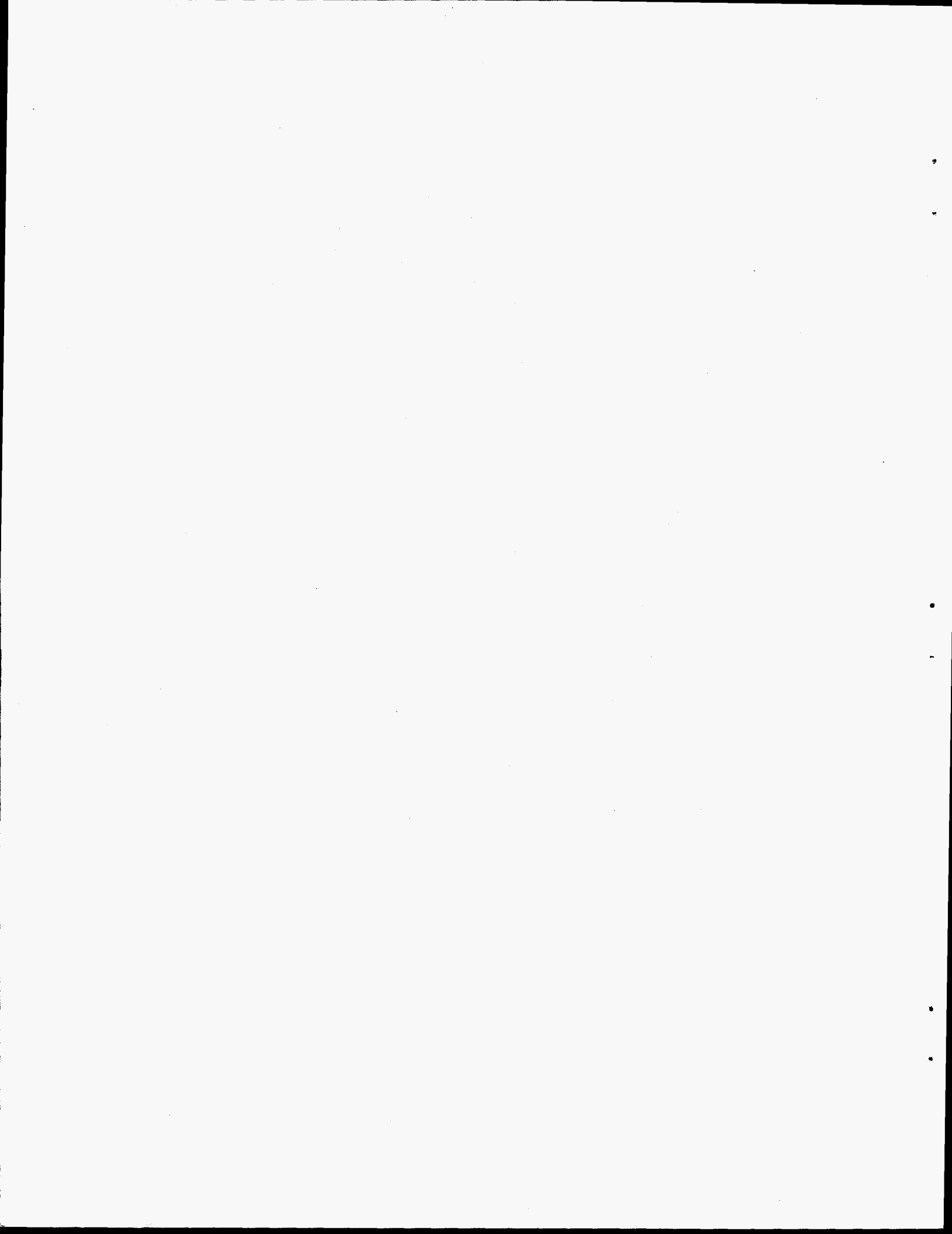
CONTENTS

LIST OF FIGURES

LIST OF TABLES

EXECUTIVE SUMMARY

Sludge pretreatment will involve some combination of washing and leaching with sodium hydroxide solutions to remove soluble salts and amphoteric material such as alumina. It is of paramount importance to prevent gelation and uncontrolled solid formation in tanks, transfer lines, and process equipment. An evaluation of results of washing and caustic leaching indicates that washing is more effective in dissolving sludge solids than subsequent sodium hydroxide treatment. Only aluminum and chromium were removed more effectively by caustic leaching than by water washing.

Operating windows are defined as the concentrations of aluminate, phosphate, and fluoride at which solids do not form in process solutions. Experimental results and model calculations found a dramatic decrease in operating window as the temperature decreased as shown in the figure below. The small operating windows at lower temperatures mean that temperatures must be maintained during processing or that concentrations of phosphate and fluoride must be kept low.
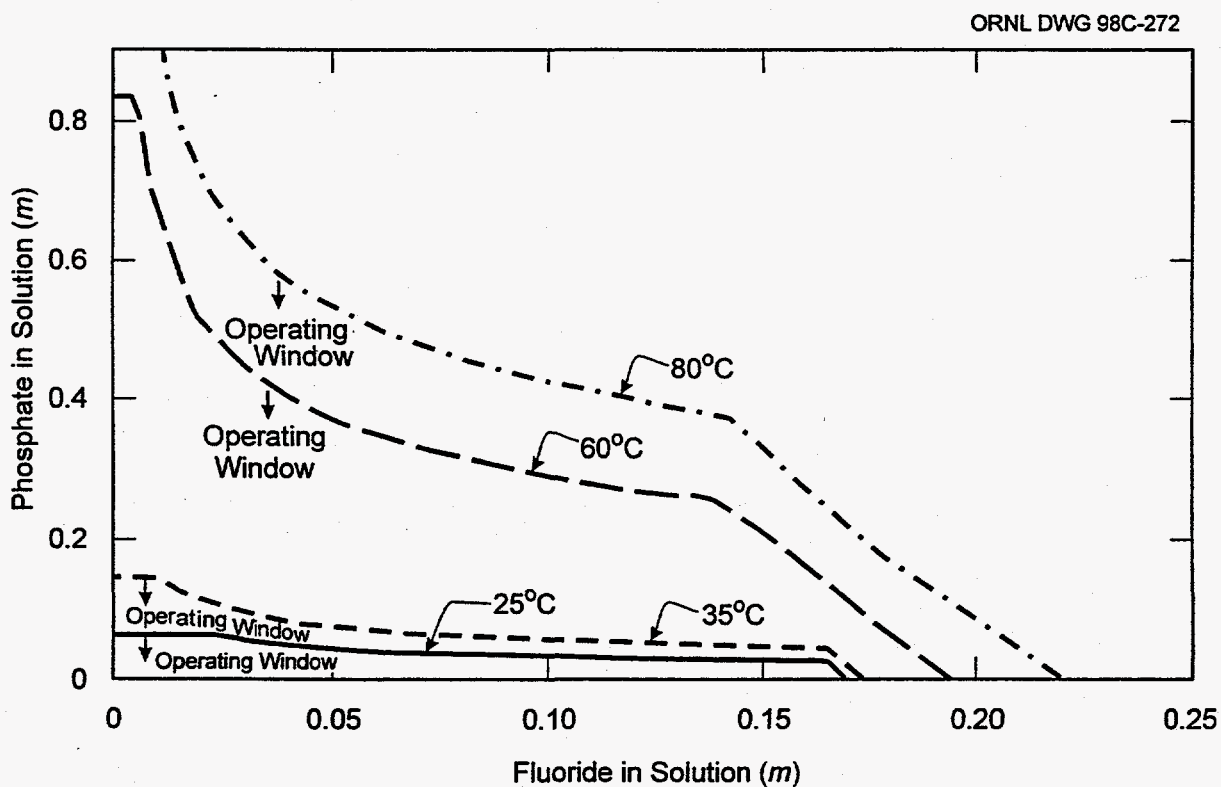
ORNL DWG 98C-272

Temperature dependence of operating windows for process solutions containing phosphate and fluoride in 3 *m* NaOH.

The operating windows for phosphate and fluoride also decrease markedly as sodium hydroxide concentration increases. This is illustrated in the figure below, which shows the operating windows for process solutions with no added NaOH, with 1 m NaOH, and with 3 m NaOH.
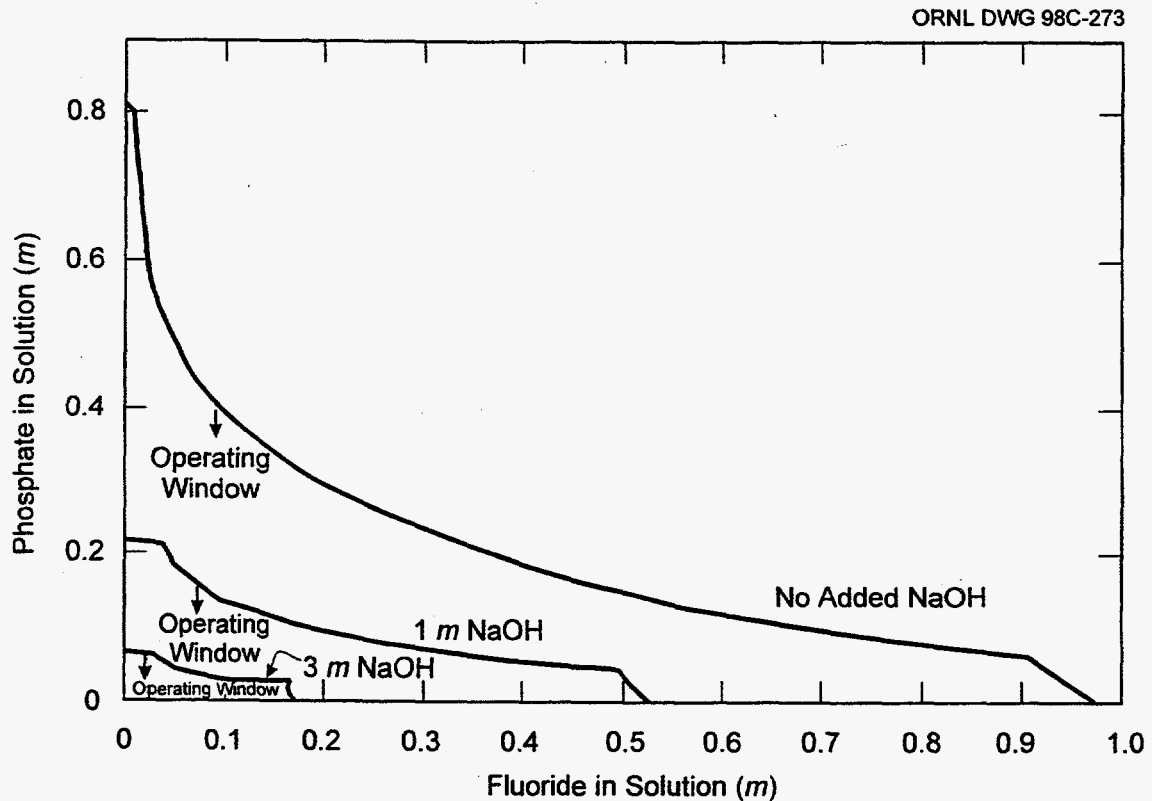
Operating windows for process solutions containing phosphate and fluoride with no added NaOH, with 1 m NaOH, and with 3 m NaOH at 25°C.

The decrease in operating windows for phosphate and fluoride with increasing caustic concentration is the opposite of that observed for alumina. As a result, operating windows for the combination of aluminate, phosphate, and fluoride are quite narrow. The total concentrations of phosphate, fluoride, and aluminate must be kept ≤0.25 m if solid formation is to be avoided in caustic treatment of sludge that contains these components. Washing out phosphate and fluoride as much as reasonably possible before caustic leaching is beneficial.

It is likely that the selection of the combination of washing and caustic leaching, as well as the volume of waste and process solutions, will have to be tailored to the specific material being treated. Sludge tests and modeling are consistent in showing that solid formation will occur in process solutions if oversight and control of solution concentrations are not maintained.

Silica will impact alumina dissolution in caustic solutions. It decreases the rate of dissolution and may lead to the formation of sodium aluminosilicates, which contain anions such as sulfate or nitrate. Because the use of caustic will increase the potential for the formation of solids containing phosphate and fluoride and can result in the formation of sodium aluminosilicates, waste to be treated by caustic leaching should be carefully evaluated to ensure that a net benefit exists.

1. INTRODUCTION

Sludge pretreatment will involve some combination of washing and leaching with caustic (sodium hydroxide). Any pretreatment process must be forgiving; that is, the range of operating conditions must be sufficiently wide to accommodate temperature variations, heterogeneous compositions, instrument inaccuracies, and operator error without causing undesirable results. It is of paramount importance to prevent gelation and uncontrolled solid formation in tanks, transfer lines, and process equipment.[1] A need therefore exists to identify conditions at which treatment is viable. The conditions to be delineated include solution compositions, temperatures, and chemical additives to control solid formation. A viable process is one that results in products that are better than the initial material from the standpoint of waste disposal while undesirable products, secondary wastes, or conditions are controlled.

Table 1 lists residual sludge solids after pretreatment by Enhanced Sludge Washing. The data used to construct Tables 1 and 2 were obtained from Penny Colton's 1997 *Pretreatment Chemistry Evaluation*.[2] The pretreatment consisted of sludge washing with inhibited water followed by caustic leaching (Enhanced Sludge Washing). Of the 18 analytes listed, only the 6 marked with an "X" in the right-hand column were affected by the water wash or the Enhanced Sludge Washing. The amounts of the other analytes remained substantially the same after pretreatment as they were before.

Table 2 gives a breakdown of the six analytes that were affected by pretreatment in terms of the material removed by water washing and the material removed by caustic leaching. Not surprisingly, most of the sodium was removed by water washing. Water washing removed 1744×10^6 mol, and subsequent leaching removed an additional $\sim35 \times 10^6$ mol. In the case of ^{137}Cs, it is unclear whether it is beneficial to remove the radioelement from the high-level waste; in any case, approximately twice as much was removed with a water wash as in the leaching. The only apparent benefit of removing silicon in caustic pretreatment is in the case where the basic treatment is followed by acid dissolution. Smaller amounts of silicon in acid solutions will lower the amounts of hydrofluoric acid that must be added to prevent the formation of silica gel. Pretreatment with water washing and caustic leaching removed approximately one-half of the silica from the sludge solids.

1

Table 1. Residual solids after pretreatment, Hanford single-shell tanks[a]

Element	Residual solids (10^6 mol)	Material affected by water wash or Enhanced Sludge Washing
Al	19.3	X
Ba	0.14	
Bi	2.5	
Ca	5.4	
Cd	0.043	
Cr	1.4	X
Fe	19.8	
Mg	2.3	
Mn	3.3	
Na	40.1	X
Ni	1.1	
Phosphate	2.8	X
Si	16.7	X
Sr	0.78	
U	3.2	
Zr	2.0	
^{137}Cs	1.3×10^6 Ci	X
^{90}Sr	34.1×10^6 Ci	

[a]Based on Penny Colton's *Status Report: Pretreatment Chemistry Evaluation FY 1997– Wash and Leach Factors for Single-Shell Tank Waste Inventory*, PNNL-11646, August 1997.

Table 2. Material removed by washing and Enhanced Sludge Washing[a]

Element	Water washing (10^6 mol)		Caustic leaching (10^6 mol)	
	Removed	Residual solids	Removed	Residual solids
Al	55.3	178	159	19
Cr	3.7	7.0	5.6	1.4
Na	1744	74.7	34.6	40.1
Phosphate	45.6	12.2	9.4	2.8
Si	4.2	25.9	9.2	16.7
^{137}Cs	9.0×10^6 Ci	5.7×10^6 Ci	4.4×10^6 Ci	1.3×10^6 Ci

[a]Based on Penny Colton's *Status Report: Pretreatment Chemistry Evaluation FY 1997–Wash and Leach Factors for Single-Shell Tank Waste Inventory*, PNNL-11646, August 1997.

More phosphate was removed by water washing (~46 × 10⁶ mol) than by the subsequent leaching (~9 × 10⁶ mol). However, the ~9 × 10⁶ mol of phosphate removed by caustic leaching could be important if phosphorous is a limiting component of waste glass. Of the 18 analytes, only aluminum and chromium were removed more effectively by caustic leaching than by water washing and are undesirable in sludge residue to be vitrified as high-level waste. This indicates that the strategy in privatization Phase I envelope D (see Sect. 2) of employing multiple washes and caustic leaching only as necessary to meet feed specifications is sound.

Four additional factors are important. First, a number of species such as nitrate, nitrite, and fluoride are not shown here as analytes. These species are generally water soluble and would be removed by water wash more effectively than by caustic leaching. Second, data shown in Tables 1 and 2 were based on specific conditions of washing at ambient temperature and leaching at ~100°C with ~3 m sodium hydroxide. Third, the data in Tables 1 and 2 are based on tests with small (≤10-g) samples that do not necessarily reflect the conditions and operations required in an operating process. Fourth, the results are given as single values. Privatization contracts will include limits on materials and processes. The range of uncertainty should be assessed so that process capabilities and limitations can be defined. At this time the operating windows and process requirements given here are also based on single-value calculations and data. Before they are used in conjunction with process control, ranges of uncertainty will have to be evaluated.

The first and most fundamental requirement, no matter what process is adopted, will be removal of sludge from the tanks. This must be done with the same concerns for process control and avoidance of solid formation as in pretreatment. Instrumentation to measure concentrations of chemical components and temperature will have to be deployed, starting with retrieval and continuing throughout all processing and transfer operations. This instrumentation should be operated with settings and alarms that are based on viable process conditions.

Finding viable process options begins with identifying treatments that are effective in separating sludge components and by identifying potential problems due to chemical interactions that could result in process difficulties or safety concerns. Solid formation in filtered leachates and wash solutions from Enhanced Sludge Washing of sludge from Hanford underground storage tanks is described in Ref. 1. Solid formation in process solutions took a variety of forms: very fine particles,

larger particulate solids, solids floating like egg whites, gels, crystals, and coatings on sample containers. Gel-like material in sludge leachate was identified as natrophosphate, $Na_7(PO_4)_2F\cdot 19H_2O$.

2. BASELINE FLOW SHEETS

Hanford tank waste treatment consists of two phases of operation in concert with the private sector.[3] Phase I consists primarily of processing double-shell tank (DST) waste, and Phase II is associated processing of primarily single-shell tank (SST) waste. The base case for Phase I divides the DST waste into four envelopes based on the characterization of the contained wastes and the constraints and requirements for fulfilling the privatization contracts for the treatment tasks. The envelopes are called the A, B, C (Phase Ia), and D (Phase Ib) envelopes, and the contracts with the private sector delineate the types and quantities of each feed that Project Hanford Management Corporation (PHMC) must deliver.

Baseline flow sheets that were developed from the *Tank Waste Remediation System Operation and Utilization Plan* (September 1997 edition[3]) are given in Figs. 1 through 9. These flow sheets provide the starting point for examination of process options.

Envelopes A, B, and C feeds are primarily supernatants (Figs. 1–6), while envelope D is sludge/supernatant slurry containing a prescribed quantity of nonsodium, nonsilicon metal oxides (Figs. 7–9). Envelope A waste "will test the production capacity and fission-product removal efficiency of the plants and will produce a final product in which the waste loading will be limited by sodium." Envelope B waste is similar to A but will be limited by concentrations of minor components. Envelope C waste contains complexing agents that may interfere with ^{90}Sr or transuranic (TRU) decontamination and require organic destruction or other mitigation technology.

The first phase (Phase Ia) of the tank privatization processing calls for starting with the decantation of the supernatant in four tanks. The supernatant in each tank is pumped to an interim holding tank, where it is sampled and prepared for pumping to the private contractor for treatment and solidification. Each tank has solids present, is at or near saturation in the liquid phase, and may be supersaturated. Pumping the supernatant to the interim tank without plugging the pipelines is the objective. Adding water and/or caustic to the tank and then mixing and settling to adjust the contents
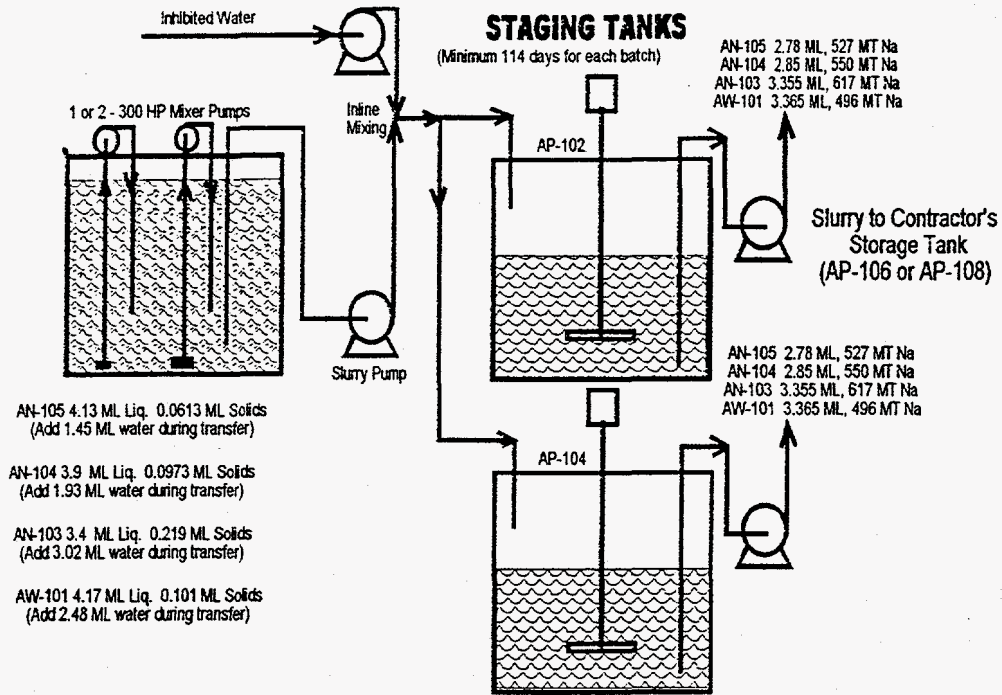
Fig. 1. Flow sheet for baseline Phase I envelope A, 2001–2003.
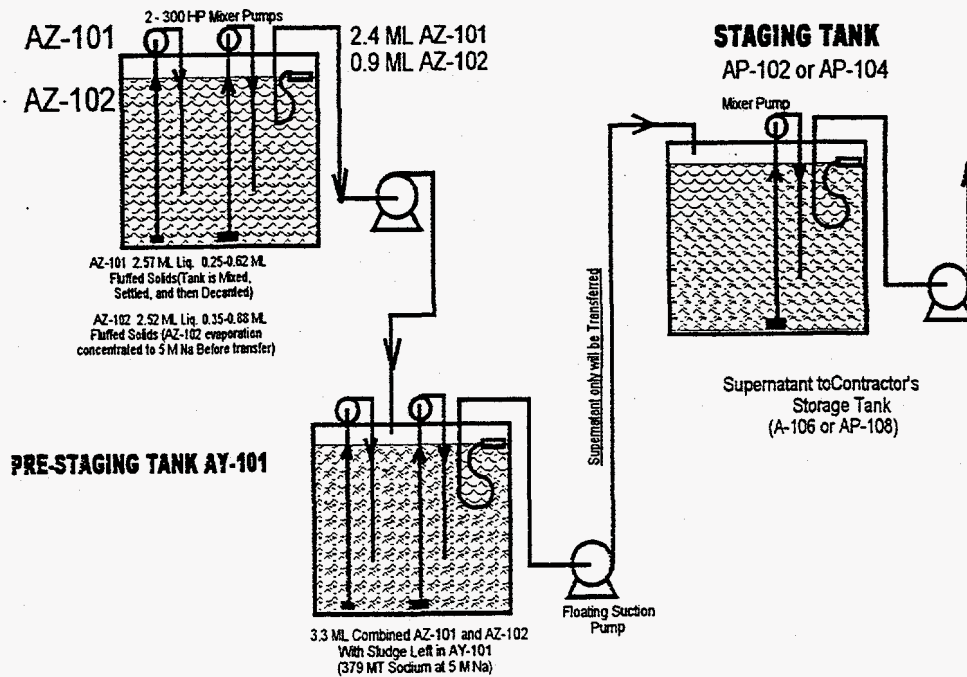
Fig. 2. Flow sheet for baseline Phase I envelope B (neutralized current acid waste supernatant), 2004.
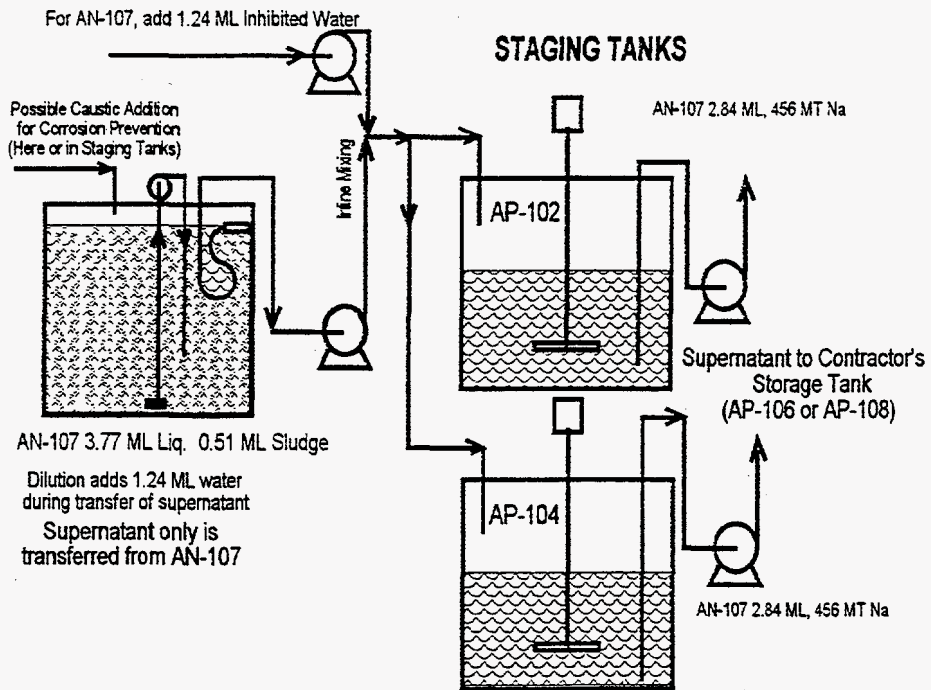
Fig. 3. Flow sheet for baseline Phase I AN-107 envelope C (complex concentrate waste), 2005–2008.
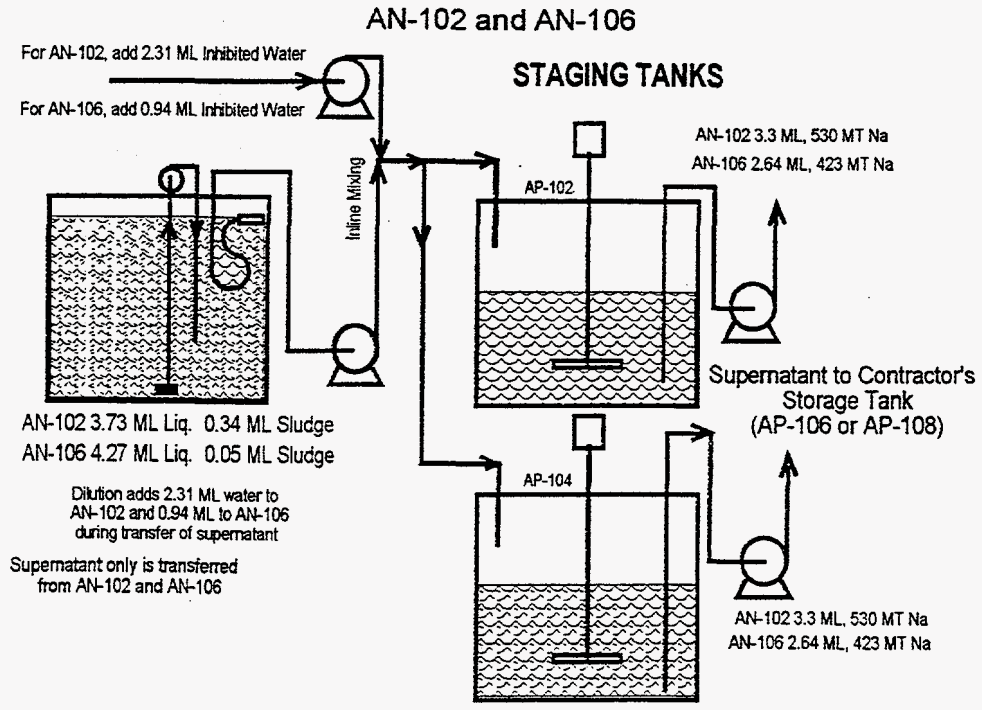
Fig. 4. Flow sheet for baseline Phase I envelope C (complex concentrate waste), 2005–2008.
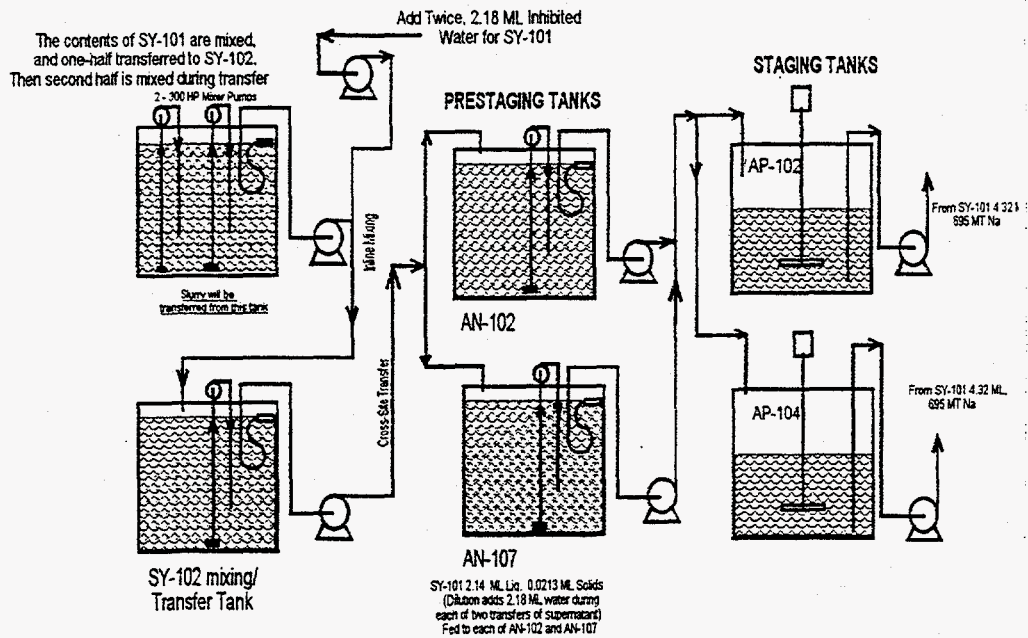
Fig. 5. Flow sheet for baseline Phase I SY-101 envelope C (complex concentrate waste), 2005–2008.
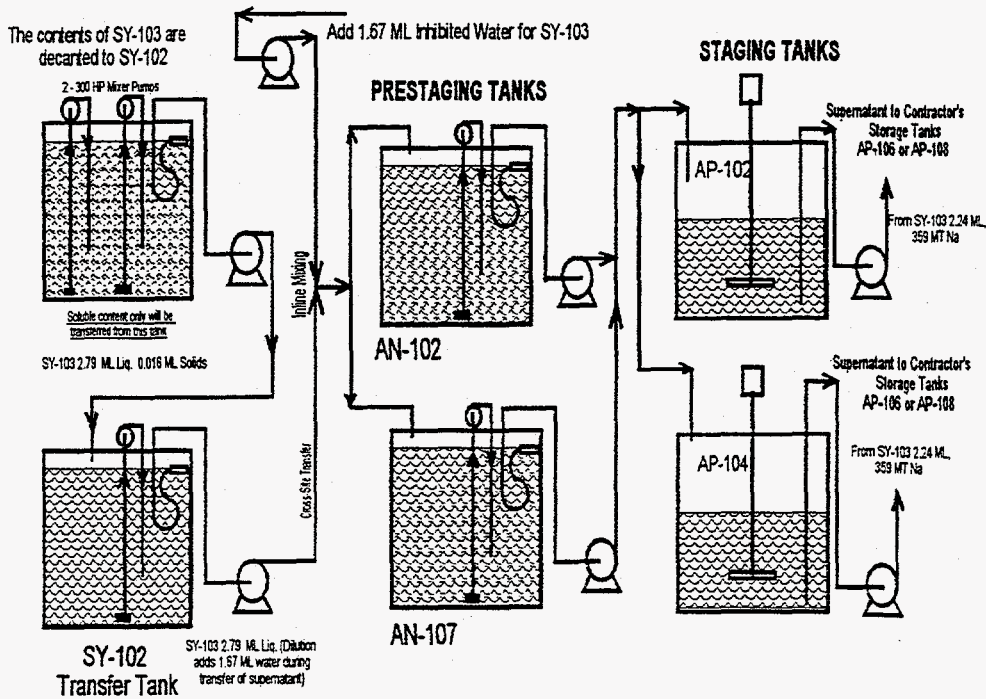
Fig. 6. Flow sheet for baseline Phase I SY-103 envelope C (complex concentrate waste), 2005–2008.

8
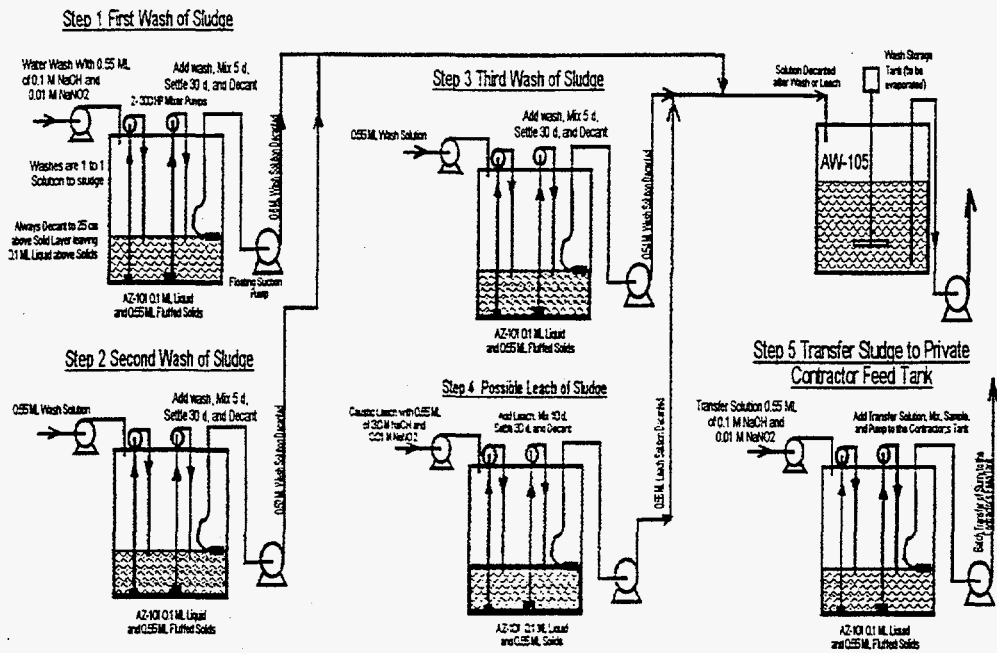
Fig. 7. Flow sheet for baseline Phase I AZ-101 envelope D (high-level waste), 2000–2003.
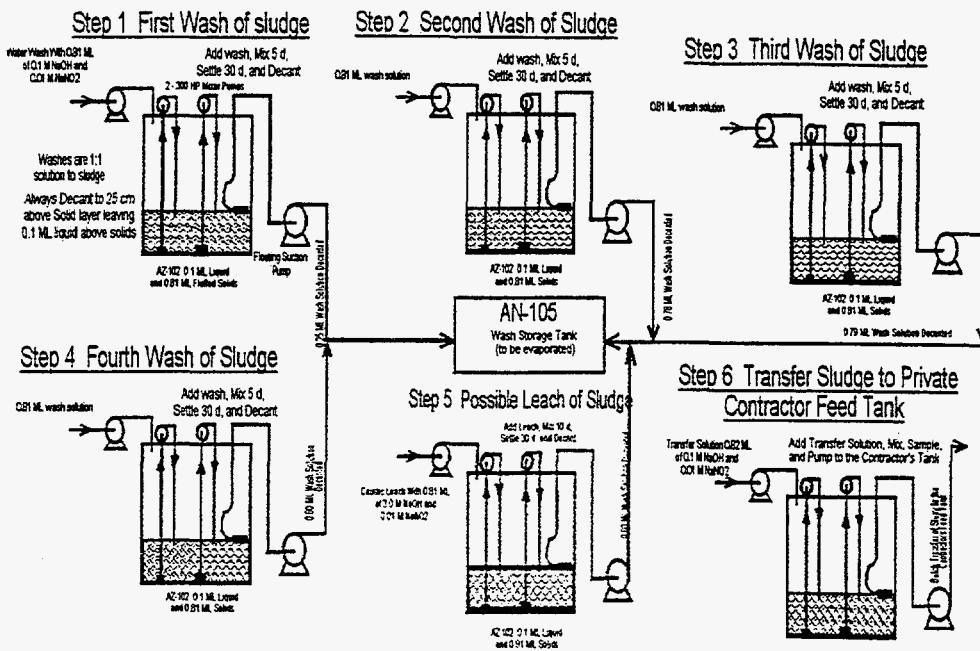
Fig. 8. Flow sheet for baseline Phase I tank AZ-102 envelope D (high-level waste), 2002–2005.
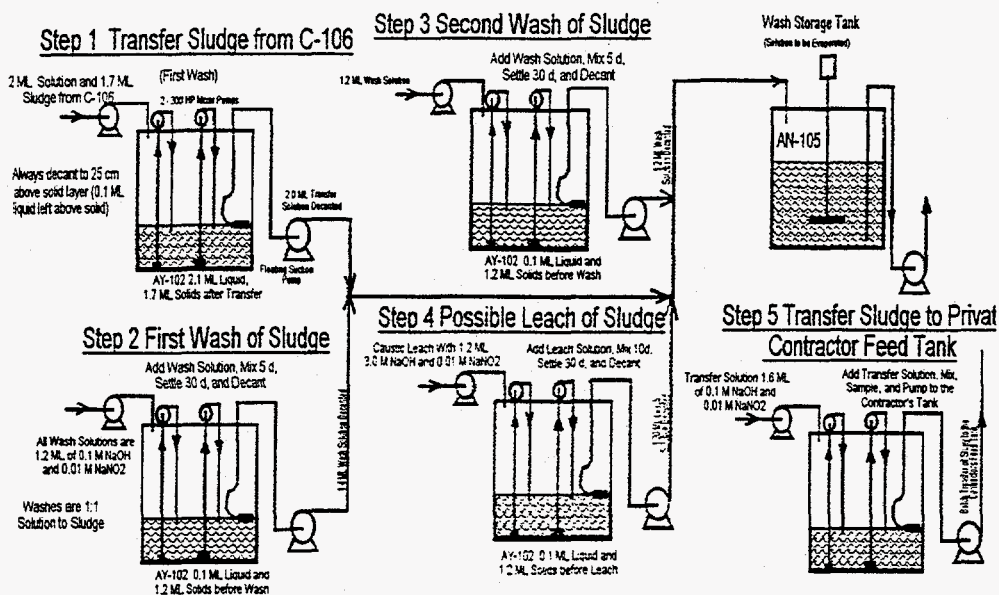
Fig. 9. Flow sheet for baseline Phase I tank AY-102 envelope D (high-level waste), 2005–2008.

to a liquid with very low suspended solids to ensure nonprecipitation, even when the temperature is reduced during transfers, is the preferred means of preventing precipitation in lines. However, all four tanks scheduled for Phase Ia are at or near the maximum liquid level and may not allow much additional dilution to be added. (AN-103 has 3.4×10^6 L, AN-104 has 3.9×10^6 L, AN-105 has 4.21×10^6 L, and AW-101 has 4.17×10^6 L.)

Because of the presence of aluminum (as sodium aluminate) and the hydroxide, reducing the concentration of components by dilution can result in the formation of gibbsite and resultant precipitation if the caustic concentration drops too low or if the temperature decreases too much. Since temperature change can occur most readily during the transfer, prevention of precipitation even with temperature decreases is probably the most desirable option. If the supernatant in the tanks cannot be diluted before transfer, precipitation problems during transfer could be greater.

2.1   PRIMARY OPTIONS

In order to prevent the precipitation, the concentration of the aluminum compounds must be kept in the soluble range during the transport phase. In addition, solids in these tanks, consisting mostly of salts produced by evaporation of the supernatant, are intended to also be dissolved and transported with the supernatant. Therefore, enough water and caustic solution must be added to dissolve the salts and keep the aluminum in solution at the temperatures that will exist in the transfer piping, assuming that the piping is at ambient conditions and is not heat traced. It is also planned to use floating suction pumps on these tanks to minimize the solids transferred, with the pumps to shut down if the solid content exceeds 100 ppm. The pumps will pump the supernatant down to about 10 in. above the sludge layer.

It would be desirable to reduce the tank supernatant temperature to approximate the piping temperature prior to transfer. This would allow any precipitation to occur in the tank, where it will not cause plugging problems, and prevent any possibility of cold lines causing precipitation during transfer. In this case, it would also be desirable to use a surface suction pump to minimize solids transport. Solids could add to the probability of seeding a precipitation during the transport. The precipitation of gibbsite usually requires a seed to begin but can exist in a supersaturated condition for long periods without seed material. Supersaturated conditions due to a decrease in temperature or dilution need to be avoided.

2.2   OTHER POSSIBILITIES

The heating of the tank contents using the mixing pumps and additional heat supplied with heating coils could help dissolve the solids. The heated solution (at a temperature much higher than the solubility temperature, probably after some water and caustic addition during heating and agitation) could then be transported through the pipelines. The heating could ensure that everything in the tank is in solution prior to transport; but, unless water and caustic are added, there would be no guarantee that precipitation would not occur in the transfer piping due to cooling in the lines. The heated supernatant would need to be kept heated and circulated to prevent hot or cold spots from developing and thus making precipitation possible.

Preheating the lines before supernatant transport with another liquid is also an option. This might leave dilution liquid in the lines, causing precipitation as supernatant mixes with the heating solution. The supernatant transport must immediately follow the mixing with the heating solution. A new place would have to be found to store the heating solution after use since storage space for liquids is at a premium. How much solution would be required is also an unknown. The piping for this process may already be in place since rinse solution is used to clean the pipes after transport. The ability to heat the solutions may not exist, but live steam is a possibility.

2.3   HANDLING ENVELOPE D TANKS

In Phase Ib, several DSTs and possibly a few SSTs will be used to supply washed sludge to the private contractors to solidify as immobilized high-level waste (IHLW). The baseline method of washing is to use inhibited water (two or three washes/mixes/decants) followed by washing with 3 M caustic (Enhanced Sludge Washing) to produce the correct amount of metal oxides for transfer to the contractors. Caustic washing may not be needed or advantageous for some of the tanks. This will have to be evaluated for each tank. The problems with the sludge washing occur as the decanted wash and leach solutions (1:1 ratio of solution to sludge for each wash) are mixed together in the wash solution storage tank. As less concentrated washes are mixed with more concentrated washes, some of these solutions could reach solubility limits for some components due to dilution. The wash collection tanks then become precipitation/settling tanks (strike tanks).

The wash in these tanks is slated to be evaporated for concentration to reduce the volume. This will probably cause precipitation of some components in the solution and may dissolve others. The concentrations of the key ions in solution will require monitoring during processing to prevent unwanted precipitation. Strict temperature monitoring and control during all phases of processing will be needed because the solubility of several of the materials depends on temperature. In order to deal with a large amount of caustic on a continuous basis, caustic recycle should be considered.

For Phase II, the SSTs will be used to supply sludge for solidification. The sludge will be mobilized and transferred to a storage/staging DST using inhibited water (a dilute solution of sodium nitrite and sodium hydroxide), at solids concentrations of 25–100 g/L equivalent nonvolatile oxides, with 100 g/L assumed for planning purposes. For all tanks transferred, this constitutes an initial

wash. Retrieved slurries that do not meet the solids content requirements (10–20% by weight) are concentrated or thickened prior to separating solids and liquids. Once in the DST, the slurry will be well mixed and then sampled for testing and qualification before transfer to the private contractor's tanks. The slurry will be stored in the DST for up to a year as a 10% slurry until the private contractor is ready for it. The private contractor will then be responsible for all of the retrieval, washing, leaching, solid/liquid separations, and solidifications of low-activity waste (LAW) and high-activity waste (HAW).

3. OPERATING WINDOWS

3.1 THE Na-F-PO$_4$-HPO$_4$-OH-H$_2$O SYSTEM

There may be limitations on the baseline flow sheets in Phase I and in flow sheets to be developed for Phase II because of the formation of solids in process solutions. Operating windows where the solids do not form were evaluated using model calculations and experimental tests with sludge and sludge simulants. The formation of phosphate and phosphate fluoride solids is described in Sect. 3.1. This is expanded to include alumina in Sect. 3.2 and sludge tests in Sect. 3.3.

In this system the term *operating window* means the set of concentrations of fluoride and phosphate at which solids do not form. The operating window will be a function of temperature, caustic concentration, and ionic strength. Even though the operating windows are expressed in terms of concentration (molality), the model evaluations are based on thermochemical activities as described in Refs. 4 and 5. The vehicle used for building the quantitative model is an adaption of the chemical equilibrium code SOLGASMIX, modified to perform aqueous electrolyte and solid calculations. This code calculates phase equilibrium by minimizing total free energy:

$$G = \sum_i n_i \bar{G}_i = \sum_i n_i \left(G_i^0 + RT \ln a_i \right) \tag{1}$$

where n_i, $\bar{G}_i$, a_i, are the mole inventory, partial molar Gibbs free energy, and activity, respectively, of species i, and the summation includes all components of the system (including water). The molar

free energies of formation G_i^0 (equal to the standard chemical potentials μ_i^0) must be obtained from literature or from data. In practice, we use the reduced form μ_i^0/RT. The activities are evaluated using the practical system where $a_i = m_i\gamma_i$ (for solutes) and $\ln a = -\phi\Sigma m_i/\Omega$ (for water, with $\Omega = 55.51$ mol/kg and ϕ is the osmotic coefficient). If temperature-dependent expressions are available for free energies of formation and activity coefficients, then Eq. (1) can be solved at any temperature. A special module has also been developed to perform nonlinear optimization for the purpose of fitting the various parameters to actual data. This is described in Ref. 5 along with data that were developed for the Na-F-PO$_4$-HPO$_4$-OH-H$_2$O system. It is useful to compare concentrations within operating windows to initial concentrations in sludge. Data on sludge in 27 tanks, provided in Ref. 6, were converted to moles of PO_4^{-3} and F^- per kilogram of sludge. The average PO_4^{-3} was 0.476 mol/kg sludge ,and the median was 0.550 mol/kg sludge. The average F^- was ≥ 0.175 mol/kg sludge, and the median was ≥ 0.082 mol/kg sludge. The values are listed in Appendix A.

Figures 10 through 13 show calculated operating windows for no added OH^-, 1 m OH^-, and 3 m OH^- at temperatures of 25, 35, 60, and 80°C. The operating windows are the areas below the lines at a given OH^- concentration and temperature. The lines at 3 m OH^- are based on model calculations alone because there are no data on the solubility of $Na_7(PO_4)_2F\cdot 19H_2O$ at OH^- concentrations above 1 m. In order to test these extrapolations, tests were run for comparison with the calculated operating windows. In Fig. 10 the filled points indicate that solids formed. Experimental details are given in Appendix B.

Solids form in process solutions because of changes in temperature, OH^- concentration, or ionic strength. This can be seen by comparing the operating windows at 80°C and those at lower temperatures. Cooling results in smaller operating windows and solid formation if the concentration at the higher temperature is outside the operating window at the lower temperature. Figure 14 shows the decrease in operating windows with temperature decreases in 3 m NaOH.

The temperature dependence of solid formation was evaluated by mixing fluoride-phosphate solutions (in 3 m NaOH) at 90–95°C and cooling until solids formed. In order to minimize supersaturation effects, the solution temperature was lowered a short interval and held constant for several hours to permit equilibration. The three initial solutions shown in Table 3 all experienced onset of precipitation in the temperature interval 52–57°C; that is, no precipitation occurred in the equilibrium solution at 57°C, but solids did form as equilibrium was reached at 52°C. The

ORNL DWG 98C-268
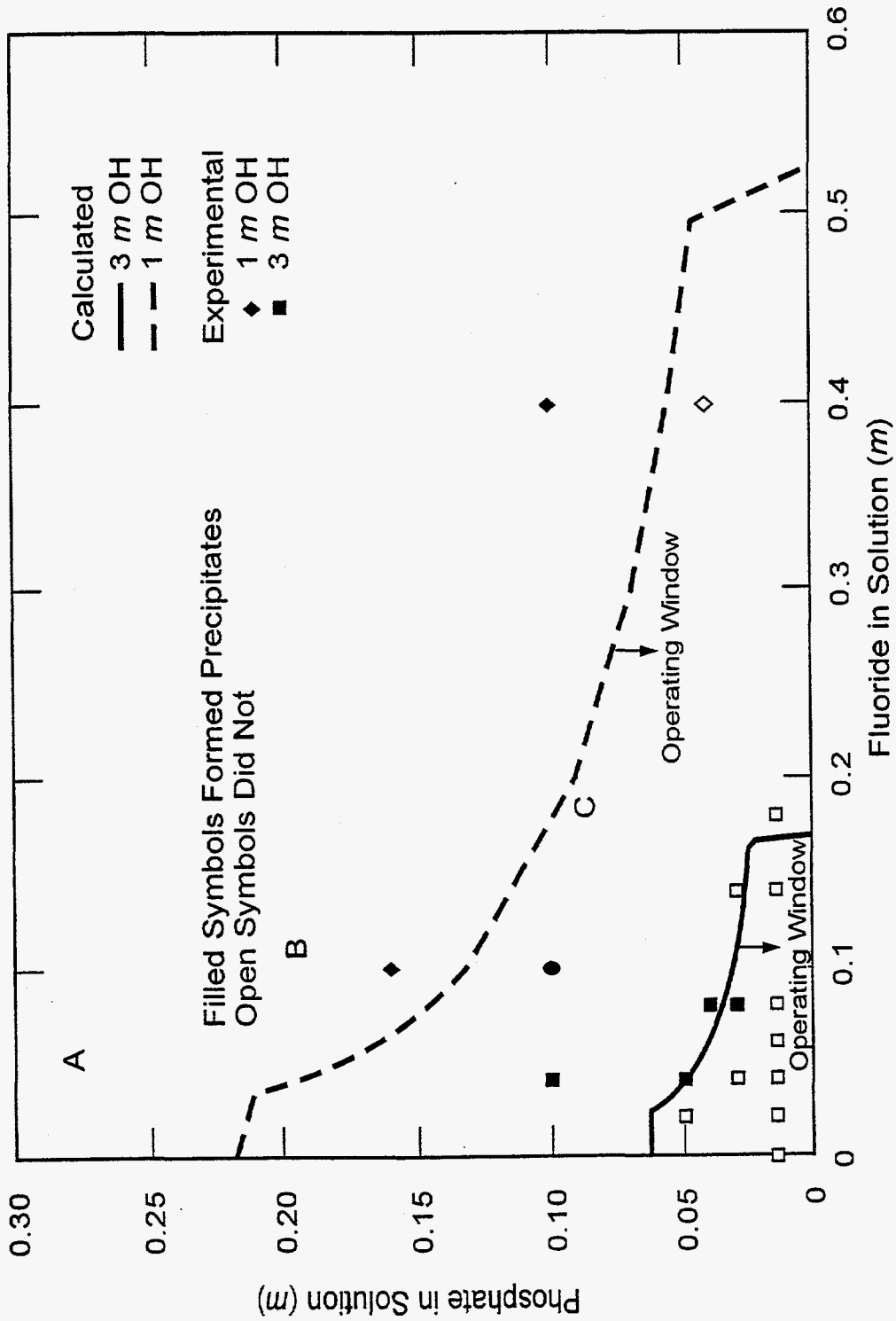
Fig. 10. Operating windows for fluoride-phosphate at 25°C.
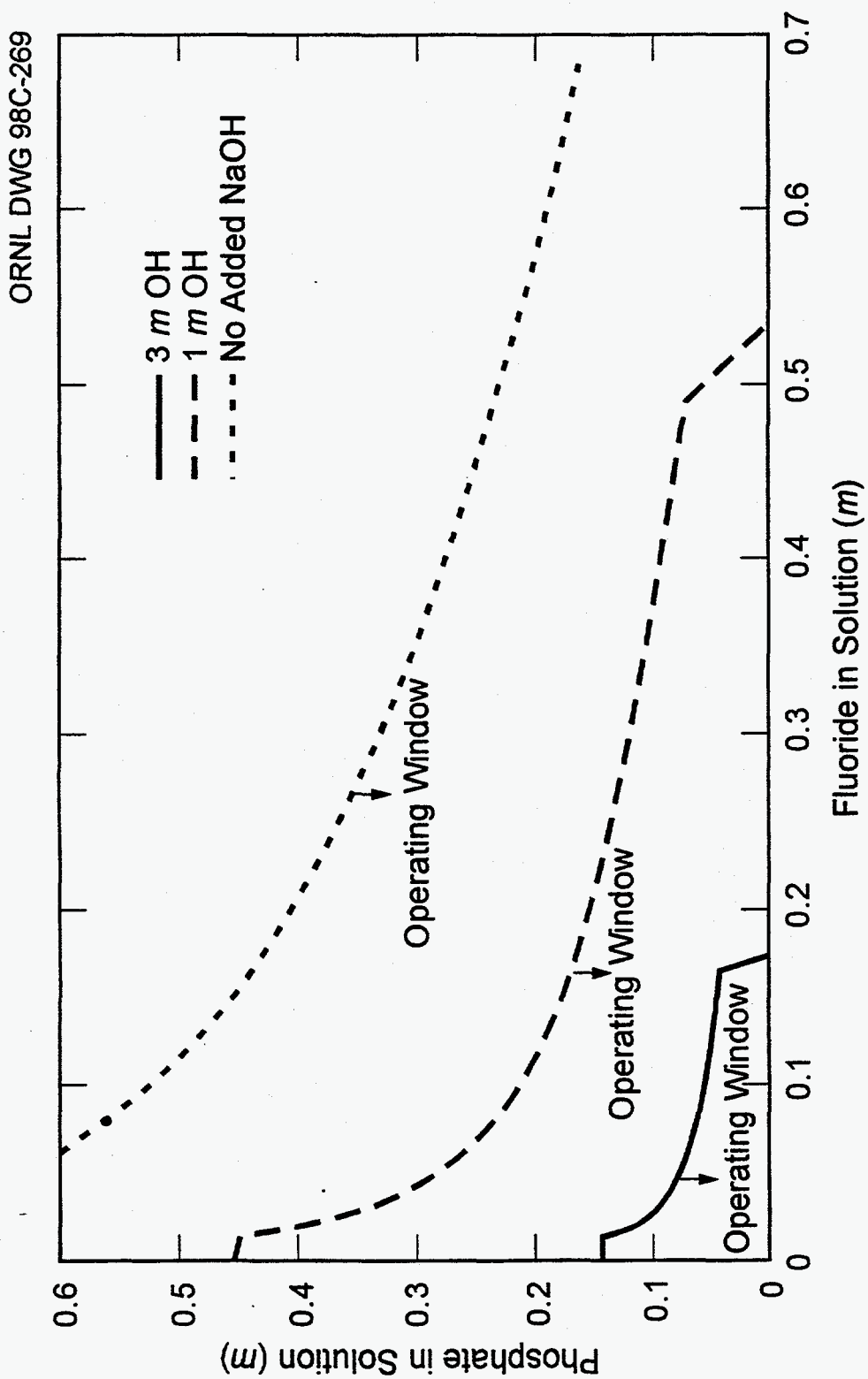
Fig. 11. Calculated operating windows for fluoride-phosphate at 35°C.
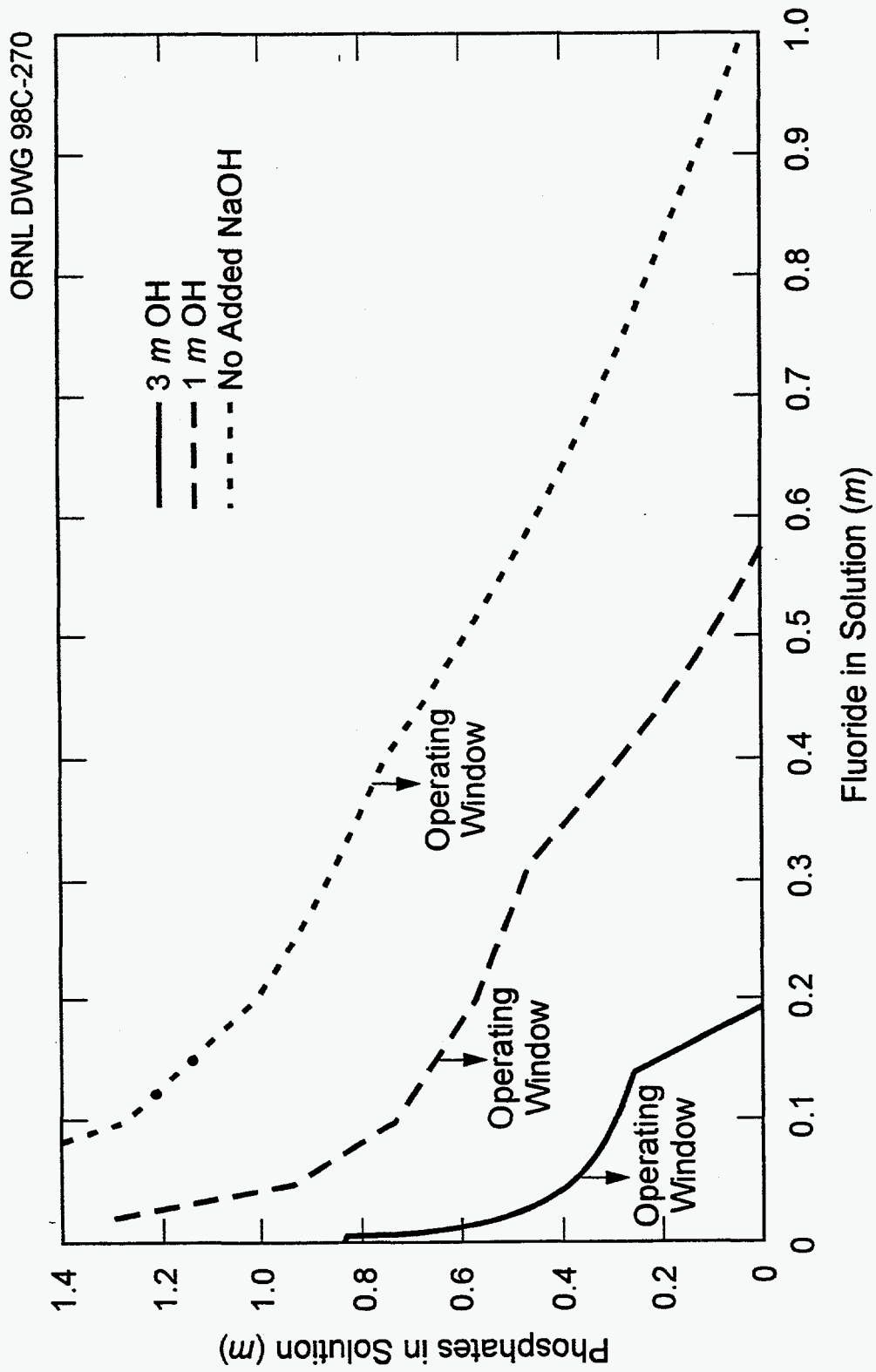
Fig. 12. Calculated operating windows for fluoride-phosphate at 60°C.
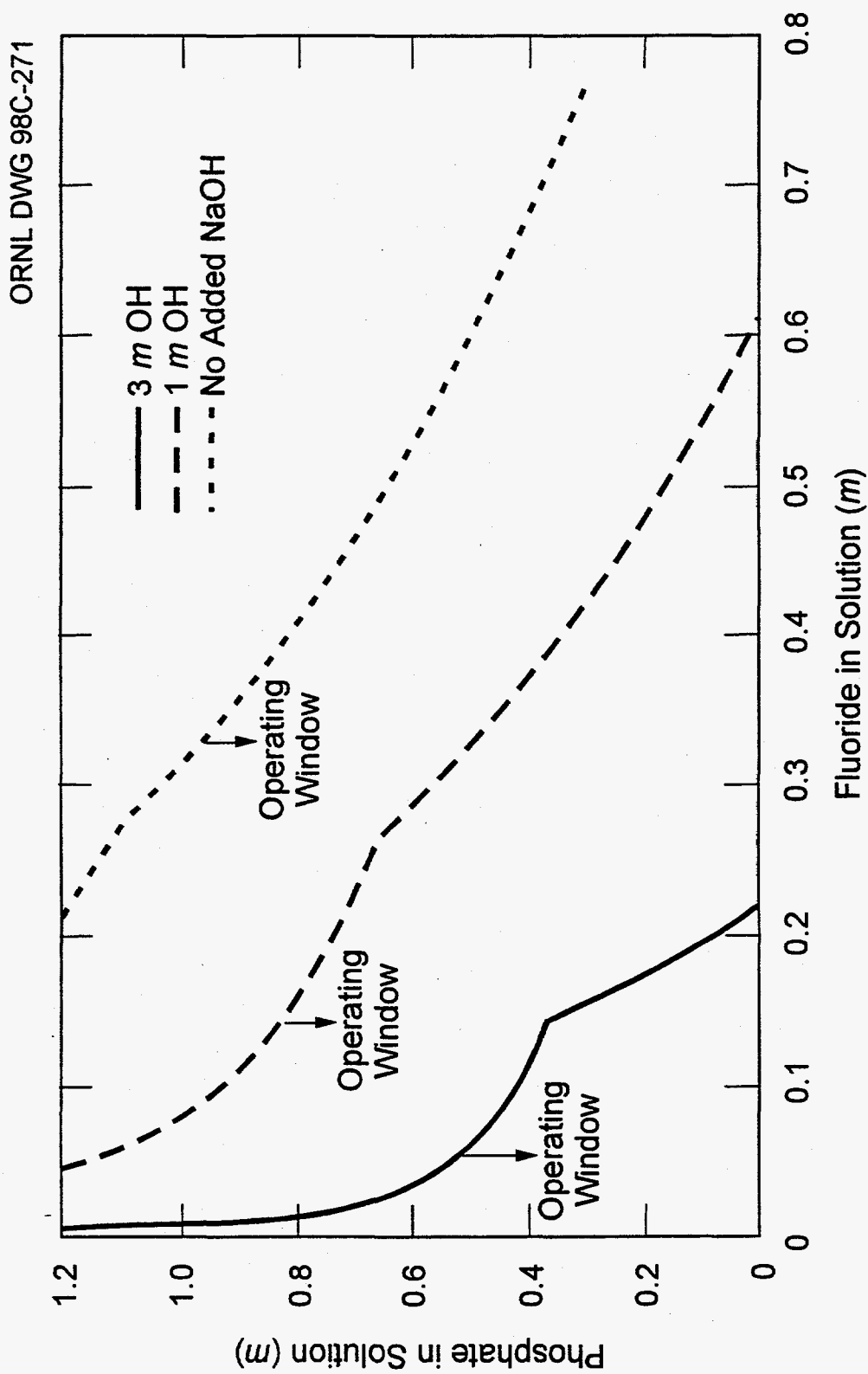
Fig. 13. Calculated operating windows for fluoride-phosphate at 80°C.
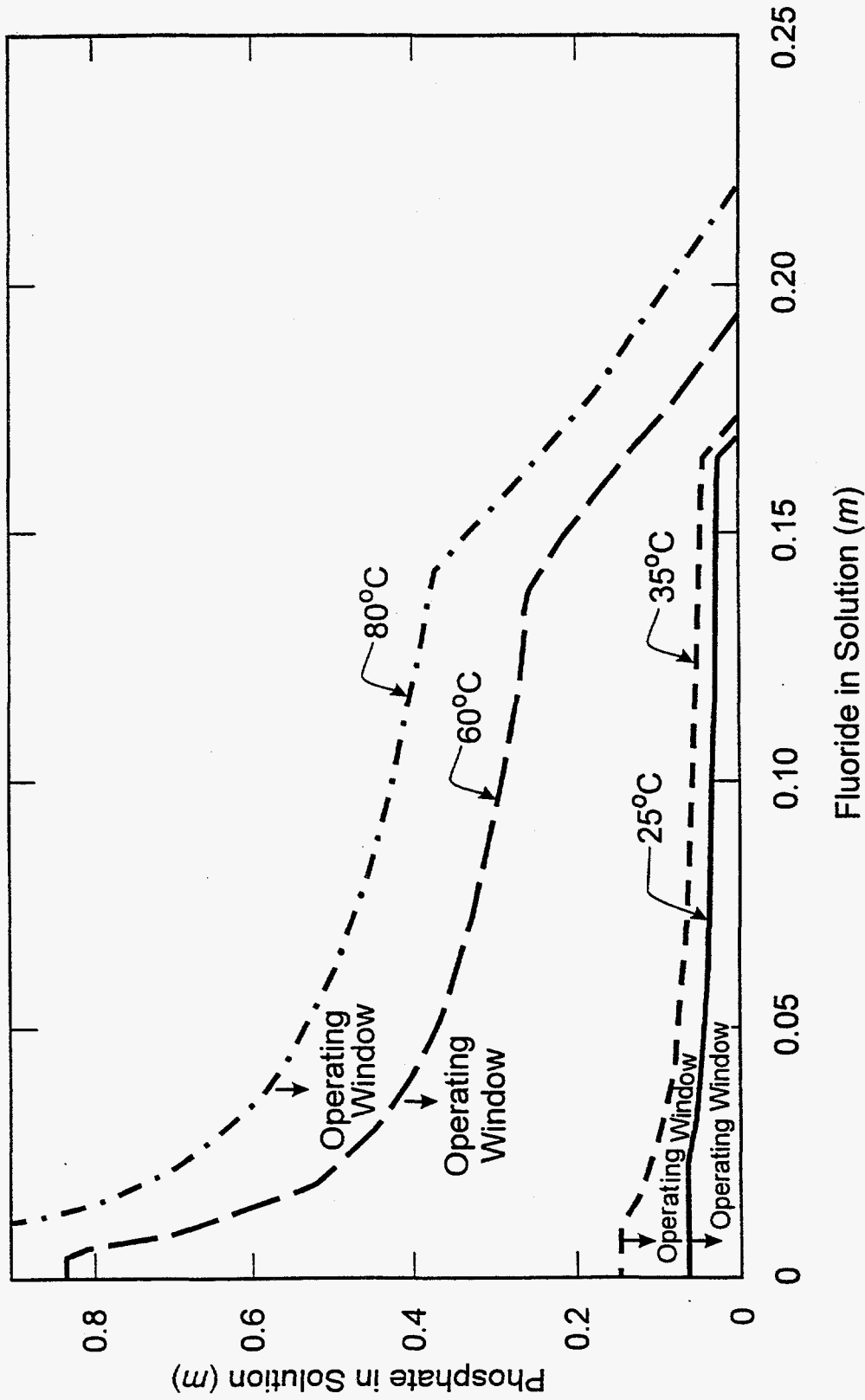
Fig. 14. Temperature dependence of operating windows for process solutions containing phosphate and fluoride in 3 m NaOH.

Table 3. Prediction of precipitation temperature

Sample	Initial concentrations (*m*)			Temperature of precipitation (°C)	
	F⁻	PO_4^{-3}	OH⁻	Data	Model
A	0.10	0.20	3	52–57	53
B	0.05	0.28	3	52–57	54
C	0.20	0.08	3	52–57	$\begin{cases} 80 \text{ (NaF)} \\ 43 \text{ (DS)} \end{cases}$

model predictions are consistent with observations in the first two cases. The third case shows inconsistency, both in the prediction of NaF precipitation and in the prediction of $Na_7(PO_4)F \cdot 19H_2O$ double-salt (DS) formation at a lower temperature. As noted in Ref. 5, the prediction of NaF is uncertain, due to the large scatter in experimental data; hence, the model is not expected to be highly accurate in this regard.

The operating windows decrease markedly as OH⁻ increases in the Na-F-PO₄ system. This is the opposite of the dissolution of alumina, which increases with OH⁻ concentration. The result of this opposition is described in Sect. 3.2.

3.2 THE ALUMINA–SODIUM PHOSPHATE–SODIUM FLUORIDE–SODIUM PHOSPHATE FLUORIDE SYSTEM

Operating windows in this system take into account the possibility of forming solid alumina as gibbsite, $Al(OH)_3$, as well as trisodium phosphate, $Na_3PO_4 \cdot 12H_2O \cdot \frac{1}{4}NaOH$ (designated in Figs. 15–22 as TSP); sodium fluoride, NaF; and sodium phosphate fluoride, $Na_7(PO_4)_2F \cdot 19H_2O$ (designated in Figs. 15–22 as DS). The ternary description of operating windows is based on the concentrations of $Al(OH)_4^-$, PO_4^{-3}, and F⁻ in solutions. Because three components are represented in a two-dimensional plot, the total concentration must be fixed. Thus, the plots depend on the concentrations as $n_{PO4} + n_F + n_{Al} = $ a fixed value, where n_{PO4}, n_F, and n_{Al} represent the molalities of phosphate, fluoride, and aluminate, respectively.

Figure 15 shows a ternary plot with the operating window for the case where $n_{PO4} + n_F + n_{Al} = 0.25 \ m$, the sodium hydroxide is $1.0 \ m$, and the temperature is 25°C. The operating window

Fig. 15. Operating window, $Al(OH)_4^-$, PO_4^{-3}, F^- at 25°C, 1.0 m NaOH, n_{PO4} + n_F + n_{Al} = 0.25 m.

Fig. 16. Operating window, $Al(OH)_4^-$, PO_4^{-3}, F^- at 25°C, 1.0 m NaOH, n_{PO4} + n_F + n_{Al} = 0.30 m.

ORNL DWG 98C-232

25°C
NaOH = 1.0 molal
Constant Inventory.
$n_{PO_4} + n_F + n_{Al} = 0.4$ molal

Fig. 17. Operating window, $Al(OH)_4^-$, PO_4^{-3}, F^- at 25°C, 1.0 m NaOH, $n_{PO4} + n_F + n_{Al} = 0.4$ m.

ORNL DWG 98C-231

25°C
NaOH = 2.0 molal
Constant Inventory:
$n_{PO_4} + n_F + n_{Al} = 0.3$ molal
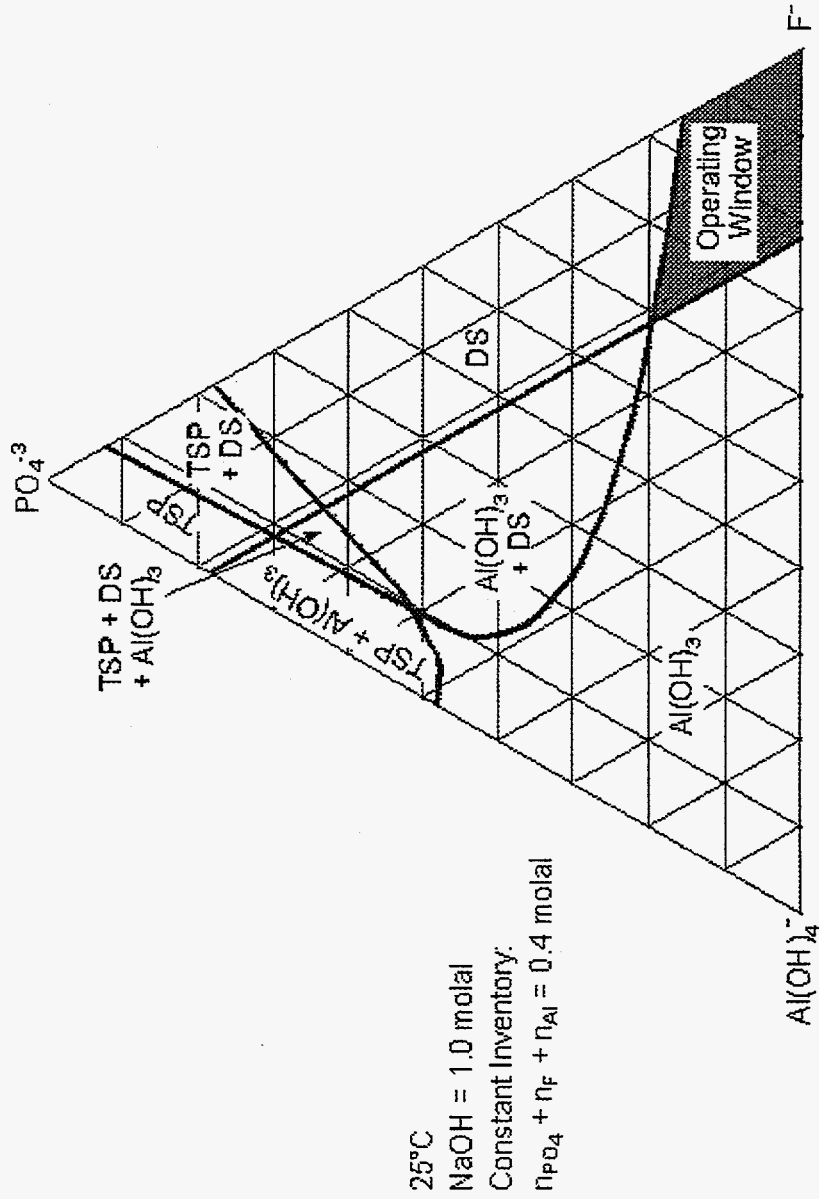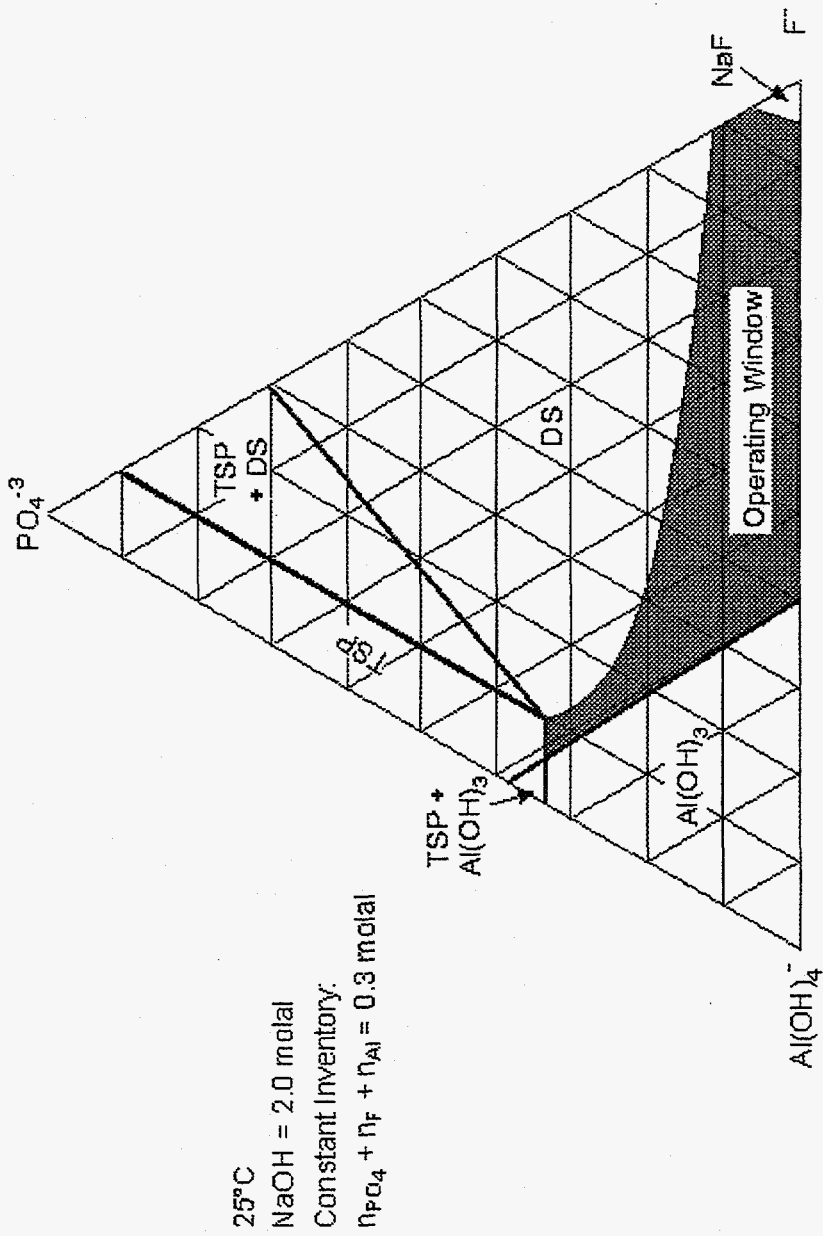
Fig. 18. Operating window, $Al(OH)_4^-$, PO_4^{-3}, F^- at 25°C, 2.0 m NaOH, $n_{PO4} + n_F + n_{Al} = 0.3$ m.

ORNL DWG 98C-230

25°C

NaOH = 3.0 molal

Constant Inventory:

$n_F + n_{Al} + n_{PO_4} = 0.3$ molal

PO_4^{-3}

TSP + DS

TSP

DS

DS + NaF

NaF

F

$Al(OH)_3$

$Al(OH)_4^-$
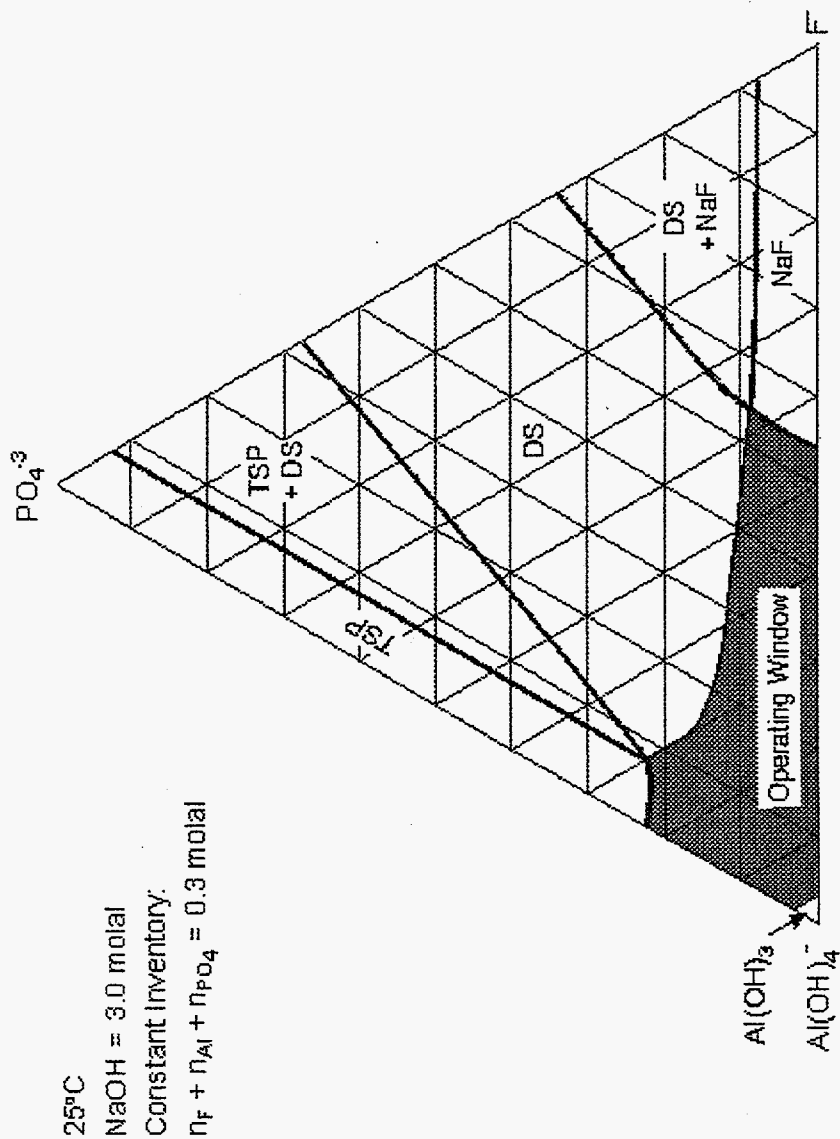
Operating Window

Fig. 19. Operating window, $Al(OH)_4^-$, PO_4^{-3}, F^- at 25°C, 3.0 m NaOH, $n_{PO4} + n_F + n_{Al} = 0.3\ m$.

ORNLDWG 98C-225

35°C
NaOH = 3.0 molal
Constant Inventory.
$n_{PO_4} + n_F + n_{Al} = 0.3$ molal
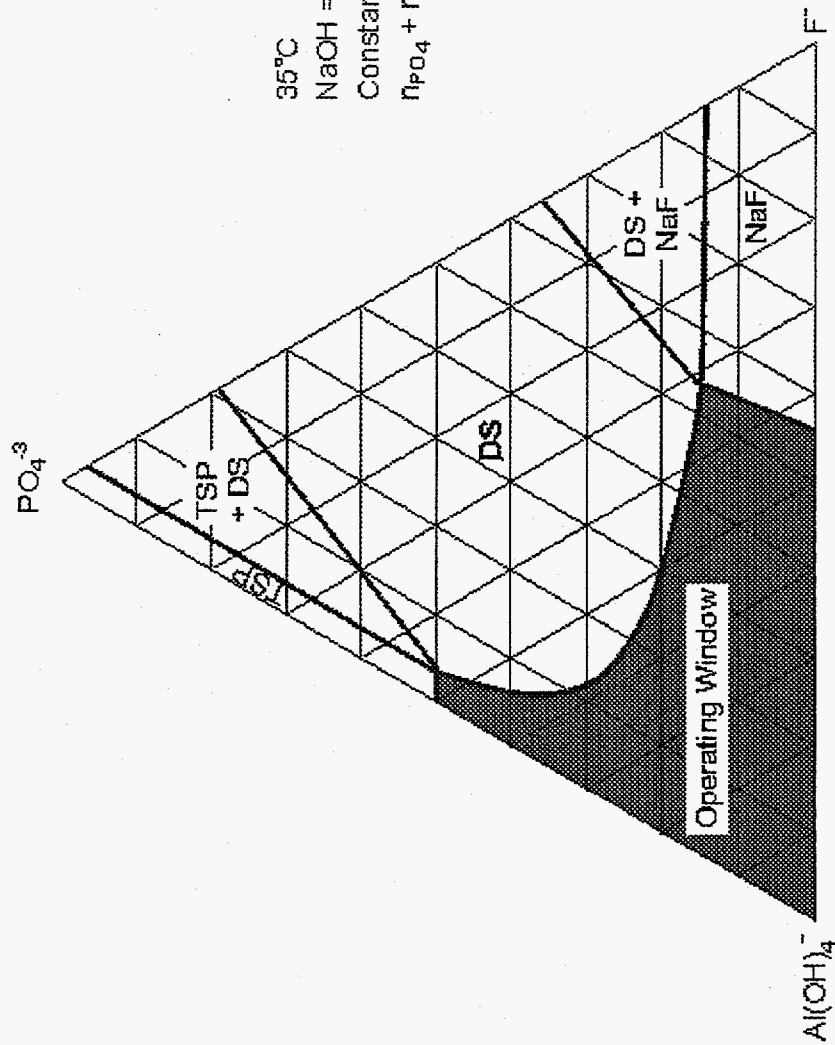
Fig. 20. Operating window, $Al(OH)_4^-$, PO_4^{-3}, F^- at 35°C, 3.0 m NaOH, $n_{PO4} + n_F + n_{Al} = 0.3$ m.

ORNL DWG 98C-234

80°C
NaOH = 2.0 molal
Constant Inventory:
$n_{PO_4} + n_F + n_{Al} = 0.4$ molal

PO_4^{-3}

Operating
Window

$Al(OH)_4^-$

NaF

F^-
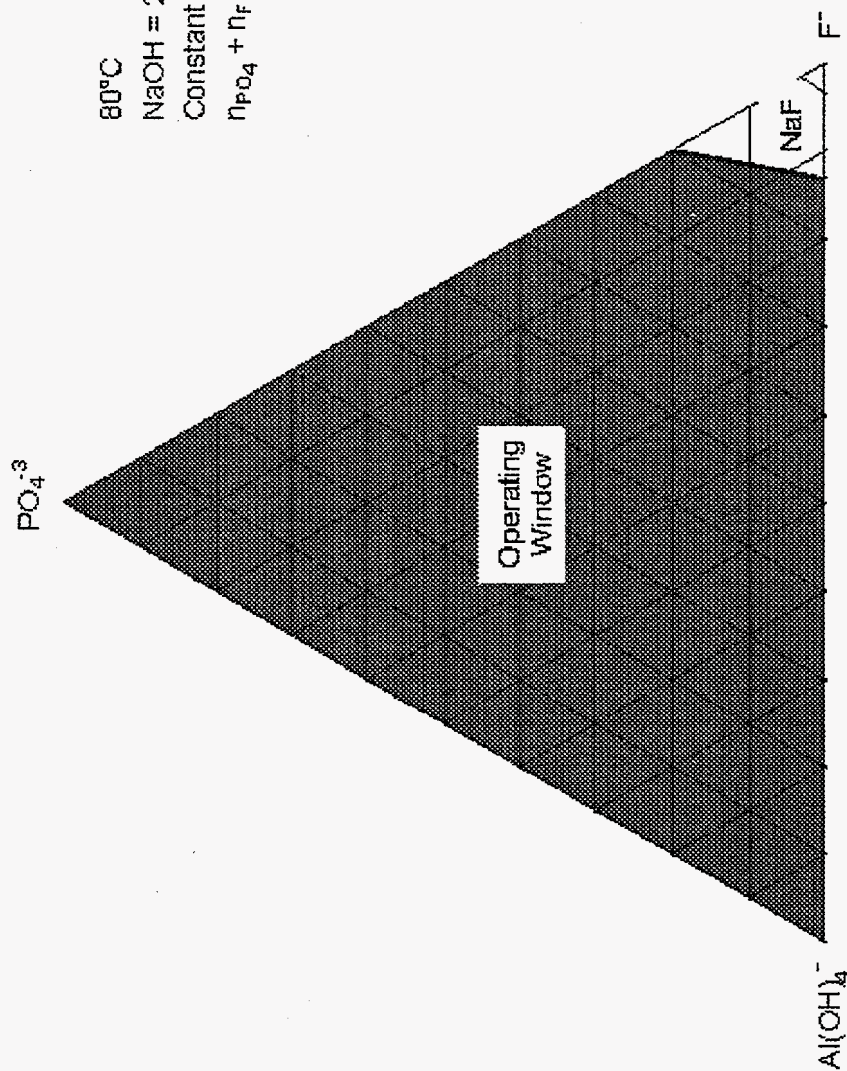
Fig. 21. Operating window, $Al(OH)_4^-$, PO_4^{-3}, F^- at 80°C, 2.0 m NaOH, $n_{PO4} + n_F + n_{Al} = 0.4$ m.

ORNL DWG 96C-236
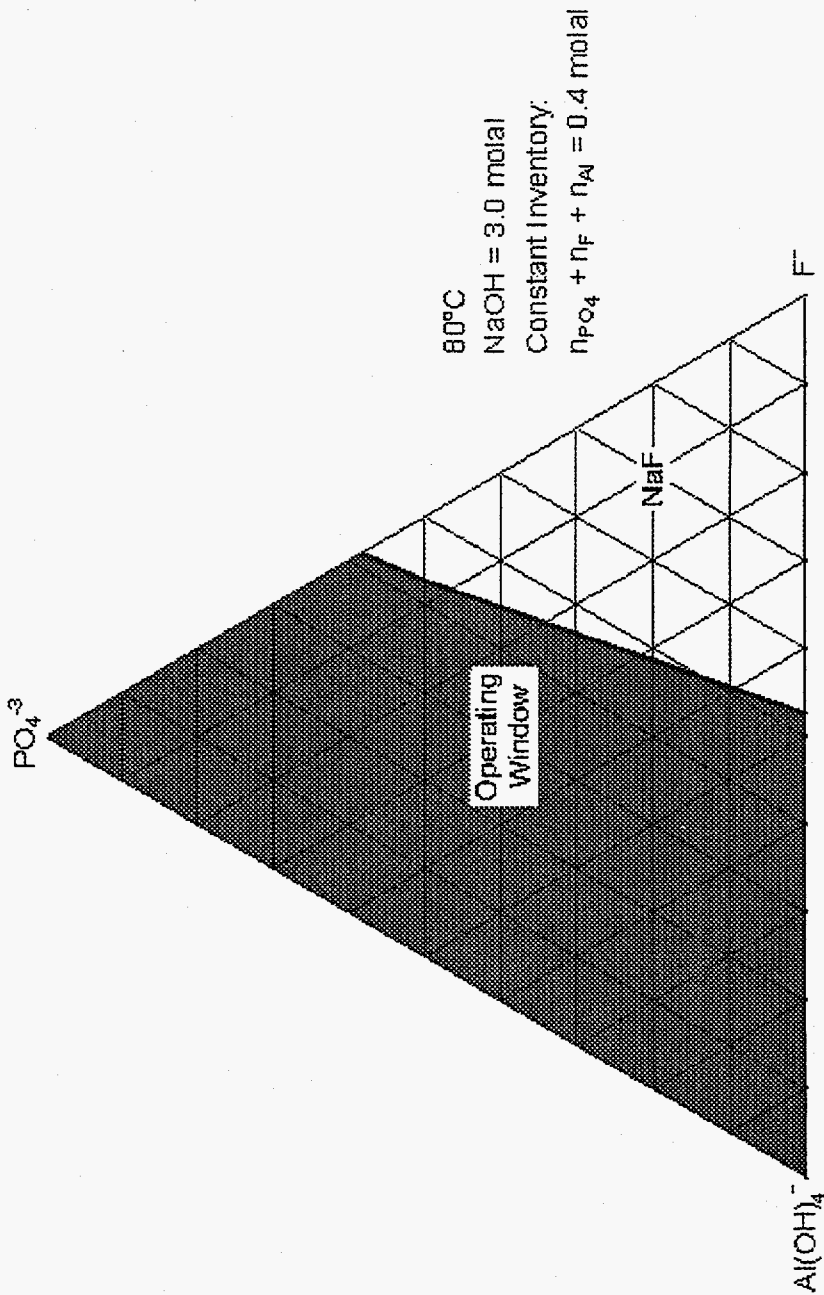
Fig. 22. Operating window, Al(OH)$_4^-$, PO$_4^{-3}$, F$^-$ at 80°C, 3.0 m NaOH, n$_{PO4}$ + n$_F$ + n$_{Al}$ = 0.4 m.

80°C
NaOH = 3.0 molal
Constant Inventory.
n$_{PO4}$ + n$_F$ + n$_{Al}$ = 0.4 molal

PO$_4^{-3}$

Al(OH)$_4^-$

F$^-$

NaF

Operating Window

is a relatively broad area toward the right of the diagram away from the aluminate corner. Figure 16 gives similar conditions, except that the fixed concentration is 0.30 m rather than 0.25 m. In this case the operating window is much narrower than in Fig. 15. This trend is continued in Fig. 17 with a total fixed concentration of phosphate fluoride and aluminate of 0.4 m. In this case the operating window is restricted to a very small area near the fluoride corner.

The effect of increasing sodium hydroxide concentration can also be examined. Figure 18 gives the operating window at 25°C for 2.0 m NaOH with a fixed phosphate fluoride and aluminate concentration of 0.3 m. With the higher caustic concentration, the operating window shifted toward the aluminate corner and moved away from the phosphate corner. This trend continues as shown in Fig. 19 at 3.0 m NaOH and a fixed concentration of 0.3 m. Here the operating window requires very low phosphate concentrations.

Figure 20 shows the effect of temperature. At 35°C the operating window for 3.0 m NaOH and a fixed concentration of 0.3 m is noticeably greater than at 25°C (Fig. 19). At 80°C, as shown in Figs. 21 and 22, the operating window is wide—even with a fixed concentration of 0.4 m, and, in the case of Fig. 21, a NaOH concentration of 2.0 m.

The comparison of the operating windows at elevated temperatures (Figs. 20–22) with those at 25°C (Figs. 15–19) shows what happens on cooldown: solids form as the area of the operating windows decreases. As shown in the figures, the type of solids that form can vary depending on the caustic concentration, with alumina predominant at lower values and phosphate or phosphate fluoride predominant at higher values. The concentrations of phosphate, fluoride, and aluminate must be kept low, ≤0.25 m total, if solid formation is to be avoided in caustic treatment of sludge that contains these components. At total concentrations greater than this, the operating windows are small unless elevated temperatures are maintained throughout all process operations.

3.3 SLUDGE TESTS

Two different types of tests were run on sludge from Hanford underground storage tank T-104 as part of this work. In one type of test, the process solutions at the process temperature were injected into 6 M HNO$_3$ and the solutions used for chemical analysis. This prevents the formation of solids and gives the gross dissolution (i.e., the total amount dissolved without permitting

solid formation). Additional portions of these samples without HNO_3 were used for observations of solid formation. These tests are useful for assessing the potential for solid formation and comparison of observations with calculations, but they do not represent Enhanced Sludge Washing as it could be practiced because the analytical results do not reflect solid formation.

In the other type of tests, the process solutions were allowed to cool to ambient without addition of HNO_3. These tests would give the net dissolution based on the process conditions (i.e., the initial dissolution less the material that may have entered a solid).

3.3.1 Net–Dissolution Tests

Tests were conducted at Oak Ridge on sludge from tank T-104 at ambient temperature, ~60°C, and ~95°C. The samples were washed with inhibited water (0.01 M sodium hydroxide plus 0.01 M sodium nitrite, then leached twice with 3 M sodium hydroxide, and finally washed three times with inhibited water. A detailed description of the tests and analytical results are provided in Appendix C.

Comparable amounts of aluminum were removed at all three temperatures. Most of the aluminum that was dissolved appeared in the first leachate solutions. There was greater removal of phosphate in the room-temperature test than in those at elevated temperatures. Most of the phosphate removed in the room-temperature test appeared in the first two washes after leaching, whereas in the tests at the elevated temperatures, it occurred during the two leaches. Gels were observed upon cooling leachates from the tests at elevated temperatures. The gel was sodium phosphate fluoride. In addition, a gel formed in the first wash after leaching in the room-temperature tests. Observations on the sample solutions are given in Appendix C.

Table 4 lists concentrations (in moles per liter) of key species in the leachates.

Table 5 lists calculated values for key species based on data in Table 4. Because the process solutions were at ambient temperature before samples were taken, the analytical results would reflect saturated concentrations if equilibrium were attained. No phosphate or phosphate fluoride solids appear in the calculated species. These solids form rapidly with cooldown, and since they were observed in the leach solutions at the time that analytical samples were taken, it is not surprising that they do not appear in the calculated results that are based on filtered samples. Gibbsite solids were

Table 4. Molar concentrations in leachates: tests at ambient, 60°C, and 95°C

Sample	Hydroxide	Sodium	Aluminum	Phosphate	Fluoride	Nitrate
1st Leach ambient	1.93	2.18	2.71×10^{-1}	3.09×10^{-2}	1.87×10^{-1}	8.60×10^{-2}
1st Leach 60°C	2.16	2.25	1.91×10^{-1}	3.05×10^{-2}	1.34×10^{-1}	5.68×10^{-2}
1st Leach 95°C	1.92	2.13	2.18×10^{-1}	3.2×10^{-2}	1.77×10^{-1}	8.73×10^{-2}
2nd Leach ambient	2.92	3.01	6.37×10^{-2}	3.02×10^{-2}	3.90×10^{-2}	1.34×10^{-2}
2nd Leach 60°C	3.00	3.06	3.85×10^{-2}	3.54×10^{-2}	2.94×10^{-2}	8.66×10^{-3}
2nd Leach 95°C	3.26	3.35	5.11×10^{-2}	2.80×10^{-2}	3.20×10^{-2}	1.14×10^{-2}

Table 5. Calculated molal concentrations in leachates: tests at ambient, 60°C, and 95°C

Sample	Hydroxide	Sodium	$Al(OH)_4^-$	PO_4^{-3}	HPO_4^{-2}	F^-	Solids
1st Leach ambient	2.01	2.57	1.87×10^{-1}	3.09×10^{-2}	1.58×10^{-5}	1.87×10^{-1}	8.40×10^{-2} mol $Al(OH)_3$
1st Leach 60°C	2.16	2.63	1.91×10^{-1}	3.05×10^{-2}	1.36×10^{-5}	1.34×10^{-1}	None
1st Leach 95°C	1.96	2.50	1.80×10^{-1}	3.20×10^{-2}	1.72×10^{-5}	1.77×10^{-1}	3.76×10^{-2} mol $Al(OH)_3$
2nd Leach ambient	2.93	3.14	6.39×10^{-2}	3.03×10^{-2}	8.16×10^{-6}	3.91×10^{-2}	None
2nd Leach 60°C	3.01	3.19	3.86×10^{-2}	3.55×10^{-2}	9.24×10^{-6}	2.95×10^{-2}	None
2nd Leach 95°C	3.27	3.45	5.13×10^{-2}	2.81×10^{-2}	6.13×10^{-6}	3.21×10^{-2}	None

calculated for the first leach at ambient temperature and at 95°C. Supersaturated solutions of gibbsite are stable for long periods if they are not seeded.[7,8]

3.3.2 Gross–Dissolution Tests

In these tests two samples of T-104 sludge were leached at 75°C. After leaching, one sample was allowed to settle at temperature and the other at room temperature. After settling, the filtered leachates were injected into 6 M HNO$_3$ to prevent solid formation. The sludge residues were then washed three times with inhibited water. One sample was maintained at 75°C throughout the washes, and the other was at room temperature. Details of the tests and analytical chemistry results are provided in Appendix D.

As anticipated, the sample that was settled at ambient temperature had much less phosphate and fluoride in the leachate than the one for which the elevated temperature was maintained. As shown in Figs. 10 and 13, a temperature decrease results in a smaller operating window. It is interesting to note that the concentrations of aluminum in the leachates were comparable.

Table 6 lists concentrations of key species in the process solutions.

Table 7 lists calculated values for key species based on data in Table 6. The analytical samples were stabilized at temperature by injection into 6 M nitric acid, so they should reflect the gross composition. Sodium phosphate fluoride was calculated in the leachate for the sample T$_1$R as observed. However, solids that were seen in the leachate from sample T$_0$R did not appear in the calculation. This could be due to a combination of calculational and analytical error. It should be noted that any calculation that is based on analytical data requires some adjustment in concentrations to achieve an anion-cation balance. The best approach is to adjust concentrations in major species such as sodium, nitrate, or hydroxide. However, it is always a matter of judgment how to compensate for the fact that analytical data as received never have a balance of charge. In one sense, the calculated values are better than analytical results in that charge balance is ensured.

4. CONTROL OF SOLIDS WITH LIME

Unwanted formation of solids can be controlled by process temperatures, by excess caustic, or by the use of additives that control when solid formation occurs or the chemical and physical form of the solids. The combination of temperature control and excess caustic in controlling alumina reprecipitation was outlined in Ref. 1. Lime, CaO or Ca(OH)$_2$, can react with phosphate to produce

Table 6. Molar concentrations in leachates and wash solutions: leaching at 75°C

	Hydroxide	Sodium	Aluminum	Phosphate		Fluoride
				P	PO_4	
T_0R						
Leach	2.19	3.67	0.14	0.022	0.015	0.11
1st Wash	0.51	1.21	0.03	0.14	0.13	0.086
2nd Wash	0.1	0.23	0.004	0.027	0.020	0.030
3rd Wash	0.02	0.068	0.001	0.0061	0.0041	0.019
T_1R						
Leach	2.10	3.78	0.099	0.18	0.13	0.15
1st Wash	0.31	0.67	0.017	0.030	0.023	0.039
2nd Wash	0.06	0.11	0.003	0.0048	0.0034	0.020
3rd Wash	0.02	0.035	0.001	0.001	0.0009	< Value

Table 7. Calculated molal concentrations in leachates and wash solutions: leaching at 75°C

	Hydroxide	Sodium	$Al(OH)_4^-$	PO_4^{-3}	HPO_4^{-2}	F^-	Solids
T_0R							
Leach	2.19	3.67	1.40×10^{-1}	2.00×10^{-2}	7.85×10^{-6}	1.10×10^{-1}	None
1st Wash	5.11×10^{-1}	1.21	3.00×10^{-2}	1.39×10^{-1}	6.46×10^{-4}	8.60×10^{-2}	None
2nd Wash	1.01×10^{-1}	2.30×10^{-1}	4.00×10^{-3}	2.38×10^{-2}	1.20×10^{-3}	3.00×10^{-2}	None
3rd Wash	2.14×10^{-2}	6.82×10^{-2}	1.00×10^{-3}	3.64×10^{-3}	1.38×10^{-3}	1.91×10^{-2}	None
T_1R							
Leach	2.14	3.48	1.01×10^{-1}	4.65×10^{-2}	2.00×10^{-5}	9.96×10^{-2}	5.22×10^{-2} mol $Na_7(PO_4)_2$ $F \cdot 19H_2O$
1st Wash	3.10×10^{-1}	6.70×10^{-1}	1.70×10^{-2}	2.48×10^{-2}	2.18×10^{-4}	3.90×10^{-2}	None
2nd Wash	6.05×10^{-2}	1.10×10^{-1}	3.01×10^{-3}	3.62×10^{-3}	3.90×10^{-4}	2.00×10^{-2}	None
3rd Wash	2.04×10^{-2}	3.51×10^{-2}	1.00×10^{-3}	6.72×10^{-4}	3.31×10^{-4}	1.00×10^{-9}	None

a calcium phosphate and can react with fluoride to produce calcium fluoride. This is a potential way to reduce the concentration of phosphate and fluoride in solution and thereby aid in preventing the formation of sodium phosphate and sodium phosphate fluoride. The lime-phosphate reaction can

produce $Ca_3(PO_4)_2$ or $Ca_5(PO_4)_3OH$ (hydroxyapatite). The lime-fluoride reaction would result in the formation of CaF_2 or $Ca_5(PO_4)_3OH_xF_{(1-x)}$. In the latter compound, the fluoride substitutes for some of the hydroxide in the hydroxyapatite. This is the reaction that occurs in tooth enamel that is treated with fluoride toothpaste or rinses. Success with lime treatment of sludge leachates and wash solutions will depend on the outcome of the competition between sodium and calcium ions to form either sodium phosphate/sodium phosphate fluoride or a calcium phosphate/calcium fluoride. This competition will be influenced by the concentration (actually thermochemical activity) of sodium ions in the solutions. High sodium-ion concentrations (activity) would tend to drive the reactions to the formation of sodium phosphate/sodium phosphate fluoride.

Lime may also react with aluminate to form a hydrogarnet. A continuous solid solution series occurs in the $3CaO \cdot Al_2O_3 \cdot 6H_2O - 3CaO \cdot Al_2O_3 \cdot 3SiO_2$ system.[9] Because of this, any use of lime in pretreatment would have to be done after inhibited water washes or caustic leaching and solid/liquid separation. If it were done before this, caustic leaching would be ineffective in reducing the amount of aluminum in sludge solids.

Two samples of Hanford T-104 sludge were treated simultaneously to evaluate the effectiveness of lime $[Ca(OH)_2]$ in preventing formation of sodium phosphate fluoride. Both samples were leached at 75°C for 24 h with 3.9 g of 3.8 M NaOH solution per gram of sludge. After leaching and settling, the samples were filtered at 75°C through 0.45-μm syringe filters. At this point in the test sequence, one of the filtered leachates was treated with 0.2 g $Ca(OH)_2$ per gram of initial sludge. This would be enough lime to convert all of the phosphate to hydroxyapatite, all of the fluoride to calcium fluoride, and all of the alumina to a hydrogarnet. The other leachate had no lime. Both samples were mixed for ~30 min and allowed to cool to ambient. The sludge residues after leaching were washed at 75°C three times for ~30 min. After each wash the solutions were filtered at 75°C, and 0.05 g $Ca(OH)_2$ per gram of initial sludge was added to one of the two wash solutions.

The leachates and wash solutions were examined periodically for several weeks. Sticky solids formed in both the $Ca(OH)_2$-treated and the untreated leachates within an hour after they were removed from heat and allowed to approach ambient temperature. No solids formed in any of the treated or untreated wash solutions. The leachates were examined periodically for several weeks, and the sticky solids persisted. However, when the leachates were examined 6 months later, the sample lime-treated no longer had the sticky solids, but the one without lime retained a mass of gel-like

material. This indicates that the initial gel formation in the limed leachate was due to the rapid formation of sodium phosphate fluoride, which over time was converted to calcium phosphate/calcium fluoride.

In these tests the cooldown to ambient was on the order of an hour. In-tank pretreatment would have much slower cooling. Two sets of samples were prepared to test solid control with lime at slower cooling rates. The sample compositions are listed in Table 8.

Table 8. Sample compositions for lime tests

Sample	Molality of sodium phosphate	Molality of sodium fluoride	Molality of sodium hydroxide	Molality of $Ca(OH)_2$
A	0.28	0.05	3.0	0.0
A′	0.28	0.05	3.0	0.54
B	0.20	0.10	3.0	0.0
B′	0.20	0.10	3.0	0.42
C	0.08	0.20	3.0	0.0
C′	0.08	0.20	3.0	0.26
D′	0.20	0.0	3.0	0.37

Examination of Fig. 10 shows that a solid should form in samples A, B, and C at 25°C.

The samples were heated at ~95°C for 4 days. No solids were seen in samples A, B, or C.

Solid lime was present in samples A′, B′, and C′. The temperature was lowered to 52°C over a period of 25 h. No solids were seen in samples A, B, or C during this cooldown, but material resembling egg whites floating in solution was seen after 5 h at 52°C in these three samples. The temperature was further decreased to 25°C over a 26-h period. In samples A, B, and C, the container walls became coated. The samples then were allowed to reach an ambient temperature of 20–25°C. When sample A was inverted after 2 weeks at ambient temperature, it formed a solid mass with no visible liquid.

In samples A′, B′, and C′, no floating material or coating of container walls occurred. However, sample D′, which also contained lime, formed a coating on the container wall at a temperature of ~50°C.

In Phase Ib pretreatment envelope D, wash solutions and leaches will be sent to a wash receiving tank as discussed in Sect. 2.3. The material in this tank will not be treated in Phase I. If lime treatment is used, it will most likely take place in the wash receiving tank. However, prevention of the formation of sodium phosphate or sodium phosphate fluoride formation would require a large amount of lime. The lime listed in Table 8 is based on the amount required to convert the phosphate to hydroxyapatite and the fluoride to calcium fluoride, plus 10% excess to maintain a calcium-ion concentration in solution. In addition, the coprecipitation of other species such as cesium or pertechnetate would have to be evaluated before implementing precipitation of phosphate and fluoride with lime.

5. RATE LIMITATIONS

When a metal oxide or hydroxide is contacted with an aqueous sodium hydroxide solution, dissolution can occur via formation of hydroxo complexes. In the case of alumina and silica, the reactions shown in Eqs. (2) and (3) are anticipated:

$$Al_2O_3 + 2OH^- + 2Na^+ + 3H_2O = 2Al(OH)_4^- + 2Na^+ ; \qquad (2)$$

$$SiO_2 + OH^- + Na^+ + H_2O = SiO(OH)_3^- + Na^+ . \qquad (3)$$
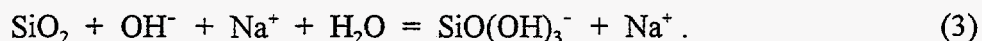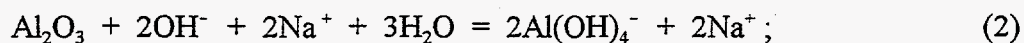
In the Al_2O_3-SiO_2-NaOH-H_2O system, the amount of residual solids and the solution composition at any given time will be determined by a number of factors, for example, (1) the mass of starting solids; (2) the volume and NaOH concentration of the initial aqueous solution; (3) the reaction temperature; (4) the relative rates of dissolution of the two starting solids; (5) the rate of formation of secondary solids (e.g., aluminosilicates, sodium silicates, sodium aluminates); and (6) the rate of formation of soluble aluminosilicate complexes.

Caustic leaching of sludge solids may be viewed as a low-temperature version of the commercial Bayer process used in extracting aluminum from bauxite. Literature on the Bayer process therefore constitutes a useful source of background information pertinent to several issues raised above. The alumina content of the feed bauxite material is typically 30–60%, and the reactive silica content is in the range 0.5–13%; other major components include iron oxides (e.g., ~20%) and titania

(e.g., 2.5%).[9] Depending on the mineralogy of the contained alumina, bauxite leaching is conducted at temperatures ranging from 377 to 525 K.[10] During the leaching process, the contained silica ("reactive" silica, typically kaolinite, $Al_2O_3 \cdot 2SiO_2 \cdot 2H_2O$) also dissolves but reprecipitates with some of the dissolved aluminum to form sodium aluminosilicates. Breuer et al.[11] investigated the effects of temperature and solution composition on the solubility of silica in Bayer liquors (caustic aluminate solutions). They reported that at 70°C, Linde zeolite A first formed and that this material subsequently transformed to the much-less-soluble basic sodalites. At higher temperatures only sodalite formed. Solubility was found to increase with temperature. It was observed, further, that the presence of anions enhanced silicate removal in the order sulfate > carbonate, phosphate, thiosulfate, nitrate > thiocyanate, sulfide, oxalate, tartrate, and citrate. According to Hudson,[10] the sodium-aluminum-silicate product must be viewed as a zeolitic material of variable composition; a wide range of sodium salts (e.g., those of CO_3^{-2}, SO_4^{-2}, Cl^-, OH^-, AlO_2^-) can be incorporated into the resulting zeolites. Cancrinite [$3(Na_2O) \cdot Al_2O_3 \cdot 3SiO_2) \cdot 2CaCO_3$] has been identified in some systems.[10]

5.1 EXPERIMENTAL TESTS OF ALUMINA DISSOLUTION RATES

A series of tests were run to evaluate how the silica-alumina interaction influences the dissolution of alumina. These tests were carried out at Penn State as part of the support of the Efficient Separations Program to the Tanks Focus Area. The experimental methodology is described in Appendix E.

5.1.1 Effect of Stirring Rate

Figure 23 shows the effects of stirring rate on alumina dissolution at 50°C. The data indicate that in the 1000- to 1900-rpm range there is no significant increase or change in the rate of dissolution. This suggests that, under the specified conditions, mass transfer in the aqueous solution is not rate determining and that the dissolution is likely limited by chemical reaction at the solid/solution interface.

37

ORNL DWG 98C-289
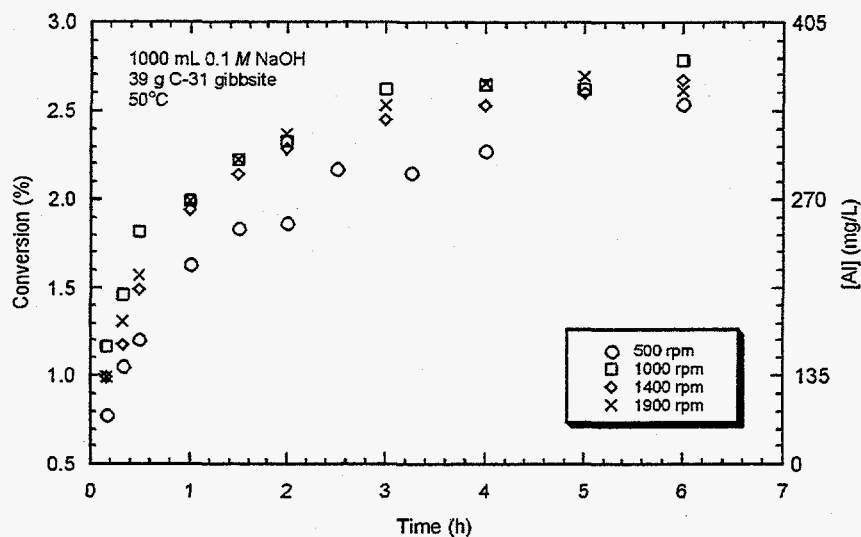
Fig. 23. Effect of stirring rate on the rate of dissolution of 39 g C-31 gibbsite in 1000 mL of 0.1 *M* NaOH at 50°C. The rate becomes independent of stirring speed at speeds greater than 1000 rpm.

An agitation rate of 1400 rpm was selected as a standard condition for the experiments described below because it provided an adequate suspension of the solids and fell within the 1000- to 1900-rpm range of Fig. 23.

5.1.2 Effect of Temperature

Figure 24 shows curves of gibbsite conversion percentage vs time at temperatures from 35–90°C. Fractional conversion (X) was calculated based on the equation:

$$X = C_A/C_{AO} \tag{4}$$

where C_A is the concentration in milligrams per liter of aluminum from the analyzed solutions and C_{AO} is the total aluminum concentration in the system (13,500 mg/L, based on 3.9 wt % C-31 gibbsite being dissolved). All curves appear to plateau beyond the first hour of the experiment, suggesting that the system may have reached equilibrium. This observation is consistent with solubility data

ORNL DWG 98C-290
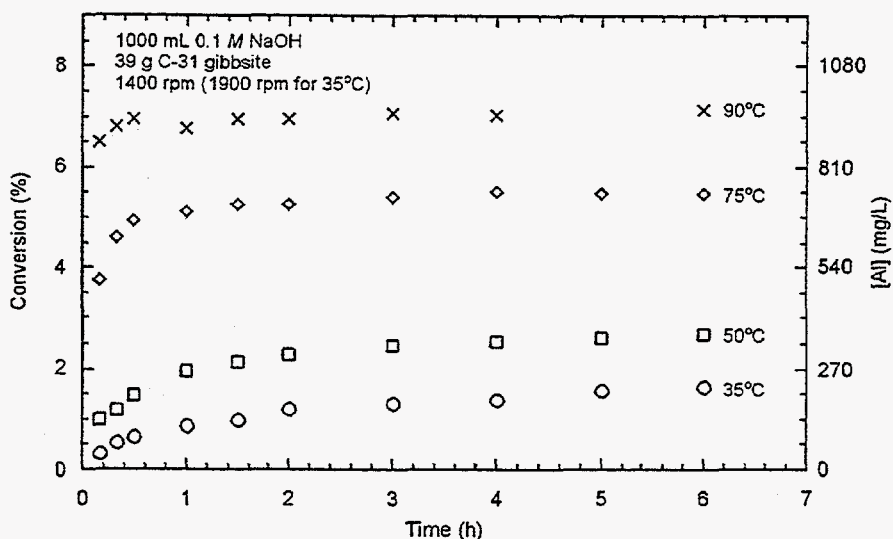
Fig. 24. Effect of temperature on the rate of gibbsite dissolution in 0.1 _M_ NaOH. The system appears to equilibrate after 2 h for the lower temperatures and after 1 h for the higher temperatures. The total aluminum concentration in the system is 13,500 mg/L, based on 3.9 wt % gibbsite being dissolved.

reported by Wesolowski[12] for gibbsite in NaOH solutions, which indicate the solubility of gibbsite to be approximately 141 ppm at 50°C, a concentration that is reached by the first hour in the 50°C experiment.

Data points before equilibrium was reached were used to extract rate constants, k, as well as to estimate the activation energy for gibbsite dissolution under these experimental conditions. The values for k at different temperatures were determined by fitting the experimental data to a second polynomial regression equation:

$$C_A = a + bt + ct^2 \tag{5}$$

where the regression coefficient b corresponds to the initial rate represented by the derivative of the concentration with respect to time, $d\,C_A/dt\,_{(t=0)}$, which also corresponds to the apparent rate constant k. Scotford and Glastonbury[13] reported the activation energy for gibbsite dissolution to be 30.6 kcal/(g·mol) for their 25–100°C experiments. Our experimental data yield an apparent

activation energy of 64 kJ/mol (Fig. 25), which compares favorably with the 76–83 kJ/mol at 20–65°C reported by Packter and Dhillon.[14]

Slope = $-E_a/R$ = -7745.4
E_a = 64.4 kJ/mol
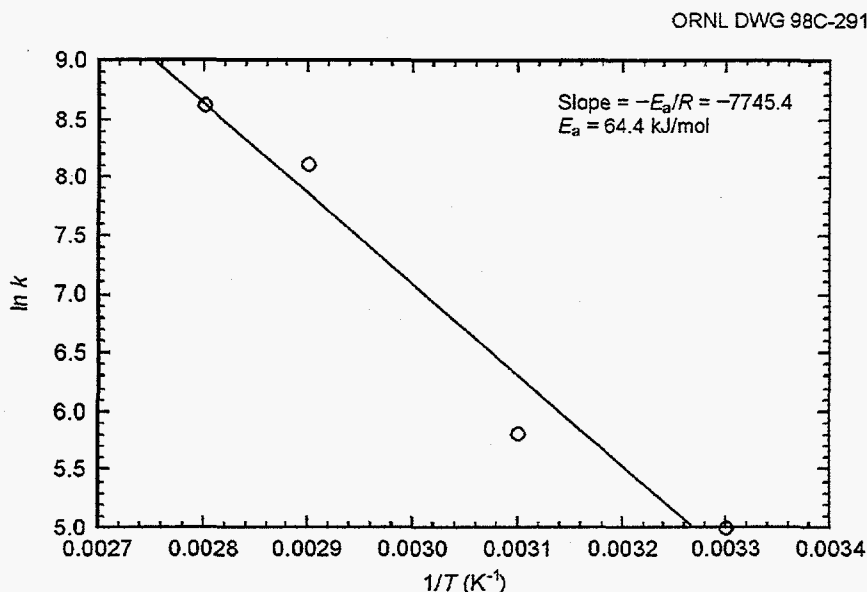
Fig. 25. Arrhenius plot for gibbsite dissolution in 0.1 M NaOH. The rate constants were determined from a second polynomial regression equation.

5.1.3 Effect of Added Silicate

Dissolved silicate (0.1–0.001 M) was added to determine what effect it would have on the overall dissolution behavior of gibbsite. Since the sludge solid material is multi-mineralogic, it is possible that for a given leach solution, the different mineral phases will dissolve, leading to the interaction of the dissolved species and possibly the formation of new solid phases and/or new soluble complexes. The dissolved species could also possibly chemisorb on solid surfaces in the sludge, which could complicate the dissolution.

Figure 26 represents the data that were obtained at different silicate concentrations for 0.1 M NaOH at 35°C. These results show clearly that the presence of silicate inhibits the dissolution of gibbsite at high pH. When the temperature is increased to 50°C (Fig. 27), the same dissolution trend is observed while an approximately twofold increase is seen in the dissolution rate of gibbsite.

ORNL DWG 98C-292
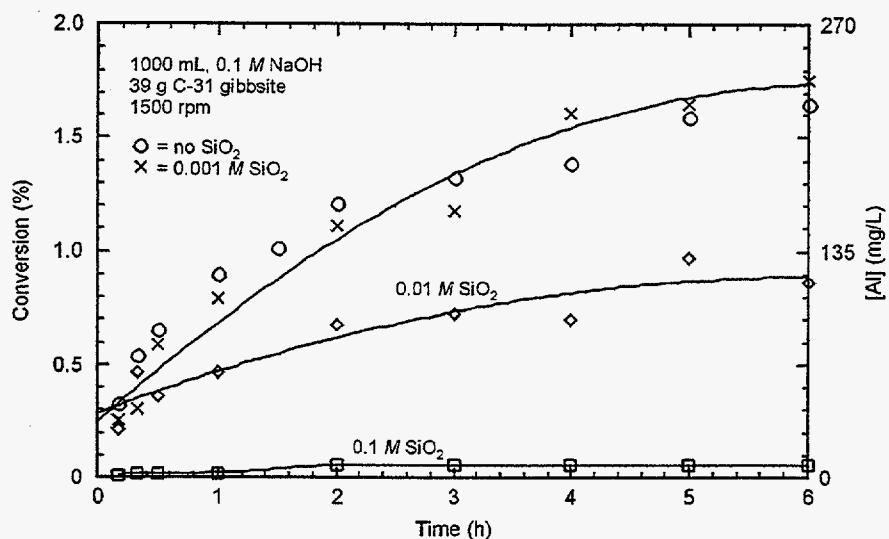
Fig. 26. Effect of silicate addition on the dissolution of gibbsite in 0.1 *M* NaOH at 35°C.

ORNL DWG 98C-293
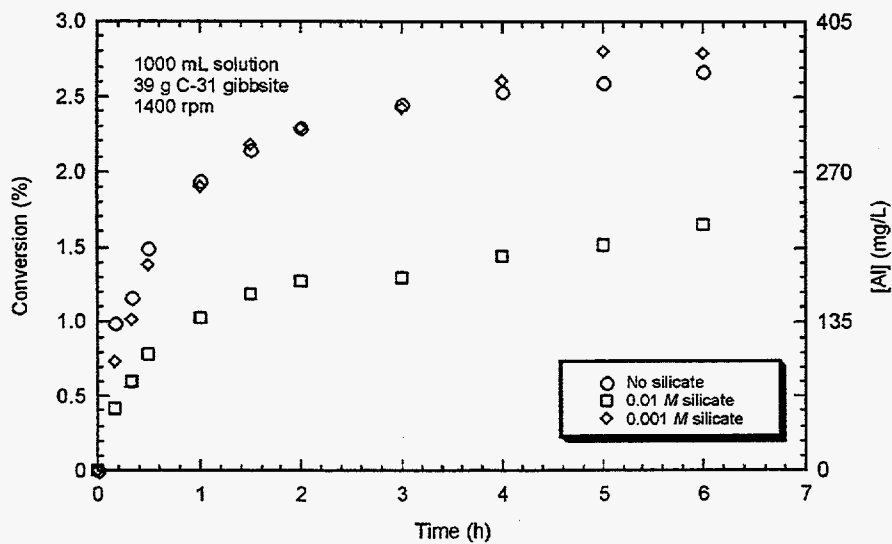
Fig. 27. Gibbsite dissolution in 0.1 *M* NaOH at 50°C.

In contrast, if the NaOH concentration is increased to 1 M and the temperature is kept at 35°C, a fourfold increase in the dissolution rate is observed (Fig. 28). Thus we can infer that a change in NaOH concentration has more of an effect on the dissolution rate than a change in temperature under these conditions. The higher the concentration of the silicate solution added, the less gibbsite dissolves. This may be attributed to surface blocking by silicate anions or to the formation of insoluble sodium aluminosilicates (SAS).
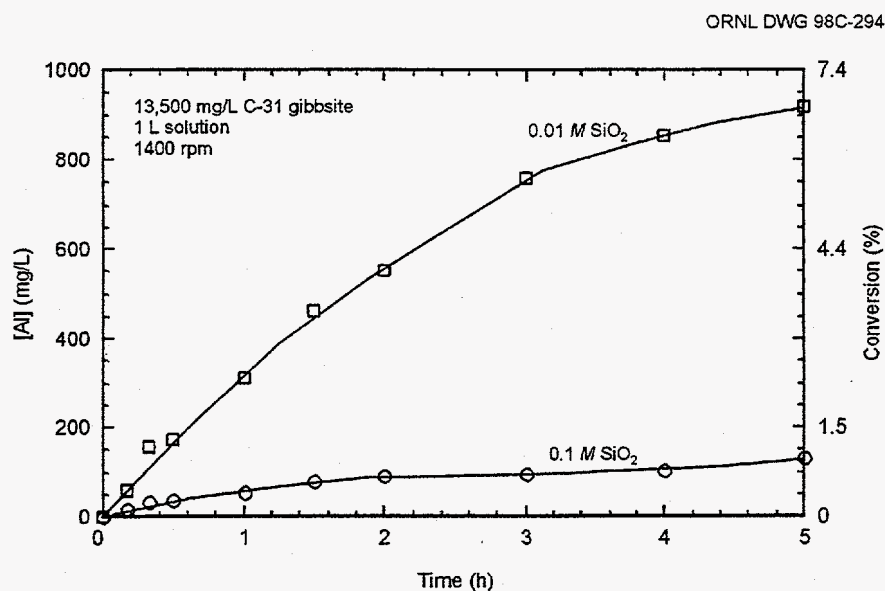
Fig. 28. Gibbsite dissolution in 1 M NaOH at 35°C.

5.2 DISSOLUTION MODEL

The plateaus in Fig. 24 suggest that with 0.1 M NaOH, dissolution reaches a steady state in 2–3 h for the temperature range of 35–90°C. A possible origin of the plateau is the exhaustion of the dissolution reagent (i.e., OH⁻ ions). However, given the relatively low conversion (<8 %), the OH⁻ concentration remains practically unchanged. It is therefore considered that the plateau is associated with the approach to the solubility limit of gibbsite at 0.1 M NaOH; that is, the reverse reaction, precipitation of $Al(OH)_3(s)$, is important under the experimental conditions.

The precipitation of $Al(OH)_3(s)$ from sodium aluminate solutions may be expressed as

$$Al(OH)_4^-(aq) + H^+(aq) \rightleftharpoons Al(OH)_3(s) + H_2O . \tag{6}$$
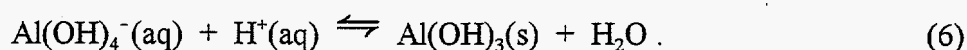
The rate law has been reported by Stratten et al.[15] as:

$$-dC_A/dt = kC_H^2 C_A^2 \tag{7}$$

where C_A and C_H represent the aluminate and proton concentrations, respectively. This rate law has been rationalized in terms of the following mechanism:

$$2\, Al(OH)_4^- \rightleftharpoons Al_2(OH)_7^- + OH^- \quad \text{(fast; equilibrium)} \tag{8}$$

$$Al_2(OH)_7^- + H^+ \longrightarrow 2Al(OH)_3(s) + H_2O \quad \text{(slow)} . \tag{9}$$
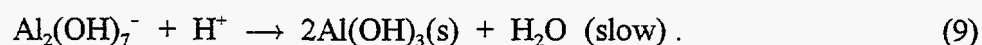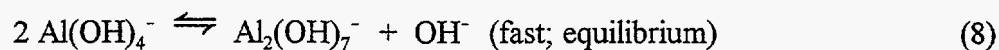
Consider the dissolution of $Al(OH)_3$:

$$Al(OH)_3(s) + OH^-(aq) \underset{k_2}{\overset{k_1}{\rightleftharpoons}} Al(OH)_4^-(aq) . \tag{10}$$
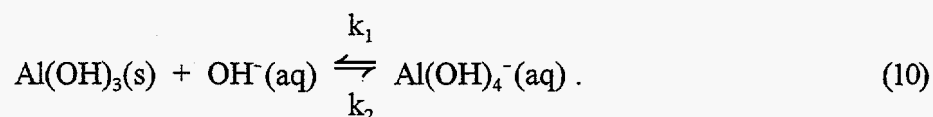
If the above precipitation rate law [Eq. (7)] is adopted for the experimental conditions of Fig. 24, then we can write the following dissolution rate expression:

$$d\, C_A/dt = k_1\, C_{OH}^n - k_2 C_H^2 C_A^2 \tag{11}$$

where C_{OH} is the hydroxide concentration and n is the corresponding reaction order. As noted above, the relatively low conversion indicates that the hydroxide (and therefore proton) concentration does not change significantly in the course of the dissolution experiments. Thus, Eq. (11) can be rewritten as

$$d\, C_A/dt = k_1' - k_2'\, C_A^2 . \tag{12}$$

According to Eq. (12), initially (i.e., for $C_A \longrightarrow 0$) the dissolution obeys a zeroth-order rate law.

At steady state (i.e., for the plateau regions of Fig. 24), $dC_A/dt = 0$ and $C_A = C_{Af}$. Thus,

$$k_2' = k_1'/C_{Af}^2 .\tag{13}$$

Combining Eqs. (12) and (13) gives

$$d\,C_A/dt = (k_1'/C_{Af}^2)\,(C_{Af}^2 - C_A^2)\,.\tag{14}$$

Using the initial conditions $C_A = 0$ when $t = 0$, Eq. (14) gives the following integrated rate law:

$$\log[(C_{Af} + C_A)/(C_{Af} - C_A)] = kt\tag{15}$$

where

$$k = 2\,k_1'/\,2.303\,C_{Af} .\tag{16}$$

Figure 29 presents the experimental data of Fig. 24 plotted in terms of Eq. (15). It can be seen that reasonably straight lines are obtained [as required by Eq. (15)]. However, contrary to expectation, the lines do not pass through zero. This discrepancy between experiment and model may be related to the rapid dissolution of surface fines.[16] Further refinement of the dissolution model must await additional experiments involving pretreatment for fines removal[16] and variations in NaOH concentration.

It was noted above that the decline in alumina dissolution in the presence of dissolved silica is related to the formation of a surface silicate layer. As a preliminary model, transport through this layer was considered to be rate limiting. For a thin silicate layer, the dissolution is expected to follow a parabolic rate law:[15]

$$\delta r = k'\,\sqrt{t}\tag{17}$$

where δr is the film thickness and k' is a constant. Equation (17) was tested against the $0.01\,M$ SiO_2 data of Fig. 28. As shown in Fig. 30, the parabolic rate law provides a good representation of the experimental data.

ORNL DWG 98C-295
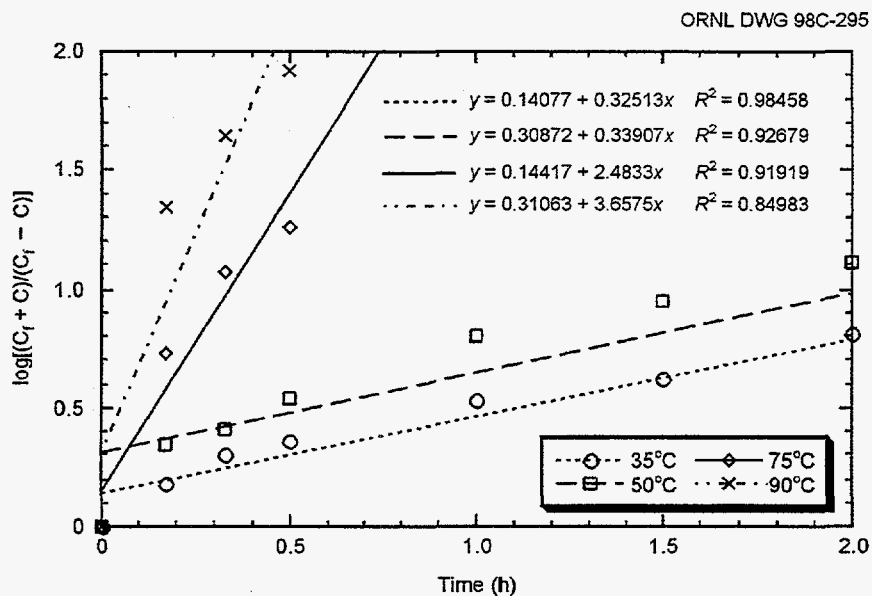
Fig. 29. Gibbsite dissolution in 0.1 M NaOH. Rate constants are extracted from the initial slopes (i.e., before equilibrium is reached).

ORNL DWG 98C-296
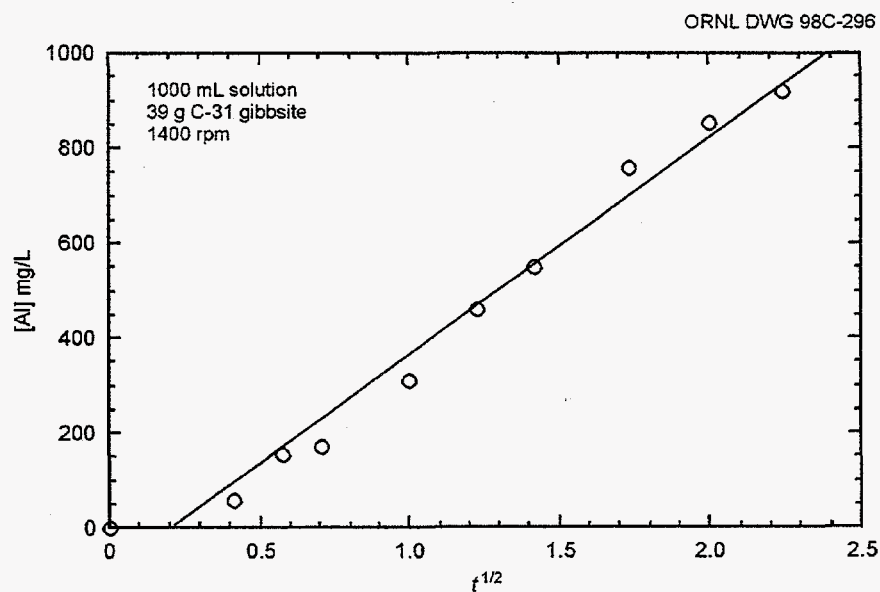
Fig. 30. Parabolic rate law representation of data from gibbsite dissolution in 1 M NaOH and 0.01 M silicate at 35°C.

6. DISCUSSION

Sludge tests and modeling are consistent in showing that solid formation will occur in process solutions if oversight and control of solution concentrations are not maintained. Operating windows narrow significantly as temperature decreases. The operating windows described in Sect. 3 were based on the indicated solution compositions. Additional components such as sodium nitrate, sodium nitrite, and sodium carbonate would increase ionic strength and further impact operating windows. Effects of ionic strength are being evaluated in ongoing studies.

It is likely that the selection of the combination of washing and caustic leaching, as well as the volume of waste and process solutions, will have to be tailored to the specific material being treated. The shifts in operating windows with caustic concentration mean that species targeted for removal should be identified before deciding on concentrations and temperatures of treatment solutions. There will be a benefit in washing out phosphate and fluoride as much as reasonably possible before caustic leaching. The wash factor for phosphate reported in Ref. 2 was 79%. However, mixing of wash solutions and caustic leachates could also result in solid formation.

It is clear that silica will impact alumina dissolution in caustic solutions. In the studies described in Sect. 5, this took the form of a decrease in rate of dissolution. However, in sludge treatment, additional anions will be present, which could result in the formation of an aluminosilicate such as a sodalite or cancrinite that incorporates anions which add to the mass of residual solids.

Because the use of caustic will increase the potential for the formation of phosphate-containing solids and can cause formation of sodium aluminosilicates, waste to be treated by caustic leaching should be carefully evaluated to ensure that there is a net benefit.

7. PATH FORWARD

There are four areas where additional effort is warranted: (1) uncertainty in model calculations and experimental data; (2) validation of the Environmental Simulation Program (ESP), which is being used at Hanford to calculate process chemical equilibria; (3) studies of the influence of silica on the dissolution of alumina and the formation of aluminosilicates; and (4) rate studies. These are being pursued in a team effort that includes Oak Ridge National Laboratory (ORNL), Mississippi State University, Numatec Hanford, and AEA Technology.

Model calculations should include uncertainty in the calculated equilibria. This can be done by employing a combination of thermochemical techniques along with an assessment of uncertainty in data for individual solid materials and in aqueous activity coefficients. Elemental chemical potentials can be extracted from calculations of chemical equilibria. They can be used to compare the free-energy difference to include a species in the equilibrium set of phases with the uncertainty in free energy. Including uncertainty will narrow the operating windows shown in Figs. 10 through 22.

The same is true of data on sludge dissolution. The enhancement by caustic leaching as shown in Tables 1 and 2 is not large in terms of the initial moles of material in the sludge. With uncertainty assigned in a statistical evaluation, the difference must become smaller. A statistical evaluation of the data in Ref. 2 will be a good starting point to determine what gain is produced by caustic leaching.

The ESP system is being used to evaluate waste treatment chemistry at Hanford. Several different approaches can be used to provide assurance that the calculations are reliable. Calculations based on the results of experimental tests have been made. These calculations provide a comparison between experimental measurements and calculations. However, they cannot ensure that the results will be valid for combinations of species that are different from the tests. Also, because the anion and cation balance is never perfect in analytical chemistry results, some heuristic adjustments are always necessary. This means that there can never be a direct comparison between model calculations and test results.

Other techniques to validate ESP include comparison calculations using another equilibrium-solver routine, comparison of standard thermodynamic values for key species with well-assessed data tabulations, and evaluation of consistency in activity coefficients using the Gibbs-Duhem equation.

The studies of the influence of silica on alumina dissolution (Sect. 5) illustrate its importance. Recent results by the Enhanced Sludge Washing Parametric Study Task at ORNL indicate that solid ·formation can play a key role during the caustic leaching phase. The caustic leaching of the washed sludge sample from Hanford tank S-101 significantly increased the sludge mass under four of the test conditions, which were the 5-h and 24-h leaches at 70°C (1 and 3 M NaOH). This weight increase is probably due to the formation of sodium aluminosilicate solids. At Pacific Northwest National Laboratory, the test results on sludge from Hanford tank BX-112 also indicated the precipitation of sodium aluminosilicate during their caustic leaches.[17] In addition to the sodium aluminosilicate solids,

sodium aluminate solids may also be formed during the caustic leaches when the sludge samples contain negligible amounts of silicon. During tests with a sludge sample from Hanford tank S-104, the wet weights of the leached solids increased in 4 and 6 M NaOH leaches that were 24 h or less. The wet mass of the sludge from tank S-104 was reduced during a 126-h leach with 6 M NaOH at 80°C.

That aluminosilicates form in caustic leachates containing aluminate and silica is not surprising. Desilication, the removal of dissolved silica, is accomplished in the Bayer process by seeding aluminate-silica caustic solutions with previous desilication products. It is surprising that Enhanced Sludge Washing resulted in a net increase in the mass of solids. The following test scheme is proposed to examine this phenomenon.

Samples of sludge from S-104 and C-107 will be washed with inhibited water until all of the water-soluble solids have been removed. A portion of washed solids will be dried to a constant weight. The dry weight of the washed solids will be compared with the dry weight of leached and washed solids to measure the net effect of solid formation and solid dissolution. Conditions to be varied include temperature (70 and 95°C), caustic concentration (1 and 3 M), and leaching time (5, 24, and 168 h). The solids will be examined by X-ray diffraction and scanning electron microscopy to determine the form of any aluminosilicates.

This information will be combined with a continuation of the kinetic studies described in Sect. 5. These data are being modeled in the FACSIMILE code, a group of computer routines for calculating the kinetics of complex processes. Rate studies will also be carried out on the precipitation of phosphate and phosphate fluoride solids, and these will be modeled as well.

8. REFERENCES

1. E. C. Beahm, C. F. Weber, T. A. Dillow, S. A. Bush, S. Y. Lee, and R. D. Hunt, *Sludge Treatment Studies*, ORNL/TM-13371, Oak Ridge National Laboratory, Oak Ridge, Tenn., June 1997.

2. N. G. Colton, *Status Report: Pretreatment Chemistry Evaluation FY 1997 — Wash and Leach Factors for the Single-Shell Tank Waste Inventory*, PNNL-11646, Pacific Northwest National Laboratory, Richland, Wash., August 1997.

3. R. A. Kirkbride, *Tank Waste Remediation System Operation and Utilization Plan*, HNF-SD-SP-012, Rev. 0, Numatec Hanford Corporation, Richland, Wash., September 1997.

4. C. F. Weber and E. C. Beahm, *Chemical Modeling of Waste Sludges*, ORNL/TM-13200, Oak Ridge National Laboratory, Oak Ridge, Tenn., October 1996.

5. C. F. Weber, "A Solubility Model for Aqueous Solutions Containing Sodium, Fluoride, and Phosphate," Ph.D. dissertation, The University of Tennessee, Knoxville, May 1998.

6. N. G. Colton, *Sludge Pretreatment Chemistry Evaluation: Enhanced Sludge Washing Separation Factors*, PNL-10512, Pacific Northwest National Laboratory, Richland, Wash., March 1995.

7. R. Den Hond, "Alumina Yield in the Bayer Process," *Light Metals 1986*, ed. R. E. Miller and W. S. Peterson, The Metallurgical Society, Inc., Warrendale, Pa., 1986, p. 125.

8. J. G. Lepetit, "Autoprecipitation of Alumina in the Bayer Process," *Light Metals 1986*, ed. R. E. Miller and W. S. Peterson, The Metallurgical Society, Inc., Warrendale, Pa., 1986, p. 225.

9. A. Atkinson, J. A. Hearne, and C. F. Knights, "Thermodynamic Modelling and Aqueous Chemistry in the $CaO-Al_2O_3-SiO_2-H_2O$ System," *Proc. Mater. Res. Soc.*, **212**, 395 (1991).

10. L. K. Hudson, *Production of Aluminum and Alumina*, ed. A. R. Burkin, John Wiley & Sons, New York, 1987, p. 11.

11. R. G. Breuer, L. R. Barsotti, and A. C. Kelly, *Extractive Metallurgy of Aluminum, Volume I. Alumina*, ed. G. Gerard and P. T. Stroup, Interscience, New York, 1963, p. 133.

12. D. J. Wesolowski, "Aluminum Speciation and Equilibria in Aqueous Solution: I. The Solubility of Gibbsite in the System $Na-K-Cl-OH-Al(OH)_4$ from 0 to 100°C," *Geochem. Acta*, **56**, 1065 (1992).

13. R. F. Scotford and J. R. Glastonburg, "The Effect of Temperature on the Rates of Dissolution of Gibbsite and Boehmite," *Can. J. Chem. Eng.*, **46**, 611 (1971).

14. A. Packter and H. S. Dhillon, "Studies on Recrystallized Aluminum Hydroxide Precipitates," *Colloid Polymer Sci.*, **252**, 249 (1974).

15. H. A. Stratten, B. T. W. Holtkamp, and P. L. deBrayn, "Precipitation from Supersaturated Aluminate Solutions: I. Nucleation and Growth of Solid Phases at Room Temperature," *J. Colloid Interface Sci.*, **98**, 342 (1984).

16. P. R. Bloom and R. M. Weaver, "Effect of the Removal of Reactive Surface Material on the Solubility of Synthetic Gibbsites," *Clays Clay Miner.*, **30**, 281 (1982).

17. G. J. Lumetta, personal communication, June 1998.

APPENDIX A

DATA ON HANFORD SLUDGE TANKS
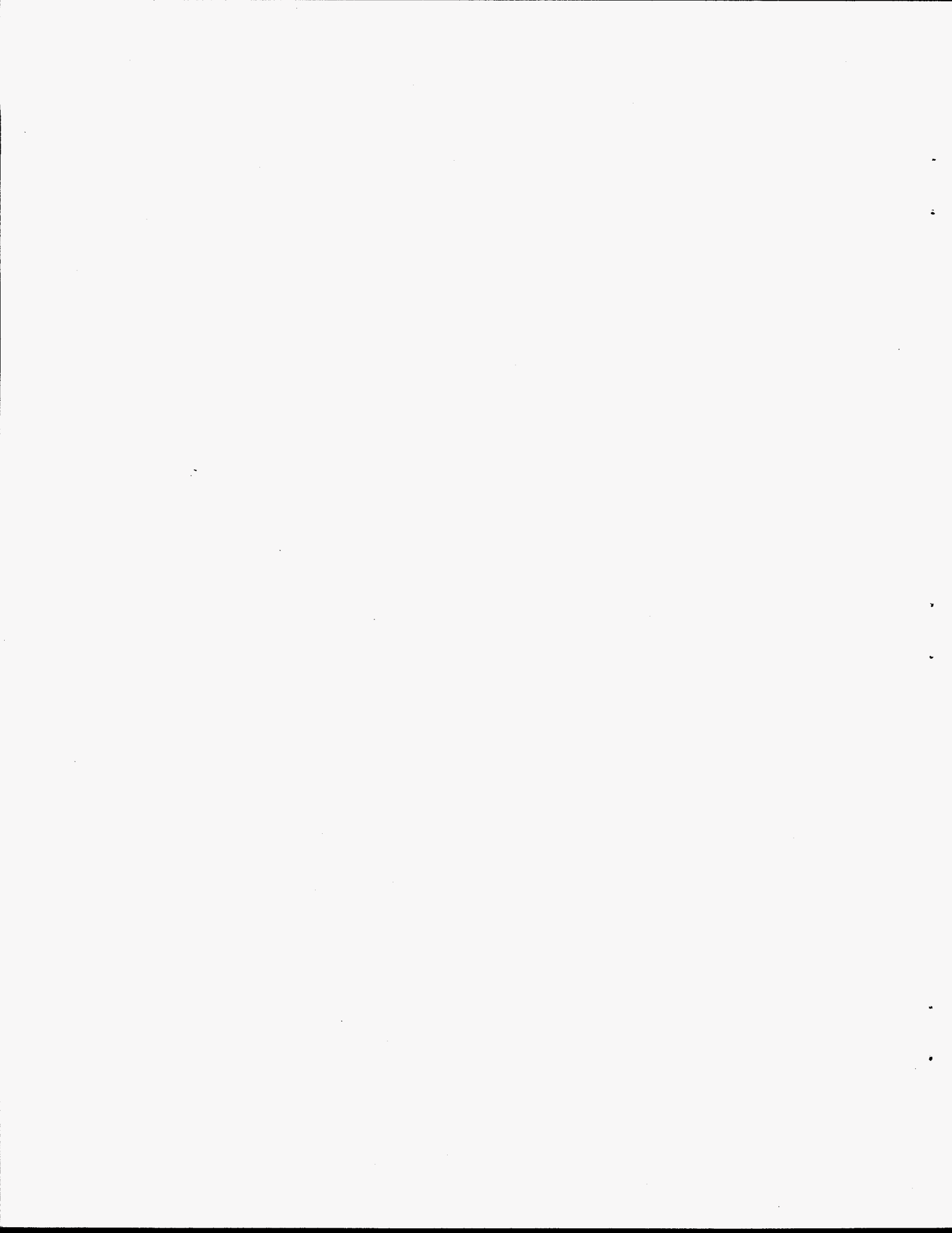
Table A.1. Sludge phosphate and fluoride in 27 Hanford tanks[a]

Sludge source	PO_4^{-3} (mol/kg)	F^- (mol/kg)		
A-102	1.66×10^{-1}	NR^b	Average PO_4^{-3}:	
A-103	6.86×10^{-2}	NR	0.476 mol/kg	
A-106	5.53×10^{-1}	NR		
			Median PO_4^{-3}:	
B-110	5.50×10^{-1}	$\geq 9.38 \times 10^{-2}$	0.550 mol/kg	
B-111	4.80×10^{-1}	$\geq 8.22 \times 10^{-2}$		
B-201	1.91×10^{-1}	$\geq 3.16 \times 10^{-1}$	Average F^-	
			≥ 0.175 mol/kg	
BX-104	1.21×10^{-1}	NR		
BX-105	6.29×10^{-1}	NR	Median F^-	
BX-107	7.42×10^{-1}	$\geq 4.78 \times 10^{-1}$	≥ 0.082 mol/kg	
C-103	1.32×10^{-1}	NR		
C-104	9.87×10^{-2}	NR		
C-105	8.00×10^{-2}	NR		
C-106	9.19×10^{-2}	NR		
C-109	6.17×10^{-1}	$\geq 2.11 \times 10^{-2}$		
C-110	6.51×10^{-1}	$\geq 7.92 \times 10^{-2}$		
C-112	9.27×10^{-1}	$\geq 7.63 \times 10^{-3}$		
S-104	3.04×10^{-3}	$\geq 7.65 \times 10^{-3}$		
T-102	4.84×10^{-2}	$\geq 1.16 \times 10^{-2}$		
T-104	7.79×10^{-1}	$\geq 4.52 \times 10^{-1}$		
T-107	1.01×10^{0}	$\geq 6.00 \times 10^{-1}$		
T-111	3.29×10^{-1}	$\geq 1.22 \times 10^{-1}$		
TY-101	7.82×10^{-1}	$\geq 1.77 \times 10^{-1}$		
TY-103	6.62×10^{-1}	$\geq 4.53 \times 10^{-2}$		
TY-104	8.27×10^{-1}	$\geq 5.64 \times 10^{-2}$		
TY-105	1.23×10^{0}	NR		
TY-106	6.09×10^{-1}	$\geq 3.68 \times 10^{-2}$		
U-110	4.62×10^{-1}	$\geq 3.91 \times 10^{-1}$		

[a]Source: N. G. Colton, *Sludge Pretreatment Chemistry Evaluation: Enhanced Sludge Washing Separation Factors*, PNL-10512, Pacific Northwest National Laboratory, Richland, Wash., March 1995.

[b]NR = Not recorded.
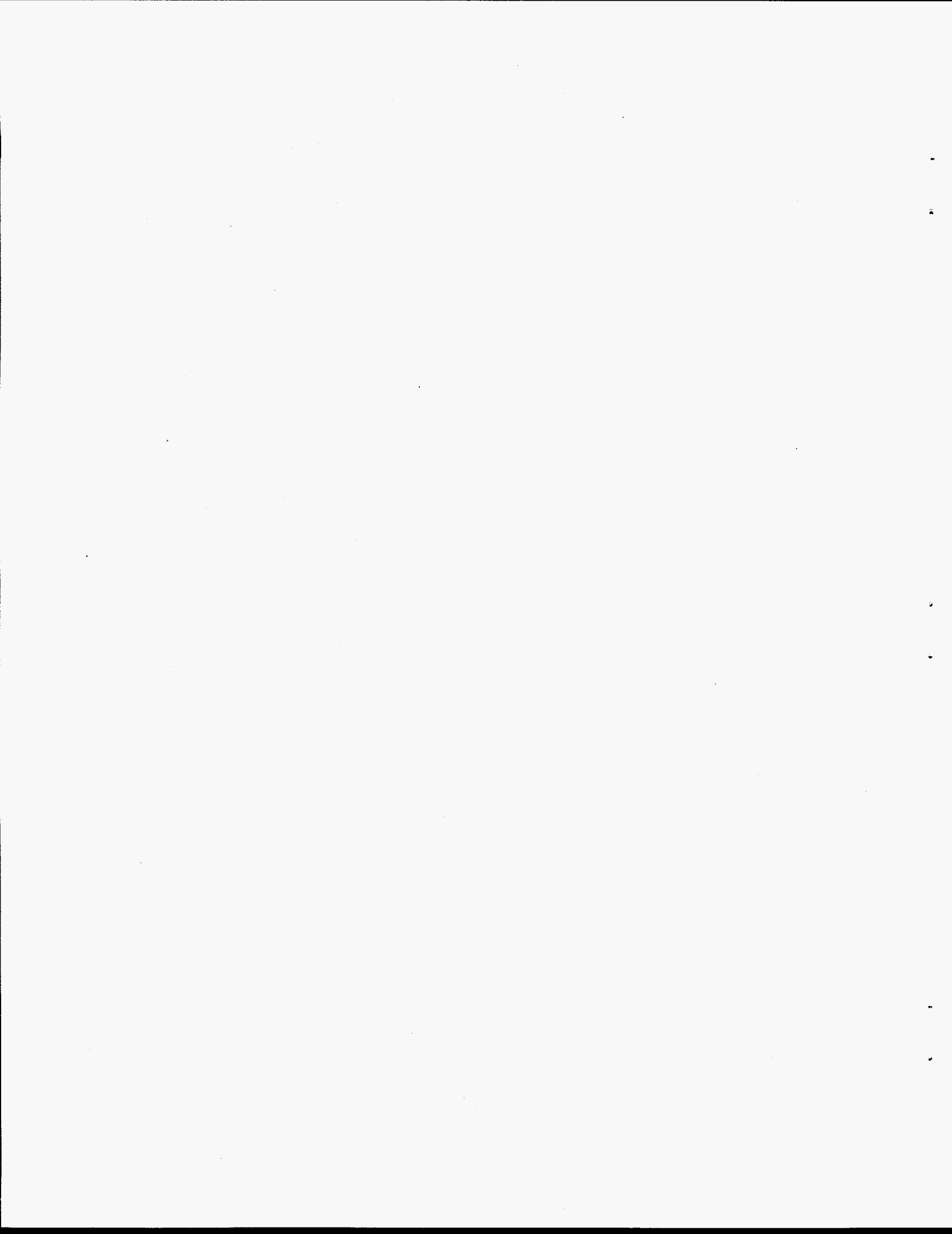
APPENDIX B

EXPERIMENTAL TESTS OF Na-F-PO_4-HPO_4-OH-H_2O MODEL CALCULATIONS
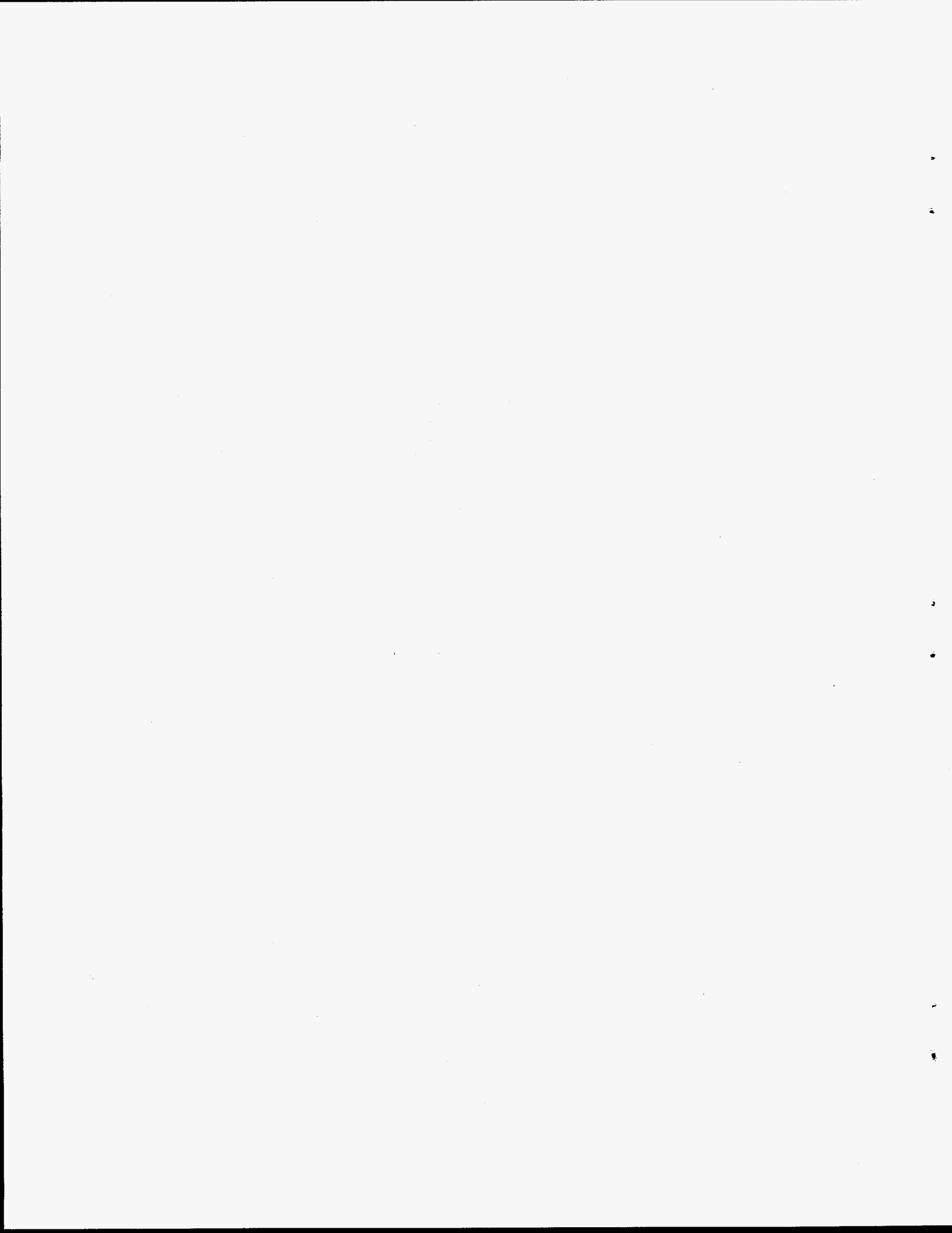
APPENDIX B

EXPERIMENTAL TESTS OF Na-F-PO$_4$-HPO$_4$-OH-H$_2$O MODEL CALCULATIONS

A series of tests were run for comparison with model calculations. Stoichiometric amounts of H$_3$PO$_4$ and NaOH were mixed to obtain initial solutions containing a mole ratio of exactly Na/PO$_4$ = 3. These solutions were mixed with solutions containing known amounts of NaF and NaOH. Reagent-grade chemicals and ultrapure water, purified through an ion-exchange membrane, were used throughout the tests.

All components were mixed at about 60°C until total dissolution was achieved. Subsequently, the solutions were cooled to 25°C and mixed for at least 1 day so they would come to equilibrium at the lower temperature. The solutions were drawn through 0.45-μm silver filters by vacuum, and the solids that were deposited on the filter media were examined. Precipitation (or lack thereof) was determined by visual examination, microscopic examination of crystals, and by X-ray diffraction.

Figure B.1 identifies the sample numbers for those tests where solid formation occurred. Figures B.2 through B.8 show the solid morphology and particle analysis that correspond to each sample where solids formed.
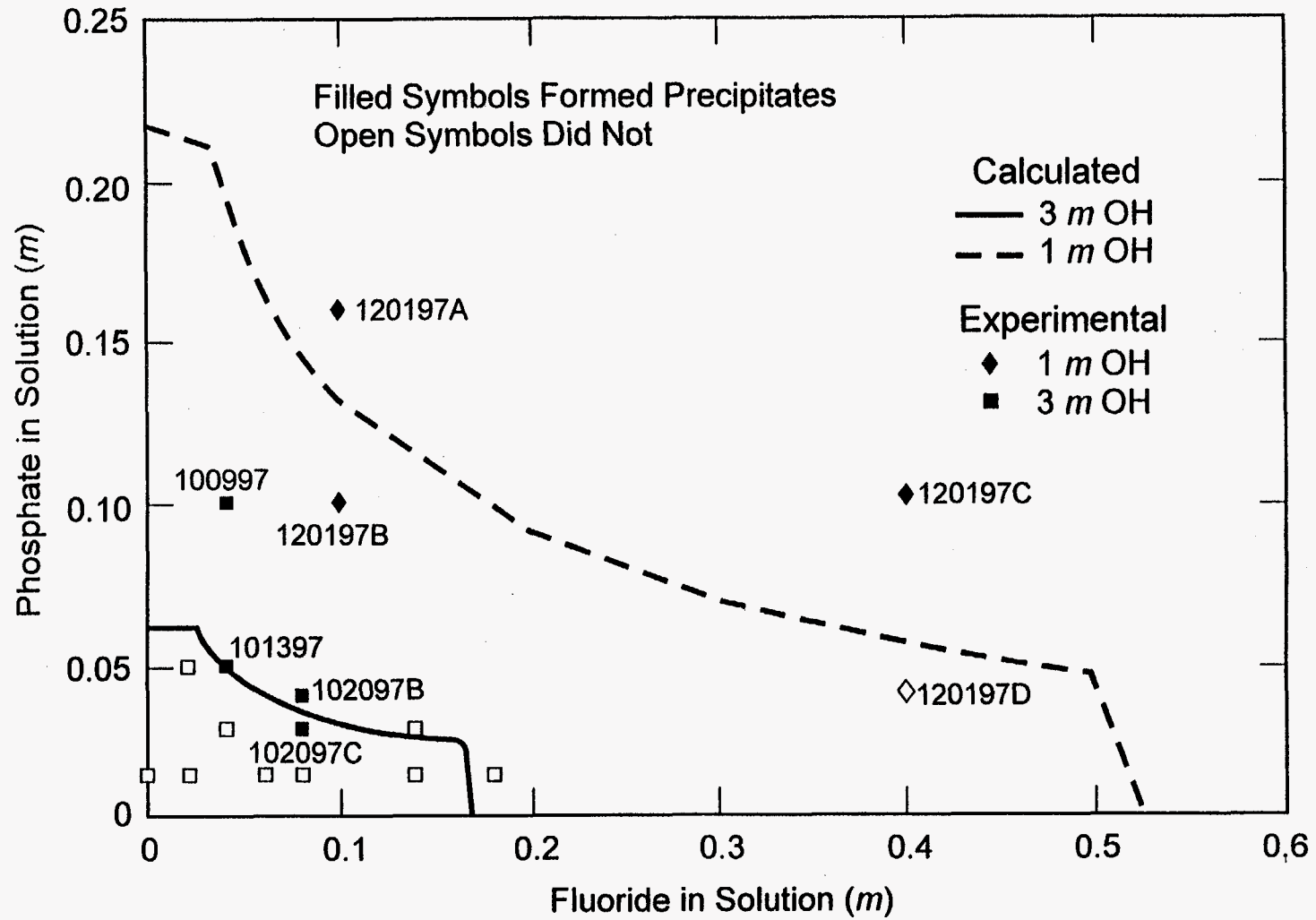
Fig. B.1. Fluoride-phosphate at 25°C.
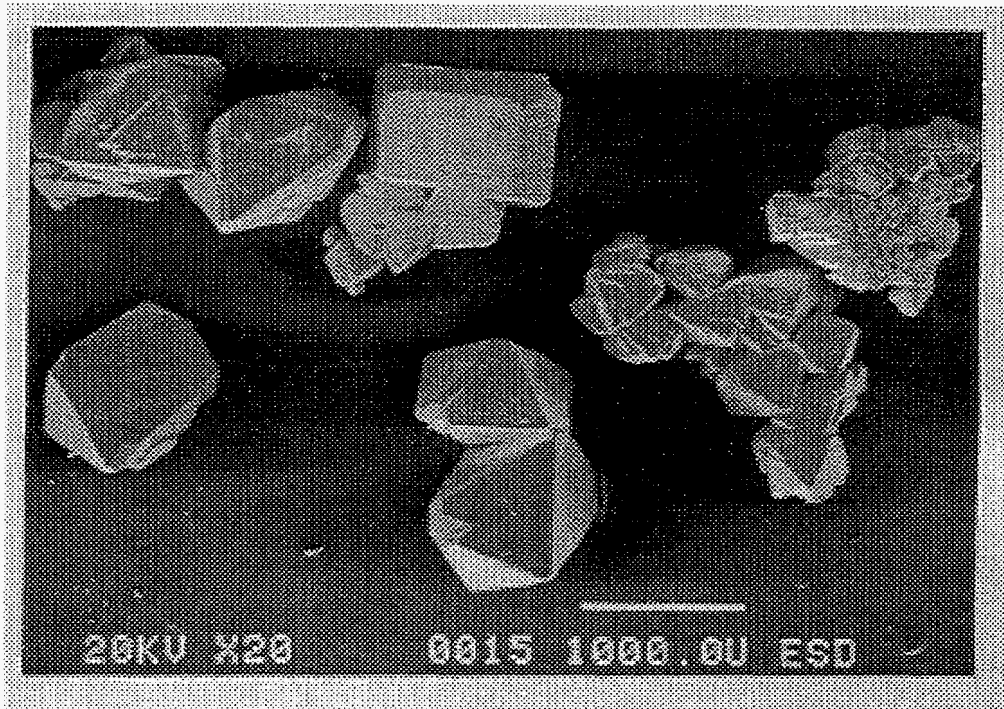
Fig. B.2. Solids formed in Test 100997.
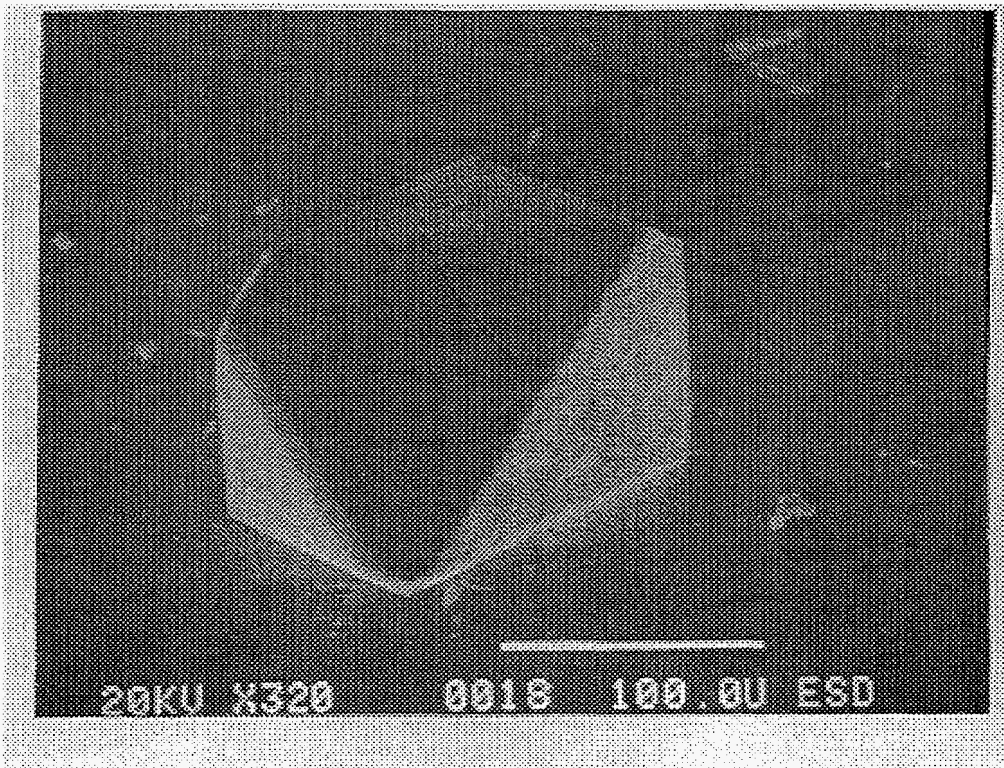
Fig. B.3. Solids formed in Test 101397.
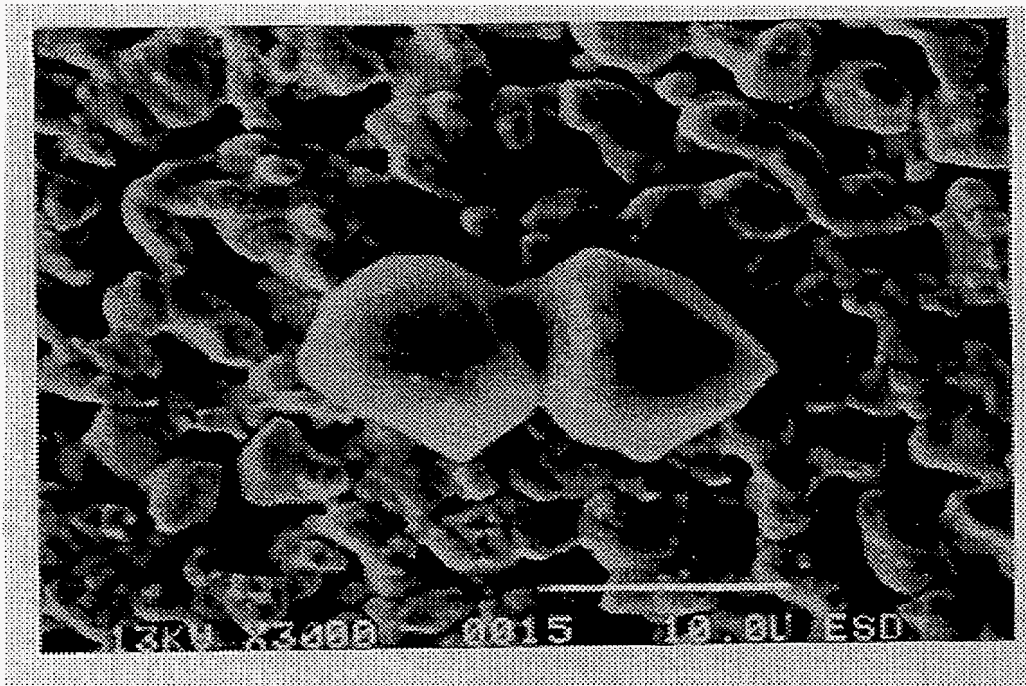
Fig. B.4. Solids formed in Test 120197A.
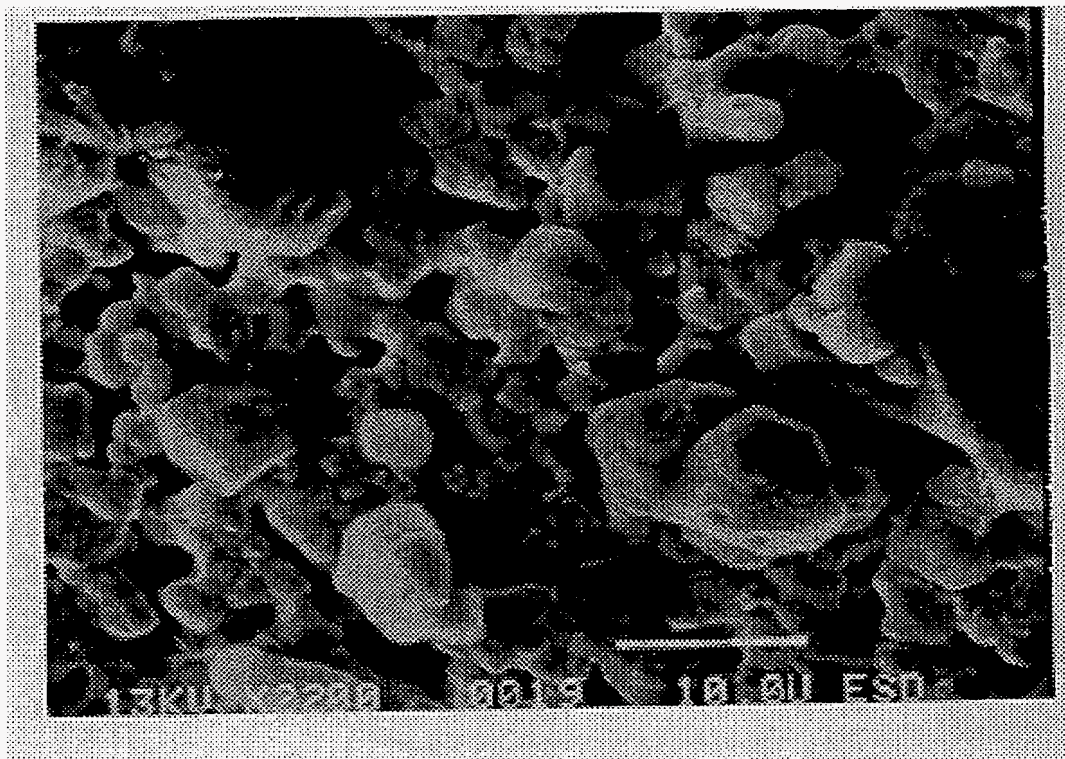
Fig. B.5. Solids formed in Test 120197B.
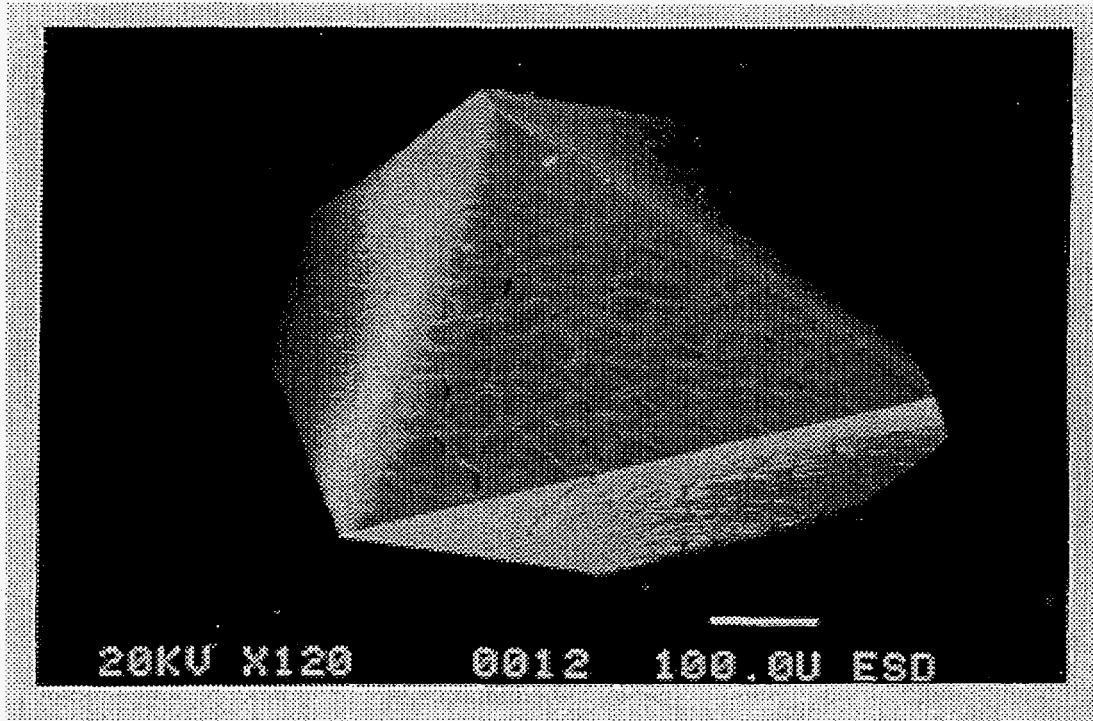
Fig. B.6. Solids formed in Test 102097B.
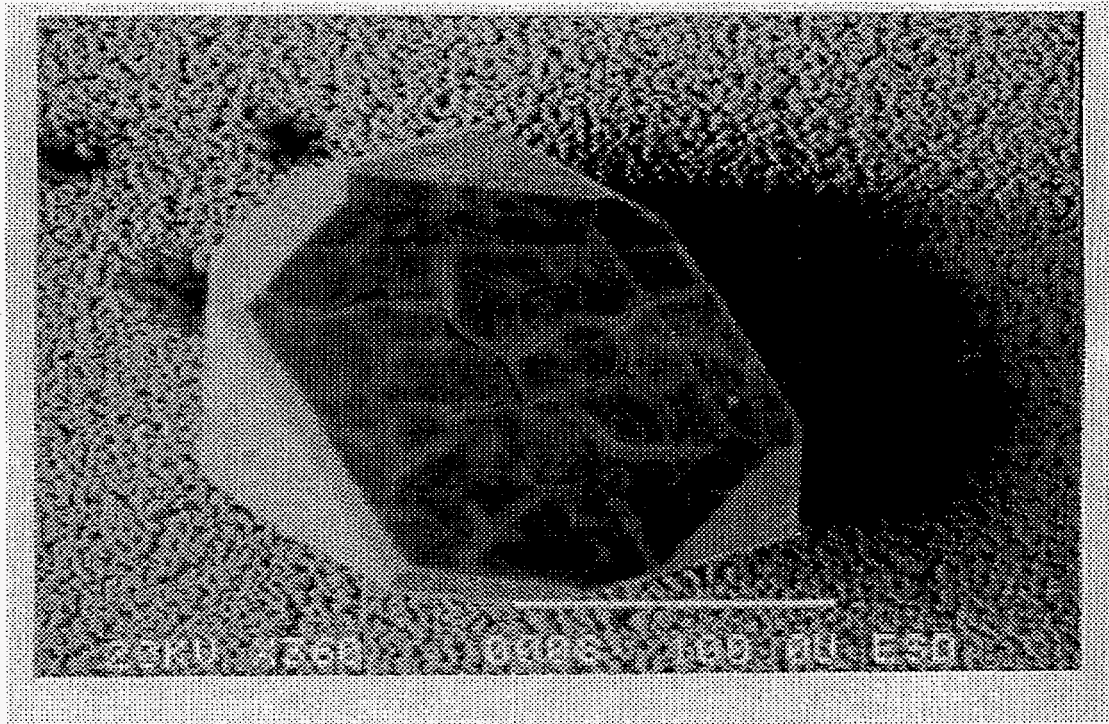
Fig. B.7. Solids formed in Test 102097C.
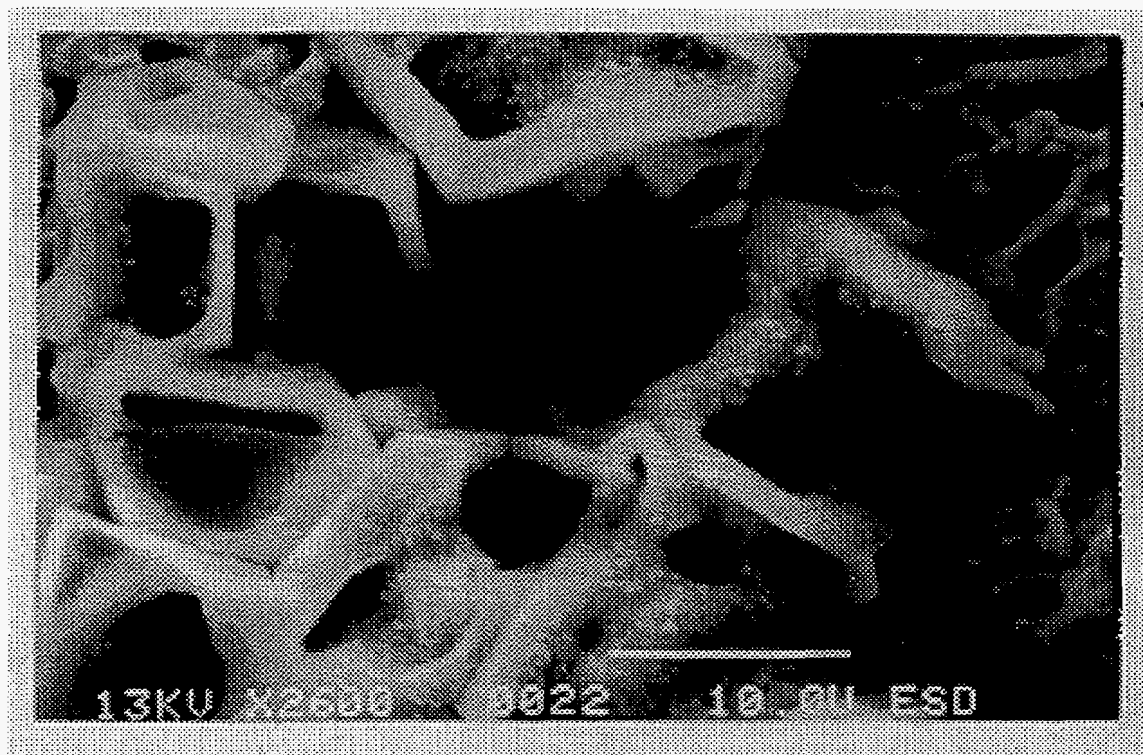
Fig. B.8. Solids formed in Test 120197C.

APPENDIX C

DETAILED DESCRIPTION OF SAMPLE T-104 ENHANCED SLUDGE
WASHING TESTS AT AMBIENT, 60°C, AND 95°C
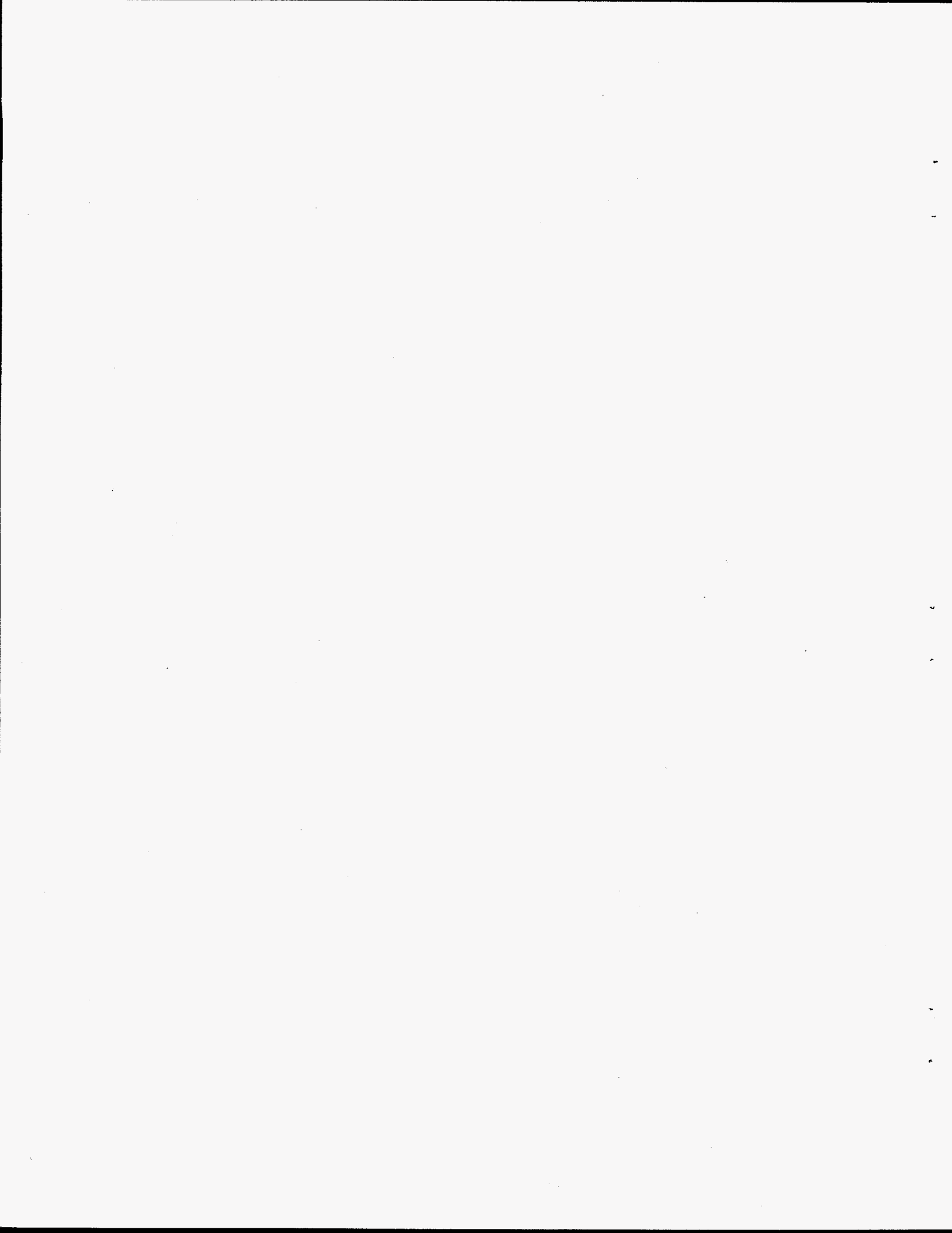
APPENDIX C

DETAILED DESCRIPTION OF SAMPLE T-104 ENHANCED SLUDGE WASHING TESTS AT AMBIENT, 60°C, AND 95°C

Labeling Setup

T_0: T-104 sample leached at room temperature (~22°C)

T_0A: 1st T_0 inhibited water wash

T_0B: 1st T_0 base leach

T_0C: 2nd T_0 base leach

$T_0D_1...D_3$: 2nd, 3rd T_0 inhibited water wash

T_1: T-104 sample leached at ~60°C

T_1A: 1st T_1 inhibited water wash

T_1B: 1st T_1 base leach

T_1C: 2nd T_1 base leach

$T_1D_1...D_3$: 2nd, 3rd T_1 inhibited water wash

T_2: T-104 sample leached at ~95°C

T_2A: 1st T_2 inhibited water wash

T_2B: 1st T_2 base leach

T_2C: 2nd T_2 base leach

$T_2D_1...D_3$: 2nd, 3rd T_2 inhibited water wash

Solutions Used

Wash Solution: $0.01\,M$ NaOH + $0.01\,M$ NaNO$_2$ (inhibited water)

Leach Solution: $3\,M$ NaOH

Solution Weights

T_0A: No weight was taken because cap sealer was used (10 mL)

T_0B: 11.51 g

T_0C: 11.44 g

T_0D_1: 10.23 g

T_0D_2: 10.19 g

T_0D_3: 10.18 g

T_1B: No weight was taken because cap sealer was used (10 mL)

T_1B: 11.39 g

T_1C: 11.34 g

T_1D_1: 10.13 g

T_1D_2: 10.18 g

T_1D_3: 10.14 g

T_2A: No weight was taken because cap sealer was used (10 mL)

T_2B: 11.41 g

T_0C: 11.32 g

T_2D_1: 10.24 g

T_2D_2: 10.22 g

T_2D_3: 10.16 g

Sludge Sample Weights

	Weight (g)		
	T_0	T_1	T_2
Initial	6.09	4.40	6.18
After 1st wash	3.83	2.94	3.87
After 1st leach	3.73	1.90	2.05
After 2nd leach	3.00	1.31	1.65
After 2nd wash	1.50	1.10	1.49
After 3rd wash	1.22	1.07	1.33
After 4th wash	1.04	1.07	1.42

Procedure

Analytical results for the initial sludge are given in Table C.1. Because of the large difference between the analytical results for P and PO_4, the phosphate analysis was rerun. Sample preparation using nitric acid microwave digestion resulted in a PO_4 concentration of 85,400 µg/g sludge. A preparation technique that employed hydroxide fusion resulted in a PO_4 concentration of 60,200 µg/g. These two values agree with the value of 73,950 µg/g reported by N. G. Colton.[6] The sludge samples were taken and placed in 50-mL centrifuge tubes using a 5-mL mechanical pipet. Using the same mechanical pipet with a new tip, the first inhibited water wash was added to each sample. The volume of the liquid added was 10 mL. The samples were then placed on the shaker (T_1 in the 60°C vessel and T_2 in the 95°C vessel), along with a water counterbalance. The heat had been turned on prior to placing the samples in the vessels. Condensate was visible in T_2 before mixing occurred. The samples were mixed for 65 min and centrifuged for 8 min. Each of the solids was observed to have three distinct layers and a volume of ~4 mL, and the liquid was a yellow color. The solutions were drawn up into plastic syringes and then pushed through a 0.45-µm polytetrafluoroethylene syringe filter. The samples were sealed back tightly and stored over night until the leach test could be performed the next day.

The first 3 M NaOH leach solution (~10 mL) was added to each sample. The samples were mixed for 4 h 46 min. The temperatures were $T_1 = 65°C$ and $T_2 = 96°C$. The samples

Table C.1. T-104 initial sludge analysis

Component	μg/g
Ag	< 2.94E+00
Al	1.82E+04
Ba	9.13E+00
Be	< 1.12E+00
Bi	1.47E+04
Br	< 19
Ca	1.70E+02
Cd	2.40E+00
Cl	760
Co	2.24E+00
Cr	8.58E+02
Cu	1.64E+01
F	8280
Fe	1.07E+04
K	8.70E+01
Mg	8.95E+01
Mn	3.18E+01
Na	7.38E+04
Ni	8.82E+00
NO_3	64300
P	4.71E+04
PO_4	23400
Sb	< 7.96E+00
Si	1.62E+03
SO_4	1.39E+04
Th	3.63E+01
U	1.02E+03
V	< 1.98E+00
Zn	2.00E+01

were allowed to slightly cool before centrifuging. After centrifuging, the liquid was decanted from each sample and filtered using the same process as before. Sample T_0 had a solids volume of ~3.5 mL, as determined by comparing it to another tube. The solids had the same distinct three layers as before. Sample T_1 had a solids volume of ~3 mL. The appearance of the three layers was not as pronounced as before. One layer was thin and two were thick. Gel was present along the edge of the solids. Sample T_2 had a solids volume of ~3 mL. Like T_1, this sample had gel present as well but was slightly visible through liquid. The samples were tightly sealed and stored over night until morning, when the next leach was scheduled.

The next day, gel was present in both $1BWT_1B$ and $1BWT_2B$. The second 3 M NaOH leach solution (~10 mL) was added to each sample. The samples were placed on the shaker and started mixing at 10:00 a.m. The temperatures at this time were $T_1 = 62°C$ and $T_2 = 93°C$. After mixing for 5 h and 30 min, the samples were allowed to cool. After centrifuging for ~10 min, T_0 had a very pale straw yellow–colored liquid with ~3.5 mL of solids. Three layers of solids were visible. T_1 had a darker yellow liquid than T_0, with ~2.5–2.7 mL of solids. Only two solids layers appeared this time (one thick layer on top and one thin one on the bottom). T_2 had ~2.5–2.7 mL of solids with two thick layers on top and one thin layer at the bottom. After the solutions were pulled off and filtered, there was no visible gel in either T_1 or T_2 solids.

The following day, T_1C had four gel granules. T_2C had slightly less than T_2B. A portion of these solids was scooped out of T_1B. In a separate weighing boat, a portion was washed with 3 M NaOH, and a portion was washed with deionized (DI) water. After ~2 min, no noticeable dissolution could be seen with the NaOH wash; partial dissolution was possible with the DI water. Most of the solids from T_2B were removed and placed into a plastic weighing boat. They were then quickly washed with three small portions of 3 M NaOH and three small portions of DI water. The solids appeared to be a pale yellow while still wet. Once dry, they were a white, clear color. These solids were collected into a bottle and sent with the rest of the washes for analyses. The results are listed in Table C.2.

The first inhibited water wash after leaching was then started. No heat was applied to the samples. The samples were taken off and centrifuged. The samples were mixed for 30 min. The liquid was pulled off and filtered. The solids volume of T_0 was ~2.7–2.8 mL. The solids volume of T_1 and T_2 were both ~2.5 mL. The tubes containing T_1 and T_2 had brown stained sides just above the liquid level.

The second wash after leaching also lasted 30 min. The samples were taken off and centrifuged. For T_0 there was no color in the liquid; for T_1 and T_2 there was a very little if any color in the liquid. There was also fine, brown solids just above the sample in both T_1 and T_2.

The third and final wash was done the following day. The samples were again mixed for 30 min, taken off, and centrifuged. The liquid was pulled off and filtered. After this

Table C.2. Composition of gel in leachate from T-104, sample T_2B, leached at 95°C

Component	µg/g
Ag	< 3.88E–01
Al	6.05E+00
Ba	< 4.21E–02
Be	< 4.82E–02
Bi	1.01E+01
Br	< 14.8
Ca	< 2.35E–01
Cd	< 6.62E–01
Cl	< 14.8
Co	< 4.33E–01
Cr	2.80E+01
Cu	< 1.26E–01
F	23300
Fe	< 1.02E–01
K	1.47E+02
Mg	< 5.93E–01
Mn	< 4.82E–02
Na	2.14E+05
Ni	< 6.77E–01
NO_3	35.0
PO_4	276000
Sb	< 6.63E+00
Si	1.99E+02
SO_4	167
Th	< 1.46E+00
U	< 2.74E+00
V	< 1.23E–01
Zn	< 8.88E–01

centrifuging, T_0 liquid had a cloudy, brown color. A second centrifugation was done. The status of the liquid was unchanged, so the samples were filtered. T_0 was slightly difficult to filter; the filter had an orange color to it after filtering was complete. The final solids volume of T_0 was ~2.3 mL. The T_1 filter had a slight orange color but was not as dark as T_0. The final T_1 solids volume was ~2.4 mL. The T_2 filter had the least color of all, with a slight orangish-brown tint. The final solids volume of T_2 was ~2.5 mL. Analytical results for the tests at ambient, 60°C, and 95°C are given in Tables C.3, C.4, and C.5, respectively.

Specific gravities were determined once all the samples had been collected, as shown in Table C.6.

Test solution appearance is described in Table C.7.

**Table C.3. Concentrations (µg/mL) in process solutions of T-104 sludge
washed and leached at ambient temperature**

Component	Wash T_0A	1st Leach T_0B	2nd Leach T_0C	Wash T_0D_1	Wash T_0D_2	Wash T_0D_3
Ag	< 1.42E–01	< 1.42E–01	< 1.42E–01	< 1.42E–01	< 1.56E+00	< 1.42E–01
Al	1.15E+01	7.32E+03	1.72E+03	2.20E+02	5.28E+01	2.44E+01
Ba	< 1.54E–02	< 1.54E–02	< 1.54E–02	< 1.54E–02	< 1.69E–01	< 1.54E–02
Be	< 1.76E–02	< 1.76E–02	< 1.76E–02	< 1.76E–02	< 1.94E–01	< 1.76E–02
Bi	8.69E+00	1.02E+01	2.17E+01	1.82E+00	9.44E+00	9.83E+00
Br	< 2.50	< 2.50	< 2.50	< 2.50	< 2.50	< 2.50
Ca	1.17E+00	4.62E–01	< 8.58E–02	< 8.58E–02	1.34E+01	5.39E–01
Cd	< 2.42E–01	< 2.42E–01	< 2.42E–01	< 2.42E–01	< 2.66E+00	< 2.42E–01
Cl	324	67.2	11.1	3.40	< 2.50	< 2.50
Co	< 1.58E–01	< 1.58E–01	< 1.58E–01	< 1.58E–01	< 1.74E+00	< 1.58E–01
Cr	5.93E+01	1.90E+01	1.05E+01	7.41E+00	< 3.99E–01	1.22E+00
Cu	< 4.62E–02	< 4.62E–02	< 4.62E–02	< 4.62E–02	< 5.08E–01	< 4.62E–02
F	564	3560	740	1940	502	54.1
Fe	2.06E+00	2.96E+00	6.79E+00	4.29E–01	< 4.11E–01	3.91E+00
K	1.77E+01	2.63E+01	2.77E+01	4.44E+00	< 8.37E+00	9.24E–01
Mg	< 2.17E–01	< 2.17E–01	< 2.17E–01	< 2.17E–01	< 2.38E+00	< 2.17E–01
Mn	< 1.76E–02	< 1.76E–02	< 1.76E–02	< 1.76E–02	< 1.94E–01	< 1.76E–02
Na	1.68E+04	5.01E+04	6.91E+04	2.90E+04	6.72E+03	1.35E+03
Ni	< 2.48E–01	< 2.48E–01	< 2.48E–01	< 2.48E–01	< 2.72E+00	< 2.48E–01
NO$_3$	28200	5330	832	125	18.2	7.20
PO$_4$	5260	2930	2870	17700	5120	548
Sb	< 2.42E+00	< 2.42E+00	< 2.42E+00	< 2.42E+00	< 2.67E+01	< 2.42E+00
Si	1.19E+01	3.46E+02	7.94E+02	1.42E+02	2.49E+02	2.64E+01
SO$_4$	1320	579	79.5	19.8	9.60	< 5.00
Th	< 5.34E–01	< 5.34E–01	< 5.34E–01	< 5.34E–01	< 5.87E+00	< 5.34E–01
U	3.98E+00	6.23E+01	5.87E+01	5.96E+00	< 1.10E+01	< 1.00E+00
V	< 4.51E–02	< 4.51E–02	< 4.51E–02	< 4.51E–02	< 4.96E–01	< 4.51E–02
Zn	< 3.25E–01	3.44E+00	2.23E+00	< 3.25E–01	< 3.57E+00	< 3.25E–01

Table C.4. Concentrations (µg/mL) in process solutions of T-104 sludge initial wash
and leaches at 60°C and final washes at ambient temperature

Component	Wash T_1A	1st Leach T_1B	2nd Leach T_1C	Wash T_1D_1	Wash T_1D_2	Wash T_1D_3
Ag	< 1.42E–01	< 1.42E–01	< 1.42E–01	< 1.42E–01	< 1.42E–01	< 1.42E–01
Al	1.85E+01	5.16E+03	1.04E+03	1.06E+02	1.84E+01	8.48E+00
Ba	< 1.54E–02	< 1.54E–02	< 1.54E–02	< 1.54E–02	< 1.54E–02	< 1.54E–02
Be	< 1.76E–02	< 1.76E–02	< 1.76E–02	< 1.76E–02	< 1.76E–02	< 1.76E–02
Bi	3.14E+00	5.28E+01	8.01E+01	3.61E+00	2.56E+00	3.22E+00
Br	< 2.50	< 2.50	< 2.50	< 2.50	< 2.50	< 2.50
Ca	9.68E–01	4.62E–01	< 8.58E–02	1.03E+00	8.58E–01	5.39E–01
Cd	< 2.42E–01	< 2.42E–01	< 2.42E–01	< 2.42E–01	< 2.42E–01	< 2.42E–01
Cl	277	37.8	< 2.50	< 2.50	< 2.50	< 2.50
Co	< 1.58E–01	< 1.58E–01	< 1.58E–01	< 1.58E–01	< 1.58E–01	< 1.58E–01
Cr	4.72E+01	6.00E+01	5.10E+01	7.32E+00	8.14E–01	1.32E–01
Cu	< 4.62E–02	< 4.62E–02	1.76E–01	< 4.62E–02	< 4.62E–02	< 4.62E–02
F	581	2540	559	84.7	13.5	7.55
Fe	8.58E–01	5.65E+00	1.08E+01	1.21E–01	< 3.74E–02	1.43E–01
K	1.66E+01	3.23E+01	5.55E+01	1.28E+01	6.09E+00	4.29E+00
Mg	< 2.17E–01	< 2.17E–01	< 2.17E–01	< 2.17E–01	< 2.17E–01	< 2.17E–01
Mn	< 1.76E–02	< 1.76E–02	< 1.76E–02	< 1.76E–02	< 1.76E–02	< 1.76E–02
Na	1.42E+04	5.17E+04	7.03E+04	8.41E+03	1.32E+03	6.41E+02
Ni	< 2.48E–01	< 2.48E–01	< 2.48E–01	< 2.48E–01	< 2.48E–01	< 2.48E–01
NO_3	21800	3520	537	46.6	8.55	5.63
PO_4	4790	2900	3360	690	54.0	11.0
Sb	< 2.42E+00	< 2.42E+00	< 2.42E+00	< 2.42E+00	< 2.42E+00	< 2.42E+00
Si	1.34E+01	2.09E+02	3.88E+02	4.13E+01	1.46E+01	7.29E+00
SO_4	1170	381	168	7.45	< 5.00	< 5.00
Th	< 5.34E–01	< 5.34E–01	< 5.34E–01	< 5.34E–01	< 5.34E–01	< 5.34E–01
U	3.58E+00	6.59E+01	6.22E+01	3.75E+00	< 1.00E+00	< 1.00E+00
V	< 4.51E–02	< 4.51E–02	< 4.51E–02	< 4.51E–02	< 4.51E–02	< 4.51E–02
Zn	< 3.25E–01	3.98E+00	1.18E+00	< 3.25E–01	< 3.25E–01	< 3.25E–01

Table C.5. Concentrations (µg/mL) in process solutions of T-104 sludge initial wash and leaches at 95°C and final washes at ambient temperature

Component	Wash T₂A	1st Leach T₂B	2nd Leach T₂C	Wash T₂D₁	Wash T₂D₂	Wash T₂D₃
Ag	< 1.42E–01	< 1.42E–01	< 1.42E–01	< 1.42E–01	< 1.42E–01	< 1.42E–01
Al	1.93E+01	5.87E+03	1.38E+03	1.74E+02	2.84E+01	1.07E+01
Ba	< 1.54E–02	< 1.54E–02	< 1.54E–02	< 1.54E–02	< 1.54E–02	< 1.54E–02
Be	< 1.76E–02	< 1.76E–02	< 1.76E–02	< 1.76E–02	< 1.76E–02	< 1.76E–02
Bi	4.37E+00	7.32E+01	1.57E+02	4.88E+00	2.52E+00	1.79E+00
Br	< 2.50	< 2.50	< 2.50	< 2.50	< 2.50	< 2.50
Ca	1.00E+00	1.03E+00	< 8.58E–02	5.17E–01	2.31E–01	1.63E+00
Cd	< 2.42E–01	< 2.42E–01	< 2.42E–01	< 2.42E–01	< 2.42E–01	< 2.42E–01
Cl	343	70.2	< 2.50	< 2.50	< 2.50	< 2.50
Co	< 1.58E–01	< 1.58E–01	< 1.58E–01	< 1.58E–01	< 1.58E–01	< 1.58E–01
Cr	6.03E+01	1.92E+02	7.73E+01	1.07E+01	1.69E+00	1.87E–01
Cu	< 4.62E–02	< 4.62E–02	2.42E–01	< 4.62E–02	< 4.62E–02	< 4.62E–02
F	597	3360	607	157	22.5	8.75
Fe	1.10E+00	4.16E+00	9.79E+00	7.70E–02	4.95E–01	1.21E–01
K	2.85E+01	5.68E+01	6.70E+01	2.00E+01	4.99E+00	3.93E+00
Mg	< 2.17E–01	< 2.17E–01	< 2.17E–01	< 2.17E–01	< 2.17E–01	< 2.17E–01
Mn	< 1.76E–02	< 1.76E–02	< 1.76E–02	< 1.76E–02	< 1.76E–02	< 1.76E–02
Na	1.73E+04	4.89E+04	7.70E+04	1.13E+04	1.87E+03	7.46E+02
Ni	< 2.48E–01	< 2.48E–01	< 2.48E–01	< 2.48E–01	< 2.48E–01	< 2.48E–01
NO₃	28200	5410	708	95.0	14.9	6.13
PO₄	6100	3050	2660	1200	137	21.5
Sb	< 2.42E+00	< 2.42E+00	< 2.42E+00	< 2.42E+00	< 2.42E+00	< 2.42E+00
Si	1.23E+01	1.10E+02	4.33E+02	4.57E+01	4.40E+00	7.11E+00
SO₄	1280	411	69.7	10.6	< 5.00	< 5.00
Th	< 5.34E–01	< 5.34E–01	< 5.34E–01	< 5.34E–01	< 5.34E–01	< 5.34E–01
U	5.67E+00	7.48E+01	8.59E+01	5.64E+00	< 1.00E+00	< 1.00E+00
V	< 4.51E–02	< 4.51E–02	< 4.51E–02	< 4.51E–02	< 4.51E–02	< 4.51E–02
Zn	< 3.25E–01	4.52E+00	2.50E+00	< 3.25E–01	< 3.25E–01	< 3.25E–01

Table C.6. Sample specific gravities

Sample	Specific gravity (g/mL)
Water	1.000
T_0A	1.036
T_0B	1.092
T_0C	1.122
T_0D_1	1.048
T_0D_2	1.014
T_0D_3	0.994
T_1A	1.026
T_1B	1.095
T_1C	1.121
T_1D_1	1.003
T_1D_2	0.997
T_1D_3	0.989
T_2A	1.036
T_2B	1.090
T_2C	1.125
T_2D_1	1.013
T_2D_2	1.002
T_2D_3	0.992

Table C.7. Appearance of T-104 process solutions after completion of tests: Samples T_0, T_1, and T_2

	Washing and leaching at ambient T_0	1st Wash and leaching at 60°C T_1	1st Wash and leaching at 95°C T_2
1st Wash	Yellow liquid No solids	Pale yellow liquid No solids	Yellow liquid No solids
1st Leach	Pale yellow liquid Small amount of gel	Yellow liquid Gel solids	Yellow liquid Small amount of gel
2nd Leach	Pale yellow liquid Small amount of gel	Yellow liquid Small amount of gel	Yellow liquid Gel solids
1st Wash	Very pale yellow liquid	Colorless liquid No solids	Pale yellow liquid No solids
2nd Wash	Colorless liquid No solids	Colorless liquid No solids	Colorless liquid No solids
3rd Wash	Colorless liquid Brown solids	Colorless liquid Small amount of brown solids	Colorless liquid Small amount of brown solids
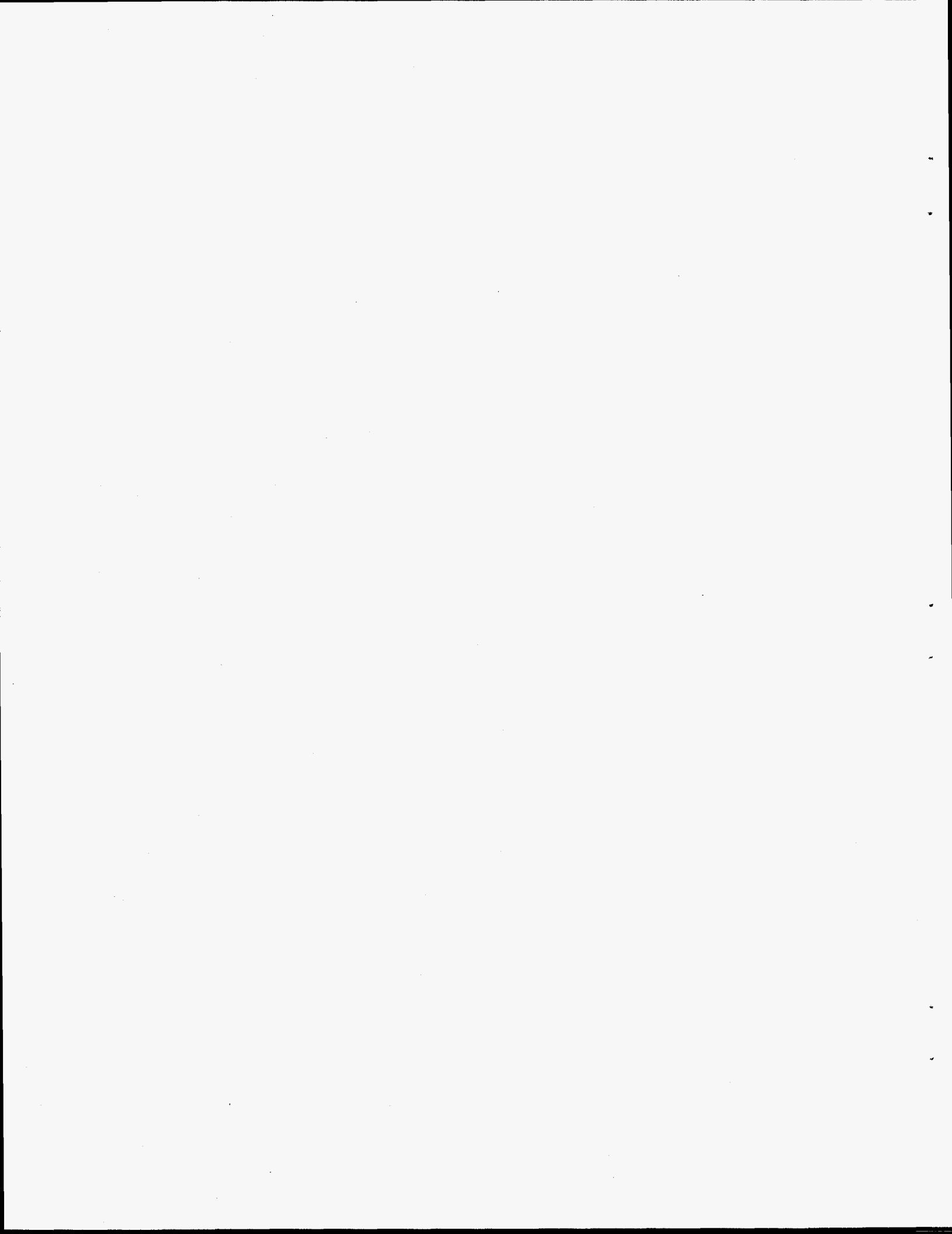
APPENDIX D

DETAILED DESCRIPTION OF SAMPLE T-104 LEACHING AND WASHING TESTS: LEACHING AT 75°C
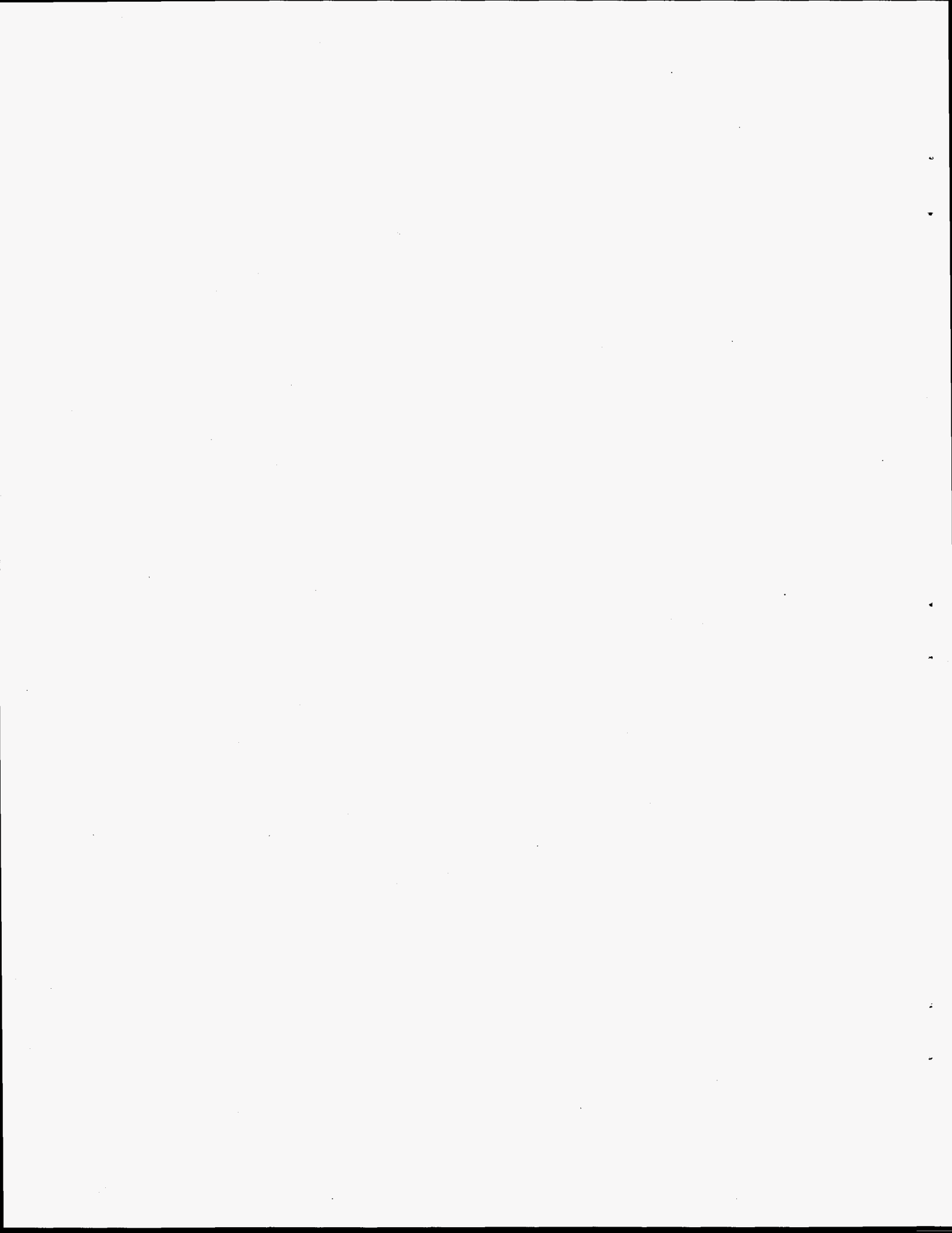
APPENDIX D

DETAILED DESCRIPTION OF SAMPLE T-104 LEACHING AND WASHING TESTS: LEACHING AT 75°C

Labeling Setup

T_0R: T-104 sample leached at 75°C, all other steps at ambient
T_0RA: Base leach
T_0RB: 1st inhibited water wash
T_0RC: 2nd inhibited water wash
T_0RD: 3rd inhibited water wash

T_1R: T-104 sample entire treatment at 75°C
T_1RA: Base leach
T_1RB: 1st inhibited water wash
T_1RC: 2nd inhibited water wash
T_1RD: 3rd inhibited water wash

Solutions Used

Leach Solution: 3.75 M NaOH
Wash Solution: 0.01 M NaOH + 0.01 M NaNO$_2$ (inhibited water)

Solution Weights

T_1RA: 11.48 g
T_1RB: 15.21 g
T_1RC: 15.2 g
T_1RD: 15.22 g

T_0RA: 11.58 g
T_0RB: 15.36 g
T_0RC: 15.27 g
T_0RD: 15.36 g
Mixing times ~24 h

Sample Weights

	Weight (g)	
	T_1R	T_0R
Initial sludge	2.92	3.54
Residue	2.72	3.87

Samples settled overnight before filtration with no centrifugation. Heated samples were filtered through heated syringes and heated 0.45-μm filters.

Analyses of process solutions are provided in Tables D.1 and D.2, and solution appearance is described in Table D.3.

Table D.1. Concentrations (μg/mL) in T-104 process solutions at 75°C throughout treatment (samples were injected into 6 M HNO$_3$ after treatment)

Component	Leach Sample→ (T$_1$RA)	1st Wash (T$_1$RB)	2nd Wash (T$_1$RC)	3rd Wash (T$_1$RD)
Al	2.66E+03	4.52E+02	7.13E+01	3.81E+01
Bi	1.16E+02	9.51E+00	3.35E+00	4.31E+00
Ca	1.41E+00	1.68E+00	1.34E+00	1.45E+00
Cl	9.36E+01	< Value	< Value	< Value
Cr	1.40E+02	2.69E+01	4.49E+00	7.06E–01
Cu	9.79E–01	2.01E–01	2.02E–01	1.51E–01
F	2.76E+03	7.33E+02	3.78E+02	< Value
Fe	1.06E+01	1.10E+00	5.67E–01	2.77E–01
K	6.05E+01	1.16E+01	3.00E+00	1.71E+00
Na	8.68E+04	1.55E+04	2.44E+03	8.11E+02
P	5.72E+03	9.41E+02	1.50E+02	2.95E+01
PO$_4$	1.27E+04	2.23E+03	3.25E+02	8.47E+01
Si	7.63E+01	4.54E+01	4.18E+01	4.28E+01
SO$_4$	1.03E+03	2.08E+02	7.18E+01	3.40E+01
Sr	8.79E–02	< Value	< Value	< Value
U	7.78E+01	1.46E+01	1.70E+00	< Value
Zn	3.39E+00	4.39E–01	< Value	< Value

A Hach 2100AN Turbidimeter was used to measure turbidity in the filtered leaches and wash solutions. The instrument is capable of reading from 0–10,000 Nephelometric Turbidity Units (NTU). Tables D.4 and D.5 give the turbidity data. The upper number in each pair is for undisturbed samples, and the lower number is for samples that were rotated three times to resuspend settled solids. Unfortunately, turbidity readings of these samples do not appear to be useful. The formation of solids, when it occurred, was rapid, so there was little meaningful variation after the initial reading. In addition, the solids sometimes coated the sample container, so there was no way to discern colloids from deposited material.

Table D.2. Concentrations (μg/mL) in T-104 process solutions leached at 75°C and all other steps in treatment at ambient (samples were injected into 6 M HNO_3 after treatment)

Component	Leach Sample→ (T_0RA)	1st Wash (T_0RB)	2nd Wash (T_0RC)	3rd Wash (T_0RD)
Al	3.69E+03	7.13E+02	1.11E+02	2.81E+01
Bi	3.19E+01	6.25E+00	2.93E+00	4.05E+00
Ca	1.18E+00	1.45E+00	1.65E+00	1.47E+00
Cl	2.71E+02	< Value	< Value	< Value
Cr	2.35E+02	4.15E+01	8.35E+00	2.06E+00
Cu	7.78E–01	8.86E–02	8.75E–02	1.01E–01
F	2.12E+03	1.63E+03	5.68E+02	3.69E+02
Fe	3.51E+00	4.93E–01	2.75E–01	2.40E–01
K	7.58E+01	1.73E+01	4.93E+00	2.13E+00
Na	8.43E+04	2.78E+04	5.35E+03	1.56E+03
P	6.83E+02	4.48E+03	8.33E+02	1.88E+02
PO_4	1.46E+03	1.19E+04	1.94E+03	3.87E+02
Si	5.50E+01	4.53E+01	3.15E+01	3.21E+01
SO_4	1.34E+03	3.34E+02	9.78E+01	< Value
Sr	< Value	< Value	< Value	< Value
U	8.01E+01	1.31E+01	< Value	< Value
Zn	3.92E+00	5.82E–01	< Value	< Value

Table D.3. Observations of process solutions of T-104 samples T_0R and T_1R

	T_0R	T_1R
Leach	Solids formed at bottom of sample	Solid formed as sample cooled. Some coating of container
1st Wash	No visible solids, possible clear gel	Became cloudy after filtration
2nd Wash	No visible solids	Became cloudy after filtration
3rd Wash	No visible solids	Became cloudy after filtration

Table D.4. Turbidity (NTU) in filtered process solutions:
sample T_1R at 75°C throughout treatment

(turbidity at ambient temperature)

| Time after test	Leachate Sample → T_1RA	1st Wash T_1RB	2nd Wash T_1RC	3rd Wash T_1RD
Initial	45.2	7.19	11.2	4.45
	62.0	4.63	12.3	18.2
3 days	38.9	1.94	1.92	4.61
	55.0	5.82	12.8	5.65
5 days	40.1	1.34	1.36	4.49
	44.5	6.87	13.4	40.2
7 days	38.8	2.35	12.7	5.03
	44.5	4.36	55.9	4.82
17 days	37.8	2.09	1.26	3.02
	40.5	3.61	2.35	34.6
24 days	37.8	6.34	3.09	1.16
	44.7	5.62	10.8	4.96
31 days	43.6	2.35	9.07	4.54
	47.5	6.20	4.46	5.65

Table D.5. Turbidity (NTU) in filtered process solutions: sample T_0R
leached at 75°C and ambient after leaching

(turbidity at ambient temperature)

Time after test	Leachate	1st Wash	2nd Wash	3rd Wash
Initial	1.34	0.86	0.90	1.20
	5.80	1.05	1.36	1.47
3 days	1.34	0.88	0.88	1.50
		1.08	1.35	2.12
5 days	2.00	0.89	0.99	1.37
	2.48	1.54	2.77	2.42
7 days	2.20	0.90	1.06	1.25
	4.20	1.02	1.94	2.22
17 days	1.66	0.93	1.38	1.67
	3.34	1.28	3.08	3.45
24 days	2.91	0.93	1.23	1.96
	2.83	1.52	1.77	1.93
31 days	2.43	1.09	1.50	1.57
	4.18	1.49	3.47	3.47

APPENDIX E

EXPERIMENTAL METHODOLOGY IN ALUMINA-SILICA TESTS
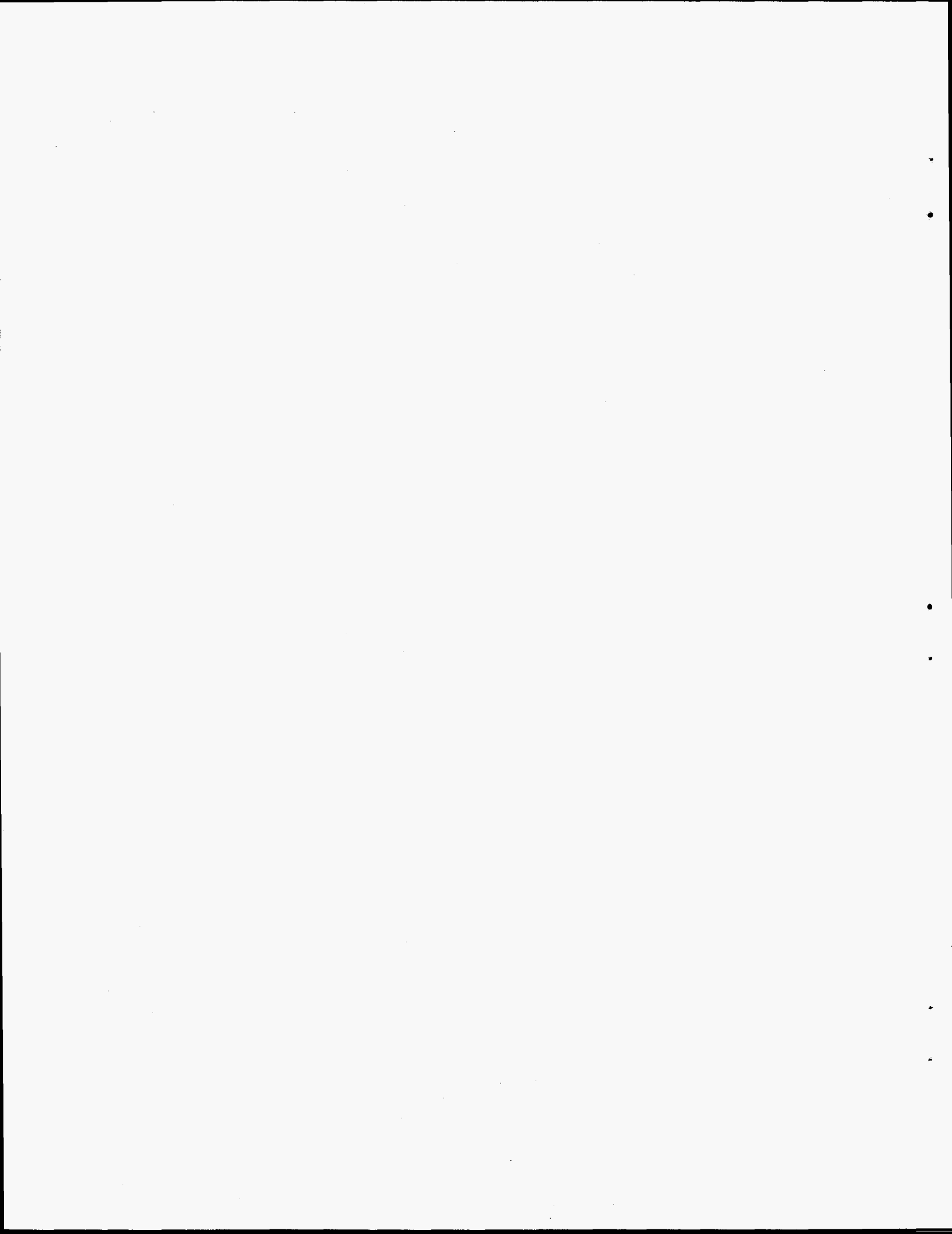
APPENDIX E

EXPERIMENTAL METHODOLOGY IN ALUMINA-SILICA TESTS

Materials

C-31 Bayer-hydrated alumina ($Al_2O_3 \cdot 3H_2O$), a synthetic gibbsite of high purity, was obtained from Alcoa. The raw product is a crystalline powder typically composed of 65 wt % aluminum oxide and 35 wt % water. The gibbsite was not pretreated prior to the experiments.

The surface area of the C-31 powder was determined using the Brunauer-Emmett-Teller (BET) technique to be 0.1–0.5 m^2/g. Sodium hydroxide (NaOH pellets, ACS reagent, 97+% purity) was purchased from Aldrich Chemical Company and diluted to the desired concentrations with deionized water. Dissolved silica used in the experiments, also from Aldrich, was in the form of sodium silicate solution that contained 14% NaOH and 27% SiO_2.

Experimental Procedure

Three types of experiments were conducted in order to investigate the effects of stirring rate, temperature, and silicate addition on alumina dissolution:

1. alumina dissolution at 50°C in 0.1 M NaOH solutions at various stirring rates to determine whether the selected experimental conditions preclude transport control on the dissolution rates;
2. alumina dissolution in 0.1 M NaOH at 35, 50, 75, and 90°C; and
3. alumina dissolution in 0.1 and 1 M NaOH solutions in the presence of varied concentrations (0, 0.1, 0.01, and 0.001 M) of silicate at 35 and 50°C.

These experiments were designed to extract dissolution trends of gibbsite under varied experimental conditions and to obtain kinetic data. The dissolution experiments were conducted in baffled 2-L Pyrex kettles (acrylic vessels were substituted for silicate experiments to avoid contamination of glass) immersed in controlled-temperature baths. The four-hole covers were fitted with a thermometer, a condenser, and a stirrer at the center connected to a constant-speed motor (Fisher Model 14-498 A). The fourth hole was used for aliquot removal with a syringe fitted with a hypodermic needle. The 5-mL aliquots were then passed through 0.45-μm nylon syringe filters to remove residual solids and large particles. Subsequently the aliquots were analyzed with a

Leeman Labs PS3000UV inductively coupled plasma spectrophotometer. Aluminum and silicon reference standards were prepared to bracket the entire range of expected elemental concentration.

At the start of the run, 1-L solutions were heated in the reactor vessels in order for the temperature to stabilize, at which point 39 g of gibbsite was added. Measurements of pH were made at the beginning and at completion of the experiments and did not change significantly, staying near pH 12.6. Stirring speed and temperature were monitored and recorded over the course of the experiment.

INTERNAL DISTRIBUTION

1–20.	E. C. Beahm	43.	B. D. Patton
21.	J. M. Begovich	44.	S. M. Robinson
22.	J. L. Collins	45.	B. B. Spencer
23.	T. A. Dillow	46.	J. S. Watson
24–38.	C. W. Forsberg	47–49.	C. F. Weber
39.	R. D. Hunt	50.	T. D. Welch
40.	R. T. Jubin	51.	Central Research Library
41.	D. D. Lee	52.	ORNL Laboratory Records–RC
42.	L. E. McNeese	53–54.	ORNL Laboratory Records–OSTI

EXTERNAL DISTRIBUTION

55. Jimmy Bell, 137 Bowsprit Lane, Kingston, TN 37763

56. Kriston Brooks, Pacific Northwest National Laboratory, Battelle Boulevard, P.O. Box 999, MS P7-43, Richland, WA 99352

57. Penny Colton, Pacific Northwest National Laboratory, Battelle Boulevard, P.O. Box 999, MS K8-93, Richland, WA 99352

58. Cal Delegard, Pacific Northwest National Laboratory, Battelle Boulevard, P.O. Box 999, MS P7-25, Richland, WA 99352

59. Zane Egan, 103 Lewis Lane, Oak Ridge, TN 37830

60. Jim Henshaw, AEA Technology, Building B220, Harwell, Didcot, Oxon, OX11 0RA, UK

61. Dan Herting, Numatec Hanford Corporation, P.O. Box 1970, MS T6-07, Richland, WA 99352

62. C. M. Keswa, Pennsylvania State University, 118 Steidle Building, University Park, PA 16802

63. Randy Kirkbride, Numatec Hanford Corporation, P.O. Box 1300, MS H5-27, Richland, WA 99352

64. Louis Kovach, Hanford, P.O. Box 1970, K6-51, Richland, WA 99352

65. Jeff Lindner, Mississippi State University, Campus Mailstop 9550, Etheredge Engineering Building, Room 320, Box MM, Mississippi State, MS 39762

66. Gregg Lumetta, Pacific Northwest National Laboratory, Battelle Boulevard, P.O. Box 999, MS P7-25, Richland, WA 99352

67. Graham MacLean, Cogema Engineering Corporation, P.O. Box 840, MS H5-27, Richland, WA 99352-0840

68. J. R. Noble-Dial, U.S. Department of Energy, Oak Ridge Operations Office, P.O. Box 2001, Oak Ridge, TN 37830-8620

69. K. Osseo-Asare, Pennsylvania State University, 118 Steidle Building, University Park, PA 16802

70. Brian Rapko, Pacific Northwest National Laboratory, Battelle Boulevard, P.O. Box 999, MS P7-25, Richland, WA 99352

71. Wally Schultz, W2S Company, Inc., 5314 Arbustos Court, NE, Albuquerque, NM 87111

72. K. E. Spear, Pennsylvania State University, 118 Steidle Building, University Park, PA 16802

73. David Swanberg, SAIC, MS H0-50, 3250 Port of Benton Blvd., Richland, WA 99352

74. John Swanson, 1318 Cottonwood Drive, Richland, WA 99352

75. Don Temer, Los Alamos National Laboratory, NMT-1 CMR, MS G740, Los Alamos, NM 87545

76. Major Thompson, Westinghouse Savannah River Company, Building C-140, Room 773-A, Savannah River Technology Center, Aiken, SC 29808

77. Rebecca Toghiani, Mississippi State University, Campus Mailstop 9595, Etheredge Engineering Building, Room 129, P.O. Box 9595, Mississippi State, MS 39762

78. George Vandegrift, Argonne National Laboratory, 9700 South Cass Avenue, Building 205, Argonne, IL 60439

79. Ray Wymer, 188-A Outer Drive, Oak Ridge, TN 37830

80–84. Tanks Focus Area Technical Team, c/o G. C. Notch, Pacific Northwest National Laboratory, P.O. Box 999, MSIN K9-69, Richland, WA 99352

85. Tanks Focus Area Management Team, c/o J. A. Frey, U.S. Department of Energy, Richland Operations Office, P.O. Box 550, MS K8-50, Richland, WA 99352

86. Technical Integration Manager (TIM), C. P. McGinnis, Oak Ridge National Laboratory, P.O. Box 2008, Oak Ridge, TN 37831-6273

87. Oak Ridge Reservation, A. G. Croff, Lockheed Martin Energy Research Corporation, Oak Ridge National Laboratory, P.O. Box 2008, Oak Ridge, TN 37831-6178